Architecture and Design of a Low Frequency Mechanical Actuation Device for Pre-Hospitalization Treatment of Myocardial Infarction Patients

by

Behrad Kajbafzadeh

B.A.Sc. (Honours), Simon Fraser University, 2010

Thesis Submitted in Partial Fulfillment of the
Requirements for the Degree of
Master of Applied Science

in the
School of Engineering Science
Faculty of Applied Sciences

Approval

Name: **Behrad Kajbafzadeh**

Degree: **Master of Applied Science (Engineering Science)**

Title of Thesis: **Architecture and Design of a Low Frequency Mechanical Actuation Device for Pre-Hospitalization Treatment of Myocardial Infarction Patients**

Examining Committee: **Chair: Dr. Jie Liang**
Associate Professor, P.Eng.
Graduate Chair, School of Engineering Science

Dr. Bozena Kaminska
Professor
Senior Supervisor

_____

Dr. Carlo Menon
Associate Professor, P.Eng.
Co-Senior Supervisor

_____

Dr. Andrew Rawicz
Professor, P.Eng.
Internal Examiner

_____

Date Defended/Approved: June 20, 2013

Partial Copyright License

SFU

The author, whose copyright is declared on the title page of this work, has granted to Simon Fraser University the right to lend this thesis, project or extended essay to users of the Simon Fraser University Library, and to make partial or single copies only for such users or in response to a request from the library of any other university, or other educational institution, on its own behalf or for one of its users.

The author has further granted permission to Simon Fraser University to keep or make a digital copy for use in its circulating collection (currently available to the public at the "Institutional Repository" link of the SFU Library website (www.lib.sfu.ca) at http://summit/sfu.ca and, without changing the content, to translate the thesis/project or extended essays, if technically possible, to any medium or format for the purpose of preservation of the digital work.

The author has further agreed that permission for multiple copying of this work for scholarly purposes may be granted by either the author or the Dean of Graduate Studies.

It is understood that copying or publication of this work for financial gain shall not be allowed without the author's written permission.

Permission for public performance, or limited permission for private scholarly use, of any multimedia materials forming part of this work, may have been granted by the author. This information may be found on the separately catalogued multimedia material and in the signed Partial Copyright Licence.

While licensing SFU to permit the above uses, the author retains copyright in the thesis, project or extended essays, including the right to change the work for subsequent purposes, including editing and publishing the work in whole or in part, and licensing other parties, as the author may desire.

The original Partial Copyright Licence attesting to these terms, and signed by this author, may be found in the original bound copy of this work, retained in the Simon Fraser University Archive.

Simon Fraser University Library
Burnaby, British Columbia, Canada

revised Fall 2011

iii

Ethics Statement

SFU

The author, whose name appears on the title page of this work, has obtained, for the research described in this work, either:

    a. human research ethics approval from the Simon Fraser University Office of Research Ethics,

or

    b. advance approval of the animal care protocol from the University Animal Care Committee of Simon Fraser University;

or has conducted the research

    c. as a co-investigator, collaborator or research assistant in a research project approved in advance,

or

    d. as a member of a course approved in advance for minimal risk human research, by the Office of Research Ethics.

A copy of the approval letter has been filed at the Theses Office of the University Library at the time of submission of this thesis or project.

The original application for approval and letter of approval are filed with the relevant offices. Inquiries may be directed to those authorities.

Simon Fraser University Library
Burnaby, British Columbia, Canada

update Spring 2010

Abstract

One of the major factors in increasing the survival rate of patients suffering from acute coronary ischemia is the speed of intervention. Two major techniques are currently in use: pharmacological and interventional. Both can be employed to recanalize thrombosed coronary arteries, but the former is slow acting and often leads to incomplete reperfusion, while the latter requires specialized personnel in a hospital with a cardiac catheterization laboratory. This thesis proposes a novel method for pre-hospitalization treatment of patients with acute coronary ischemia that can be safely applied by a minimally trained individual prior to or during patient transportation to hospital. It consists of applying low frequency mechanical vibration to the left intercostal space of patient's chest during diastole of the heart cycle to induce vibration on the heart and thus on the coronary arteries. Additionally, the method includes application of direct, distal, mechanical, arterial deformation to induce pressure change and turbulence in the blood flow. Mechanical vibration increases coronary blood flow, acts as a strong vasodilator, and relieves heart spasms likely to be seen in heart attack patients. Direct arterial deformation generates turbulence in the blood, which amplifies mixing of clot busting agents with thrombi. Furthermore, it imposes shear stress on the clot wall to achieve clot displacement and/or disruption. In order to investigate the impact of mechanical actuation on clot lysis and also to examine feasibility of a device for application of mechanical vibration on the chest of myocardial infarction patients, three major studies are presented that also form the three objectives of this work: the first study introduces an electromechanical apparatus to study the effects of mechanical vibration and deformation on disrupting blood clots in-vitro with and without combined use of thrombolytic agents. The second study describes the design and architecture of a prototype device for application of Diastolic Timed Vibration (DTV) on the chest of heart attack patients for increasing the coronary blood flow, and improving the weak relaxation of the ill myocardium. The final experiment herein presents a preliminary investigation on a human subject to determine whether direct distal arterial deformation could cause turbulence in the blood flow as a means for better mixing of fibrinolytic agents with clot and also to induce stress on the clot and the clot wall.

Keywords: Heart attack; non-invasive treatment; low-frequency mechanical vibration and deformation; coronary ischemia; arterial thrombolysis; reperfusion

Acknowledgements

I would like to thank Dr. Bozena Kaminska and Dr. Carlo Menon, my co-senior supervisors, for their continuous support and guidance during the course of this thesis work and also for providing me with directions.

I am indebted to Dr. Marcin Marzencki for his help and expertise for all the experiments done in this work: in-vitro studies, DTV device development, and ultrasound image acquisition.

My sincere thanks go to Dr. Kouhyar Tavakolian for his guidance and insight for the DTV design and architecture chapter.

I would like to thank Mr. Farzad Khosrow-Khavar for helping me understand certain concepts of myocardial infarction localization algorithms and ECG signal processing necessary for developing the DTV hardware.

My sincere thanks go to Dr. Andrew Rawicz; without his help I would have not been able to understand concepts of blood flow characteristics and behaviors under mechanical vibration.

I would also like to thank the personnel at the UBC Animal Farm for their help and hospitality during the in-vitro experiments and Andrew Hofmann for his insight and helpful observations.

I would like to express my gratitude to Mr. Kris Dickie for his help with ultrasound imaging acquisition.

Table of Contents

List of Tables

List of Figures

xi

List of Acronyms

AV   Atrioventricular

aVF   Augmented Lead - Foot

aVL   Augmented Lead – Left Arm

aVR   Augmented Lead – Right Arm

Cath lab   Cardiac Catheterization Laboratory

DTV   Diastolic Timed Vibration

ECG   Electrocardiogram

EDV   End-Diastole Velocity

EMS   Emergency Medical Service

FFT   Fast Fourier Transform

HIFU   High Intensity Focused Ultrasound

IHD   Ischemic Heart Disease

IV   Intravenous

LA   Left Arm

LF   Left Foot

MI   Myocardial Infarction

NI   National Instruments

PCI   Percutaneous Coronary Therapy

PSV   Peak Systolic Velocity

PTCRA   Percutaneous Transluminal Coronary Rotational Atherectomy

RA   Right Arm

RI   Resistive Index

S/D Ratio   Systolic/Diastolic Ratio

SA   Sinoatrial

STEMI   ST Elevation Myocardial Infarction

VI   Virtual Instrument

1.   Introduction[1]

Ischemic heart disease (IHD) is one of the leading causes of death contributing to 12.8% of mortality worldwide [5]. It is a consequence of reduced blood supply to the heart muscle through coronary arteries [6]. IHD is considered to be an on-the-rise pandemic that took lives of 7.3 million people in 2008 [7]. In the same year in the United States alone, there were over 405 thousand IHD driven deaths [8]. It is estimated that more than 915 thousand Americans experience a new or recurrent coronary attack every year with approximately one death every 40 seconds [8].

Acute myocardial infarction (MI) – also referred to as ischemic heart disease or heart attack – is a consequence of a complete or prolonged obstruction of a coronary artery. Coronary arteries transfer oxygenated blood to myocardium, and therefore, a complete loss of flow in these vessels can potentially lead to a regional necrosis. Coronary artery perfusion loss is usually due to formation of a thrombus in the artery stenosis site. Rupture of atherosclerosis lesions in the coronary artery stimulates platelet aggregation and coagulation cascade, which can lead to clot formation [9], [10] and reduction of the lumen diameter of the affected vessel. Studies show that necrosis occurs approximately between 15 and 30 minutes after the onset of ischemia [10] providing a very narrow window of opportunity for preventing cell death.

1.1. Motivation

Since the amount of myocardial muscle loss is proportional to the ischemic time [11], rapid therapy application after the onset of symptoms is crucial for increasing patient's chance of survival. Therefore, techniques that can be applied quickly after the

---

[1] This work shares wording and content with published and unpublished (at the time of this submission) articles that the author of this thesis has been one of the major contributors [1], [2], [3], [4].

1

onset of symptoms, before or even during patient transportation to a specialized facility, could potentially save many lives and are subject of intense multidisciplinary research.

In a severe case, when a major epicardial coronary artery becomes blocked, the resulting heart muscle injury may introduce ST segment elevation in patient's electrocardiogram (ECG) signal. This condition is referred to as ST Elevation Myocardial Infarction (STEMI). Presence or absence of the elevated segment allows the emergency or hospital personnel to rapidly decide whether to induce thrombolysis [10], which is use of specific means, i.e. pharmacological or interventional, to break down blood clots. There are two major reperfusion options available to STEMI patients [12]: fibrinolytic therapy and percutaneous coronary therapy (PCI). Fibrinolytic therapy is a pharmacological approach employing clot-busting drugs while in the PCI method, a balloon or stent are inserted into the patient's circulatory system, guided and inflated inside the stenosed artery to restore patency. In very severe cases, an open heart surgery might be required. The choice of reperfusion procedure depends on the estimated transportation time to hospital with a cardiac catheterization laboratory (cath lab), elapsed time from the onset of the symptoms, and the risk of bleeding.

Beneficial effects of thrombolytic therapy have been demonstrated in controlled clinical trials proving to accelerate clot lysis [13], [14] and preserve left ventricular function [15], [16]. Unless contraindicated, administration of fibrinolytics is the first recommended choice, when patient transfer time to an angioplasty facility is greater than 90 minutes (door-to-balloon inflation time). The administration is preferably performed within 30 minutes of emergency medical service personnel arrival (EMS-to-needle time). However, it has been reported that only 50-60% of the patients achieve TIMI 3 (normal flow) within the first 90 minutes of fibrinolysis [17], [18], and 1% of the patients may experience intracranial hemorrhaging with a fatality rate of 60% [19].

Over the years, in the United States, the average door-to-balloon time has improved quite significantly in meeting the target 90-minute time frame suggested by AHA [20], [21]. However, not every patient receives proper care in a timely manner, which is usually due to one or more of the following reasons [22]:

- Busy PCI centers may have to transfer patients to another facility.

2

- In cases where the patient does not arrive by EMS, diagnosis can take longer in the ER.

- Not all hospitals run their cath lab 24 hours a day, 7 days a week.

- In most PCI centers, staff is off-site during off hours. They would require longer time to arrive to the facility.

- Lack of optimal coordination among EMS services, STEMI referral hospitals, and STEMI-receiving hospitals.

Furthermore, door-to-balloon times could be significantly higher in remote or rural areas due to unavailability of a hospital equipped with a cath lab. In developing countries, numbers are speculated to be worse.

Given the importance of immediate initiation of treatment after the onset of STEMI symptoms, this thesis focuses on an adjunctive safe noninvasive therapeutic method that can be applied by the EMS personnel and/or minimally trained individuals present at the scene to help in starting the pre-hospitalization treatment after the onset of STEMI symptoms. The method is a combination of two approaches called Diastolic Timed Vibration (DTV), which consists of application of external mechanical actuation to the chest of the STEMI patient at certain frequencies only during the diastole phase of the heart pumping cycle, and distal arterial mechanical deformation, which consists of application of mechanical vibration to an artery distal to the stenosis site. Such mechanical approach can be a safe adjunct method to clot disruptive drug therapy accelerating reperfusion of occluded vessels. Application of mechanical stimulus can increase mixing of thrombolytic drugs and improve drug penetration to the occlusion site and thus allow lower doses during pharmacological therapy leading to lower risk of bleeding, especially interesting for patients with contraindications to thrombolytic drug use.

1.2. Objectives

As mentioned earlier, the main goal of this work is to introduce a method consisting of direct arterial mechanical actuation and deformation, and diastolic timed

vibration (DTV) to achieve thrombolysis, improve coronary blood follow, and relieve heart spasms likely to be seen in heart attack patients. The following three studies form the objectives of this work, which aim at achieving the aforementioned goal.

1. Design of an electromechanical setup as a simplified model of heart coronary arteries and capillaries to study the impact of distal and proximal application of mechanical vibration and deformation on vessel-like narrowings occluded with animal blood clot.

2. Architecture and design of a proof-of-concept DTV apparatus for application of mechanical vibration on the chest of STEMI patients and examination of major contributing factors to the efficacy and safety of the device.

3. Examination of different methods for quantitative analysis of the effects of distal mechanical deformation of a human subject artery on the blood flow.

1.3. Thesis Organization

This work is organized as follows. After the introduction, in chapter 2, required background information is presented. Furthermore, a review of current reperfusion methods is provided along with shortcomings of these methods. State of the art with regard to efficacy of noninvasive mechanical vibration on STEMI patients is also discussed in this chapter. Afterwards, in chapter 3, an electromechanical setup is presented, which was used to perform in-vitro studies. Results and analysis of the acquired data are described in the same chapter. In chapter 4, the design, features, and requirements of a proof-of-concept Diastolic Timed Vibrator device are discussed with presentation of experimental results. Chapter 5 discusses different approaches taken in order to quantitatively examine the efficacy of direct distal mechanical arterial deformation in causing turbulence in blood flow. A discussion underlines the principal concepts and proposes a combined therapy method. Finally, a conclusion accompanied by a sketch of future works finish this thesis work.

2. General Background and Literature Review

Chapter 2 presents general background information, which was required for conducting this research, and various methods of thrombolysis and their potential drawbacks. Certain background information and literature review specific to components of this research are discussed in respective chapters later herein.

This chapter is organized as follows: first, detailed description of heart electrical activity, electrocardiogram, arrhythmias and ECG lead calculations are presented. Subsequently, various common or in-research reperfusion methods are presented along with availability and safety remarks. Finally, efficacy of mechanical vibration on thrombosis is reviewed.

2.1. Electrocardiogram (ECG)

ECG is an important diagnostic tool and usually the first used in diagnosing conditions of heart problems. The following subsections introduce ECG in more depth.

2.1.1. Heart Electrical Activity

Human heart is equipped with a natural pacemaker called sinoatrial (SA) node. SA node is a small mass in the heart made of specialized cells and is responsible for generating electrical impulses in the myocardium. It is located in the right atrium (upper right chamber of the heart), which is responsible for receiving deoxygenated blood. Left atrium, on the other hand, receives oxygenated blood from the lungs. The electrical impulses generated by the SA node travel through specialized conduction pathways initially to the right and left atria. This process initiates contraction of atrial muscles, which, in turn, pumps the blood out of the right atrium through tricuspid and mitral valves to the ventricles. Left ventricle is responsible for pumping blood out of the heart muscle

to the lungs (for oxygenation) whereas right ventricle pumps blood to the rest of the body.

While causing atrial muscle contraction, the electrical impulse approaches the atrioventricular (AV) node. AV node is also a set of specialized group of cells and is mainly responsible for delaying the electrical impulse by about 100 ms before reaching the Bundle of His and the left and right bundle branches. Bundle of His and its branches are designed for conducting the electrical impulse along the dividing wall (septum) in the heart and leading it, through the Purkinje fibers, to the inner wall of the ventricles. Through this path, as the electrical signal travels, it causes the ventricles to contract and pump the blood out of the heart. The reason for the 100 ms time delay at the AV node is to allow the atria to fully deplete the blood into the ventricles before ventricles contract, and also to achieve high cardiac throughput [23].

The contraction and relaxation of the heart muscle generate an electrical current that distributes to the whole body and results in potential differences at different locations of the body. Given the different timings at which the heart muscle cells contract as the electrical impulse from the SA node travels down the Bundle of His, one can expect to see different electrical potentials at different timings. These electrical potentials are vectors and as such are represented with a magnitude and direction (cardiac vectors). The simplest way to measure and represent the overall electrical activity of the heart is by placing two electrodes at the opposite sides of the heart muscle. This way the cardiac vector is projected on the line joining the two surface electrodes. Plotting the potential difference between the two surface electrodes as a function of time yields electrocardiogram or ECG of the heart [23]. Figure 1 shows the schematic of a normal ECG of the heart [24].

2.1.2.   Structure of ECG Signal

The description of each segment (wave) of the ECG signal is as follows. Figure 1 is referenced in this example.

- P-wave corresponds to the onset of atrial contraction.

- QRS complex is for representing the onset of ventricular contraction.

6

- PR distance represents the time the heart takes from the start of atrial contraction to the beginning of the ventricular contraction.

- T-wave depicts ventricular relaxation.

- QT interval shows the duration of ventricular contraction.

Typical amplitude of the R-wave is 1 mV with minimum and maximum figures, depending on the subject and their health condition, at 0.4 to 4 mV, respectively [23].
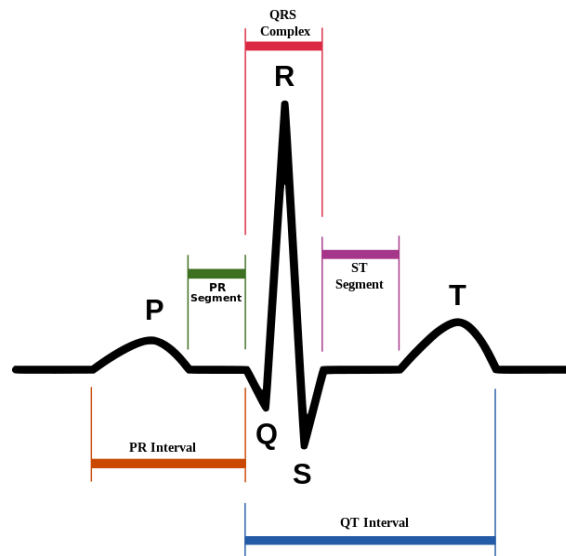
Figure 1. ECG structure.

2.1.3.   Arrhythmia

As mentioned earlier, the heart electrical activity is generated by the SA node and travels through a predefined conduction path with a delay at the AV node. However, any interruption, non-conductivity, or non-responsiveness of the conduction path leads to change in the overall shape of the ECG signal known as arrhythmic ECG. This condition is referred to as arrhythmia (abnormal heart rhythm) and is reflected in patient's ECG with abnormal ECG amplitude, wave timings and intervals, absence of certain waves and the overall change in the shape of the ECG signal. In general, issues with the SA node and/or the specialized conduction path cause irregular heartbeat and reduced cardiac output. In turn, arrhythmia can be caused by myocardial infarction, a condition

that supply of blood is interrupted to certain areas of the heart muscle leading to death of that segment, and in very severe cases the issues can be fatal. Figure 2 shows premature ventricle contraction (PVC) ECG [25]. PVC occurs as a result of ventricular contraction happening before the atrial contraction.
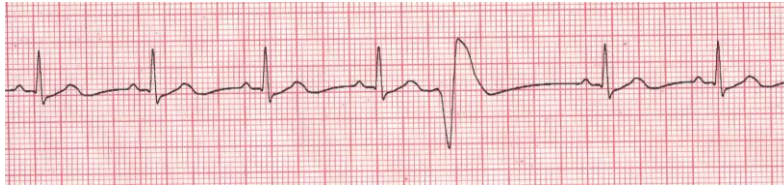
Figure 2. Premature ventricular contraction.

Figure 3 shows elevation in the ST segment of the heart ECG signal [26]. ST elevation in the ECG indicates, among other life threatening conditions, severe myocardial infarction, which requires immediate attention. To be diagnosed as ST elevation, the Q-wave time length must be greater than 0.04 seconds and its depth must be at least one third of the height of the R-wave in the QRS complex.

Figure 3. ECG with ST segment elevation.

2.1.4.   ECG Leads

Since the ECG signal is formed by plotting the projection of cardiac vectors over the line joining two surface electrodes as a function of time, the location of the electrodes and also the calculation method becomes of paramount importance, which are all discussed in the following.

Electrode Placement and Lead Calculations

The ECG electrodes for projecting cardiac vectors can be placed in one of the two possible ways (or can be a combination of both): three electrodes on three limbs, and/or six electrodes on the chest wall.

Three main leads and an additional three augmented leads, collectively called frontal plane leads, are possible by placing the electrodes according to the Einthoven's equilateral triangle (Figure 4). The purpose of these leads is to provide a two dimensional view of the heart electrical activity.
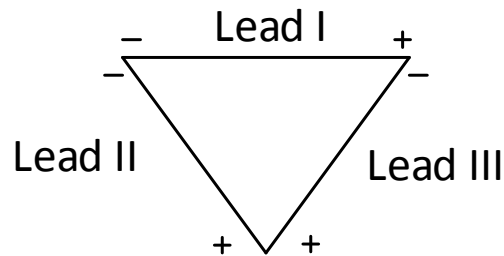
Figure 4. Einthoven's equilateral triangle.

The three main leads are Lead I, Lead II, and Lead III. Each of the leads is the projection of the cardiac vector between their respective electrodes. Table 1 shows the three possible configurations and calculation of the potentials.

Table 1. Leads I through III placement and calculation.

Lead Number	Projection Calculation
Lead I	Left Arm (LA) – Right Arm (RA)
Lead II	Left Leg (LL) – Right Arm (RA)
Lead III	Left Leg (LL) – Left Arm (LA)

Einthoven's triangle also allows for three augmented leads. Augmented leads provide viewing the heart electrical activity from different angles as the projections are at a different direction. This is done by measuring the potential between a limb electrode and the average of the other two limb electrodes. Table 2 shows the three different scenarios.

Table 2. Augmented leads calculations.

Lead Name	Projection Calculation
aVR (augmented - right arm)	RA – ½ (LA + LL)
aVL (augmented - left arm)	LA – ½ (RA + LA)
aVF (augmented - foot)	LL – ½ (RA + LA)

In order to view the entire cardiac vector, six additional electrodes are placed on the chest, which project the cardiac vectors onto a transverse plane and hence reconstructing the whole cardiac vector when combined with frontal plane leads. In this method, potential of each electrode is measured with reference to the average of the three limb electrodes (Table 3).

Table 3. Projection and calculation of chest electrodes.

Lead Name	Projection Calculation
V_1	V_1 + ⅓ (LA + RA + LL)
V_2	V_2 + ⅓ (LA + RA + LL)
V_3	V_3 + ⅓ (LA + RA + LL)
V_4	V_4 + ⅓ (LA + RA + LL)
V_5	V_5 + ⅓ (LA + RA + LL)
V_6	V_6 + ⅓ (LA + RA + LL)
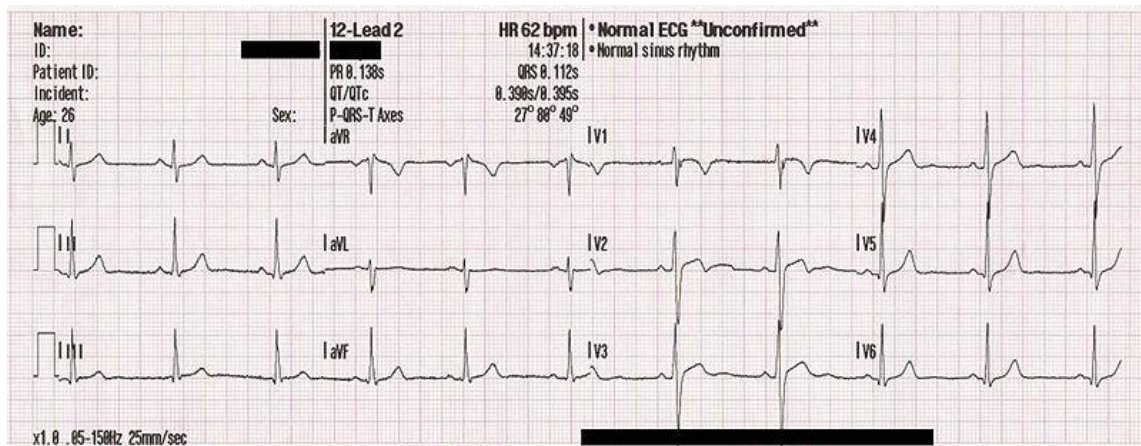
Figure 5. Representation of a 12-lead ECG.

Combination of the six leads from the frontal plane and the six leads from the transverse plane form the standard 12-lead ECG. 12-lead ECG generally allows for rapid

identification of MI, decreased time to reperfusion and is recommended by the American Heart Association [27]. Figure 5 shows a 12-lead ECG waveform.

It is worthwhile mentioning that to achieve 12-lead ECG, only 10 electrodes are needed. Three for frontal plane leads, and six electrodes for the transverse plane. A 10th electrode is used as a reference to patient's right leg. This is generally to reject common mode noise in the system.

2.2. Atherosclerosis and Coronary Thrombosis

Atherosclerosis is a condition caused by plaque buildup in the arteries. Plaque buildup stiffens as well as reduces the diameter of the arteries [28]. Over time, if the size of the plaque grows large enough to obstruct blood flow, heart attack can occur. However, plaques do not need to be completely obstructing the artery to cut the blood flow. Existence of vulnerable plaques in the artery is a major risk factor. A vulnerable plaque progresses very rapidly and also is prone to cause thrombus [29]. Thrombus is formed when the plaque ruptures under hemodynamic stress. Once rupture occurs, the body reacts by forming a clot around the ruptured area. Clot formation is the natural reaction of body to the lesions [9], [10], [30]. Clearly, the clot, in turn, narrows the artery diameter and eventually leads to occlusion. This condition generally leads to coronary thrombosis (heart attack).

2.3. Reperfusion Methods

This section reviews various reperfusion methods available to STEMI patients. Both invasive and non-invasive methods are discussed.

2.3.1. Percutaneous Coronary Intervention (PCI)

PCI, also known as coronary angioplasty, is an invasive non-surgical procedure by which the cardiologist guides a deflated balloon or stent using a catheter through femoral or radial artery to the stenotic coronary artery. Once in place, the balloon is inflated to widen the stenosed artery [31]; stents are more commonly used as they

11

permanently keep the artery open. Although very successful, this method requires substantial infrastructure, i.e. cath labs, and is rather expensive. However, PCI is the preferred method of treatment over other options.

Ideally, in order to prevent necrosis, patients must be transferred to a cath lab within 90 minutes of onset of symptoms. However, this is not always possible due to busy PCI centers and patient transfer to another facility, longer diagnosis time in the ER, limited operational hour of cath labs, and unavailability of staff is during off hours [22]. Therefore, commencement of treatment even before arrival of EMS or to the ER could efficiently minimize the size of necrosis region of heart muscle.

2.3.2.   *Thrombolysis by Clot Dissolving Agents*

Pharmacological thrombolysis is use of clot dissolving agents to break down thrombi in the vessels. It is a rather slow process with a success rate between 40 and 50% within the first 90 minutes of the procedure [17], [18]. Although minimal, generally 1% of patients experience intracranial hemorrhaging out of which only 40% survive [19]. This procedure can be started by the EMS personnel while the patient is en route to the hospital. Thrombolytics are administered intravenously.

Intra-Arterial Thrombolysis

Intra-arterial thrombolysis is generally used for stroke patients and is only effective within three hours of the onset of stroke symptoms. This method is invasive and includes injection of clot busting agents directly to the clot site using catheters [32]. Invasiveness of the procedure requires access to specialized cath labs.

2.3.3.   *Atherectomy*

It is a minimally invasive surgical procedure to remove the plaque buildup by using specialized surgical blades passed to the plaque site on the artery wall via a catheter. There are different methods for this purpose, the most popular of which is known as percutaneous transluminal coronary rotational atherectomy (PTCRA). In this method, small whirling blades selectively remove plaques on the coronary wall.

A comparison between PTCRA and balloon angioplasty was done by comparing and analyzing data from 12 studies for patients that were not suitable for surgery [33]. It was concluded that although PTCRA could benefit patients with complex atherosclerosis lesions, no further evidence was found to support use of PTCRA in lieu of angioplasty. In fact, patients that underwent PTCRA found to be more likely to suffer from post procedural complications [33].

2.3.4. *Ultrasound Assisted Lysis*

Ultrasound thrombolysis has been a topic of research for many years since late 1970s [34], [35]. It is believed that therapeutic ultrasound energy can selectively break fibrin matrix in the thrombus, which in turn, leads to disruption of the blood clot [36], [37]. In general, there are four approaches to ultrasound thrombolysis [34]:

1. External transducer catheter-delivered ultrasound.

2. Transcutaneous delivery of external High Intensity Focused Ultrasound (HIFU) with or without administration of thrombolytic agents or similar methods.

3. Catheter-delivered transducer-tipped ultrasound with localized clot breaking agent administration.

4. Transcutaneous delivery of low frequency ultrasound in conjunction with IV thrombolytic agent delivery.

The following four subsections briefly introduce and discuss the above four methods.

External Transducer Catheter-Delivered Ultrasound

This is an invasive method, which has been shown through different studies, in-vitro, animal, and human, to work very effectively [35], [38], [39], [40] . Hong et al. studied clot disruption capability of the ultrasound energy delivered by a catheter in-vitro. They studied the effects of clot age, use of clot busting drugs, and wire probe length and concluded that all their sample clots were broken down in less than three minutes

regardless of the probe size and age. Use of thrombolytic agents proved little to no effect in the process [39]. In another study, 18 dogs received 1 – 4 hour old human blood clot with very high success rate of recanalization with application of catheter-delivered ultrasound [40]. In order to evaluate the ability of percutaneous coronary ultrasound in humans with acute myocardial infarction, Rosenschein et al. conducted a research on 15 patients with TIMI 0 or 1 flow. High intensity low frequency ultrasonic ultrasound was used to target the thrombus site. Ultrasonic waves, when aimed at a liquid, cause generation of cavitation. Cavitation can cause mechanical agitation and also induces shear forces on the cell structures damaging the cell [41]. The procedure was followed up by an angiogram where it confirmed TIMI grade 3 flow in 87% of the patients. The degree of flow remained constant at TIMI 3 except for 1 patient that experienced recurrent ischemia on the fifth day after the procedure [42]. Similarly, Hamm et al. in their in-vivo and in-vitro studies on 14 patients with acute MI demonstrated effectiveness and safety of the catheter-delivered therapeutic ultrasound in dissolving thrombi [38].

Current standard invasive and interventional techniques for coronary thrombolysis use balloon angioplasty and coronary arterial stent to open the narrowed artery with success rates higher and adverse effects lower than catheter-delivered ultrasound approach [34], [43], [44]. Therefore, use of catheter-delivered ultrasound for treating coronary thrombosis seems not to be best choice.

High Intensity Focused Ultrasound (HIFU)

HIFU has been studied as another tool to disrupt thrombus. Use of high intensity/power ultrasound focused on a desired segment and the resulted heat causes damage to the cells. By choosing the right frequency and duty cycle, damage to arterial wall can be prevented.

Rosenschein group used an acoustic lens on a diagnostic imaging ultrasound probe to focus the ultrasound energy. Finding the best parameters (40% duty cycle with pulsed-wave ultrasound, average power of 25 ± 5 watts/cm^2), they disrupted clots in an immersed bovine arterial segment. The procedure took less than two minutes and no arterial damage was observed [45]. In a more recent study, a 1.51MHz focused ultrasound transducer was used for in-vitro and in-vivo studies on rabbits. Pulse lengths between 0.1 and 10 ms with 300 W power were chosen. For in-vitro experiments, clots

from arterial blood of a rabbit were placed into a 2 mm of diameter of a tube. The tube was hit with a 30 MHz ultrasound. For in-vivo experiment, they initiated clots in rabbits femoral arteries and used a 23 MHz Doppler ultrasound. In-vitro studies showed 99.2% success rate. The clot erosion volume seemed to be dependent on the exposure power, and pulse length. Higher pulse lengths resulted in smaller debris size. The in-vivo study showed bleeding with 10 ms pulses, and with 1 ms length pulses although bleeding was limited to one case, only partial flow restoration in 6 of the 10 clots occurred [46].

In general, HIFU appears promising for thrombolysis purposes; however, more work needs to be done to determine safety and feasibility of this approach.

Catheter-Delivered Transducer-Tipped Ultrasound Adjunct with Fibrinolysis Agents

Catheter-delivered transducer-tipped ultrasound is clinically used for removal of deep venous thrombi [34]. Tachibana used a 1.3 MHz transducer-tipped catheter to deliver 0.3 W/cm^2 ultrasound energy for one minute in conjunction with use of urokinase (an enzyme used for thrombolysis) in-vitro. The approach lead to increased thrombolysis success [47]. In another study by the same team, it was shown that a 70 kHz ultrasound in conjunction with urokinase and a contrast agent offers a more successful thrombolysis rate. Presence of microbubbles in the contrast agent resulted in a success rate of 33-51% [48]. Destruction of microbubbles by the ultrasound energy allows for local delivery of drugs in the bloodstream. Furthermore, ultrasound energy lowers the energy needed for cavitation. Microbubbles lower the required cavitation energy and therefore ultrasound destruction of microbubbles can cause microjets that can impose stress on the clot and lead to clot disruption [49].

Siegel and Luo used a 120 kHz catheter-delivered transducer-tipped ultrasound system in conjunction with a fibrinolysis agent for their in-vitro studies and observed 20-40% success rate in disrupting the clots [50]. To further examine the feasibility of catheter-delivered ultrasound, Atar et al. performed an in-vivo experiment on 14 dogs with and without use of microbubbles (i.e. ultrasound was not used). 5-7cm clots were induced into femoral arteries of the dogs. A 1.1 MHz catheter was used to deliver ultrasound energy, microbubbles and clot busting agents. On the contralateral side, a clot with the same size was injected, but no microbubbles were used and only fibrinolytic

agents were injected. Overall, 28 segments were studied out of which only 50% achieved TIMI 2 or 3 flow without the use of microbubbles as opposed to 86% success rate in presence of the two components, i.e. microbubbles and fibrinolytic agents. Later angioscopy confirmed the results of the experiments [51].

Transcutaneous Delivery of Low Frequency Ultrasound in Conjunction with IV Thrombolytic Agent Delivery

It is very well documented that ultrasound facilitates thrombolysis in presence of fibrinolytic agents [52], [53]. It is believed that ultrasound, in both perfused and static systems, augments the delivery of lytic enzymes into the blood clot as well as disrupting the fibrin bundles into smaller diameter size bundles [53], which, in turn, provides the more binding sites to the clot busting drugs and also reduces flow resistance during exposure time [53].

Initial in-vitro studies dating back to 1992 demonstrated a synergistic effect between fibrinolytics and ultrasound. In-vitro studies showed success when ultrasound was used as a facilitation means to deliver three different thrombolytic drugs [54]. Later studies confirmed this and demonstrated that ultrasound energy did not adversely affect functional activity or molecular structure of thrombolytic agents used in previous studies [34]. Furthermore, there have been studies concentrated on the frequency range most effective for disrupting clots. In one study, it was shown that lowering the frequency to 25 kHz from 250 kHz effected higher clot disruption [55], which is believed to be due to lower tissue heating and deeper penetration of longer wavelength ultrasound [34].

In-vivo studies have also been conducted to determine feasibility of noninvasive ultrasound assisted lysis. In one study, researchers used transcutaneous ultrasound in conjunction with thrombolysis agents and achieved, in 100% of the cases, TIMI 3 flow after one hour of therapy. In order to prevent tissue damage from heating, pulsed ultrasound wave (duty cycle = 30%) was used [56].

Use of microbubbles in transcutaneous low frequency ultrasound has been studied in the past and is an ongoing topic of research. A comparison between use of microbubbles in conjunction with ultrasound and use of ultrasound or microbubbles alone showed that 76% of clotted vessels in a rabbit model were recanalized compared to 9% and 0% recanalization rate of standalone ultrasound and microbubbles,

respectively [57]. Other studies have also confirmed effectiveness of low frequency ultrasound combined with microbubble presence in dissolving blood clots [34], [58].

It has been shown that application of ultrasound in acute myocardial infarct animal models leads to improvements in the ST segment elevation of the ECG, even if the dose is not enough to lead to reperfusion. This is believed to be due to vasodilation and enhanced tissue reperfusion effects of ultrasound energy [59], [60].

Coronary Thrombolysis and Transcutaneous Ultrasound

As mentioned earlier, access to cath lab within the 90-minute door-to-balloon timeframe may not be possible in all cases and there has always been a need for a noninvasive approach. Siegel et al. studied canine models with induced acute myocardial infarction. This was achieved by sending a catheter to the dog's coronary artery as a means for directing a guidewire to the artery. A 3 V battery was connected between the catheter and the dog's skin to cause acute thrombus. Within 60-120 minutes, an acute thrombus was formed, which was akin to type of thrombus seen in humans. A total of 51 dogs underwent transcutaneous ultrasound with a custom 27 kHz probe. Combination of ultrasound and fibrinolytic agents lead to greater TIMI 3 flow compared to cases where only fibrinolytic agent was used (more than four times greater in 90 minutes of procedure) [61], [62], [63]. ECG waveforms from the dogs treated with fibrinolytic mediated ultrasound showed better and greater degree of normalization of the ST segment elevation [64]. Use of pulsed wave vs. continuous wave ultrasound did not display any advantage in achieving TIMI 3 flow [34].

Safety

Safety of therapeutic ultrasound as a thrombolysis means has been investigated in several researches. It is dependent on the frequency, intensity and tissue characteristics. In a review article, ultrasound has been presented to be a safe method for thrombolysis [34]. However, other studies have shown different results, depending on the intensity and frequency of ultrasound. Frizzel et al. in an in-vitro study demonstrated that ultrasound at therapeutic and above therapeutic levels can very well lead to formation of thrombi [65]. In another study, tissue temperature was shown to rise by an average of 12°C, from 30°C to 42°C, within 10 minutes after the initiation of application of therapeutic ultrasound (20 kHz, 1.5 W/cm^2) on rabbits. Skin temperature, on the other

hand, showed greater increase. At 5-minute mark, it went up to reach 63.8°C and at 10-minute mark of ultrasound treatment it reached 73.3°C [57].

In a study on pigs, an ultrasound with a frequency of 750 kHz and intensity of 1.5 W/cm^2 was applied to pigs' ear veins. Tissue temperature was shown to increase to 52-54°C. Later examination of the veins by electron microscopy revealed superficial and also structural damage to the veins [66].

2.4. Effects of Mechanical Actuation on Blood Flow and Reperfusion of Clotted Vessels

Efficacy, and important parameters of mechanical vibration and contributing factors, as the main motivation for this research work, in improving or even restoring blood flow is discussed in this section.

2.4.1. Mechanical Actuation for Thrombolysis

Several studies have been conducted to evaluate the efficacy of mechanical vibration in removing/breaking thrombi. The efficacy of mechanical vibration in thrombolysis has been attributed to superior deep penetration [67], [68], and unique internal transmission characteristics through arteries and epimyocardium and, in general, body tissues [69], [70], [71], [72]. Low frequency mechanical vibration is a means for disrupting blood clots [73], and has been thought to improve mixing of clot busting drugs with clots in in-vitro models [74]. Furthermore, in open animal model studies, external tapping of acute thrombosed coronary arteries has been shown to cause blood flow restoration [75]. Sheer stress, strain and also stretch mechanisms caused by mechanical vibration are thought to be contributing factors to myocardial reperfusion [76], [77].

In one study, thirty patients with upper and/or lower extremity (iliofemoral, iliofemoropopliteal, femoropopliteal, subclavian) thrombosis were examined. After application of percutaneous mechanical vibration for an average time of 145 minutes in conjunction with fibrinolytic agents, it was concluded that percutaneous mechanical

throbectomy can be considered as an effective means for restoring blood flow, although continued surveillance is required to monitor for potential complications [78].

In a meta-analysis study of cystic fibrosis patients, various physical therapy modalities were examined. Thirty five trials were statistically analyzed for different combinations of modalities. The standard physical therapy, which includes postural drainage, percussion, and vibration showed significantly greater sputum expectoration than no treatment method. Additionally, when combined with exercise, standard therapy significantly increased the efficacy of the treatment than standard therapy alone [68].

An In-Vitro Flow Model for Examination of Noninvasive Low Frequency Vibration on Thrombolysis

Yohannes and Hoffman [79] conducted an in-vitro experiment to determine whether low frequency vibration in the range of 100 Hz would lead to thrombolysis. In their experiment, a 2 cm slab of beef was placed on the chest of a teddy bear with an indwelling catheter penetrating through the bear's thorax. A 90% stenosis site was developed in the catheter by a width-adjustable clamp. In order to simulate arterial pressure, the catheter was connected to a pressurized heparinized IV system. Thirty test runs with 2-hour old clots injected into the catheter were conducted. A twenty-minute observation period was allowed for each trial to ensure stability of the occlusion site. Tests were randomized into vibration and no-vibration groups. Each test was run for 45 minutes.

In the vibration group, catheter reflow occurred within an average time of 90 seconds in 88% of the trials whereas in the no-vibration group reflow did not occur at all. It was concluded that vibration application on a thrombosed site could indeed assist in clearance of thrombus [79].

2.4.2.   *Mechanical Vibration Frequency*

One of the reasons for heart blood pumping failure in myocardial infarction patients has been attributed to incomplete left ventricular relaxation of the heart muscle. It is believed that weak or incomplete relaxation of the left ventricle causes higher diastolic pressure and could impede blood flow in the coronary arteries during the diastole cycle [80]. In an open heart canine model study it was shown that application of

50 Hz sinusoidal vibration with 2.1 mm of stroke magnitude during diastole on the epicardium leads to improvement in systolic pressure of the depressed heart with incomplete left ventricular relaxation [80]. The reason for using 50 Hz frequency was due to the fact that the resonance frequency of the heart is estimated to be at around 50 Hz [71], which ensures maximum transfer of vibrational energy to the heart muscle as the impedance/resistance of the system is minimum at resonance. Application of mechanical vibration must only occur during the diastole phase of the heart cycle to avoid dampening of heart pumping force.

2.4.3. Mechanical Vibration Application Timing

Experiments show that administration of mechanical vibration during the systole phase of an ill heart leads to depressed left ventricular pressure during systole, which is detrimental to blood flow and heart muscle health [81].

In a study by Kikuchi et al. eight coronary perfused canine left ventricles were examined. Coronary flow was graded and controlled for achieving different degrees of ischemia. They applied 50 Hz, 2 mm amplitude mechanical vibration to the canines during diastole, with no vibration applied during systole. With higher degrees of ischemia the relaxation time of the heart would increase; however, the relaxation time showed decrease with application of vibration and was directly dependent on the amplitude of vibration. It was concluded that mechanical vibration applied during diastole of an ischemic heart improved the relaxation time during diastole [82].

In order to evaluate the effect of low frequency mechanical vibration on human heart, Takagi et al. [83] conducted experiments to understand whether this approach would improve systole pressure reduced by incomplete relaxation, and help in improving left ventricular relaxation of the heart muscle. Low frequency mechanical vibration is shown to be a coronary vasodilator in arteries with spasm [84], usually the case with heart attack patients [85]. They showed that application of 50 Hz, 1 mm amplitude mechanical vibration in an open-chest canine model increased the left ventricular pressure during systole and also accelerated the relaxation rate during diastole.

In a 46-patinet study, in order to study the efficacy of external mechanical vibration on left ventricular relaxation time, a vibrator was attached to the precordium of

human subjects, would vibrate at 50 Hz with 2 mm of amplitude and the device would only operate during diastole phase of the heart cycle. The experimental group included subjects with normal, hypertrophied (thickened heart muscle), and failing ventricle. In all the cases no change in heart rate and peak left ventricular pressure was observed, although the relaxation time showed reduction and was correlated with magnitude of vibration and also the impaired relaxation [67].

2.5. Summary and Conclusions

This chapter presented the first objective of this thesis with an in-depth overview of electrocardiogram and causes and physiology of the heart's electrical activity as well as discussion of various reperfusion methods for treatment of (coronary) thrombosis and the efficacy of mechanical vibration in disrupting thrombus. Also presented was safety of discussed methods.

In general, all the methods discussed in this chapter require presence of trained personnel and specialized equipment for commencement of the treatment. Pharmacological, ultrasound, and PCI methods all require access to specialized facilities and personnel: ultrasound thrombolysis can have very detrimental effects depending on the frequency, intensity, duration, and tissue characteristics. Heating of the tissue, adhesion, thrombosis are all the side effect of ultrasound thrombolysis, although mostly dependent on the characteristics the ultrasound wave. On the other hand, use of thrombolytic agents might lead to intracranial hemorrhaging and, consequently, death in most cases. PCI, although the gold standard for thrombolysis, requires access to cath labs and trained personnel.

Given the promising research work done in studying efficacy of mechanical vibration in disrupting blood clots, issues with availability of invasive methods such as percutaneous coronary intervention, and safety and availability concerns with use of therapeutic ultrasound for thrombolysis, it seems that use of low frequency mechanical actuation as a more available, noninvasive, adjunct thrombolysis method can open a new path towards, at least, initiation of pre-hospitalization for STEMI patients. To further pursue this goal, an electromechanical apparatus was developed to study the exact mechanism of actuation of the thrombosed vessel resulting from transcutaneous

application of mechanical vibration. Next chapter presents the research work, which is one of the objectives of this thesis, aimed at understanding efficacy of low frequency mechanical vibration in precipitating the lysis process in-vitro.

3. Low Frequency Mechanical Actuation Accelerates Reperfusion In-vitro[2]

This chapter presents the first objective of the thesis by describing an electromechanical setup used for performing in-vitro studies in order to study thrombolytic effects of low frequency mechanical vibration.

Yohannes and Hoffmann [79] studied the impact of mechanical vibrations applied through an attenuating barrier on recanalization of a thrombosed flow system. They hypothesized that localized transcutaneous low frequency mechanical vibration may serve as a safe and practical method to accelerate clot dissolution and aid in reperfusion. Nevertheless, the model for stenosis site in their study was a simple vessel deformation, rather than a narrowing; therefore, the actual lumen area remained unchanged. Furthermore, the pressure was gravitationally applied instead of creating a pressurized flow system. Finally, the actual frequency and amplitude of mechanical actuation was only assumed, not measured.

Effect of low frequency mechanical vibration on clearing thrombus has been a target of research. Wobser [73] demonstrated that mechanical vibrations delivered by an intragastral resonator can disrupt big blood coagulate. The Trellis Thrombolysis Catheter system is an FDA approved commercially available device which uses low frequency vibration to oscillate a wire within the catheter as an adjunct to fibrinolytic therapy to disrupt or help dissolve blood clots in treatment of deep vein thrombosis [78]. Furthermore, Folts [75] reported efficacy of direct external tapping on the stenosed site in clearing acutely thrombosed arteries in open animal models. Therefore, given the greater penetration depth of lower frequency mechanical vibrations, ease of actuation, and the absence of unwanted heat generation, application of low frequency mechanical vibration has been proposed as a safe and effective substitute to ultrasound that can be

---

[2] This chapter is based on published and unpublished (at the time of this submission) articles that the author of this thesis has been a major contributor [1], [2], [3], [4].

adjunctly used with fibrinolytic medications [3], [68], [79], [86]. In addition, simplicity of the procedure allows for its application in the field by minimally trained emergency personnel or even by a bystander immediately after the onset of symptoms.

It is hypothesized that application of mechanical stimulus can increase mixing of thrombolytic drugs and improve drug penetration to the occlusion site and thus allow lower doses during pharmacological therapy, leading to lower risk of intracranial hemorrhaging, which is especially interesting for patients with contraindications to thrombolytic drug use. While previous research has demonstrated the beneficial effect of mechanical actuation on accelerating reperfusion, the exact mechanism of actuation of the thrombosed vessel resulting from transcutaneous application of mechanical vibration has not been explored in detail. Vibration applied externally to the torso can both induce vibration of the blood carrying vessels and their deformation. This chapter presents a thorough investigation of various methods of mechanical actuation and the corresponding effect on accelerating reperfusion.

The goal of this work is to present an electromechanical apparatus to verify the effectiveness of various methods of low frequency mechanical actuation on accelerating reperfusion in-vitro. To this end, a stenosed, partly occluded heparinized flow system subject to arterial-like pressure variations with one of three actuation methods applied is studied: direct vibration of the occlusion site, deformation of vessel 20 mm proximal to the occlusion sites and deformation of a larger vessel 60 cm distal to the occlusion sites. It is hypothesized that vibration of vessels induces turbulence and thus promotes mixing and penetration of antithrombotic agents in the bloodstream which should lead to accelerated reperfusion. Vessel deformation on the other hand, induces local pressure variations that result in both increased mixing of drugs in blood and mechanical deformation of the blood clot and thus its accelerated disintegration. These hypotheses are herein investigated.

3.1. Materials and Method

The experiments described in this chapter were performed at the University of British Columbia Farm, 6182 South Campus Road, Vancouver, BC, Canada, in accordance with ethics approval 2009s0630.

3.1.1. Flow System

A schematic of the setup prepared for this experiment is shown in Figure 6. It is intended to model a stenosed arterial system subject to systemic pressures.
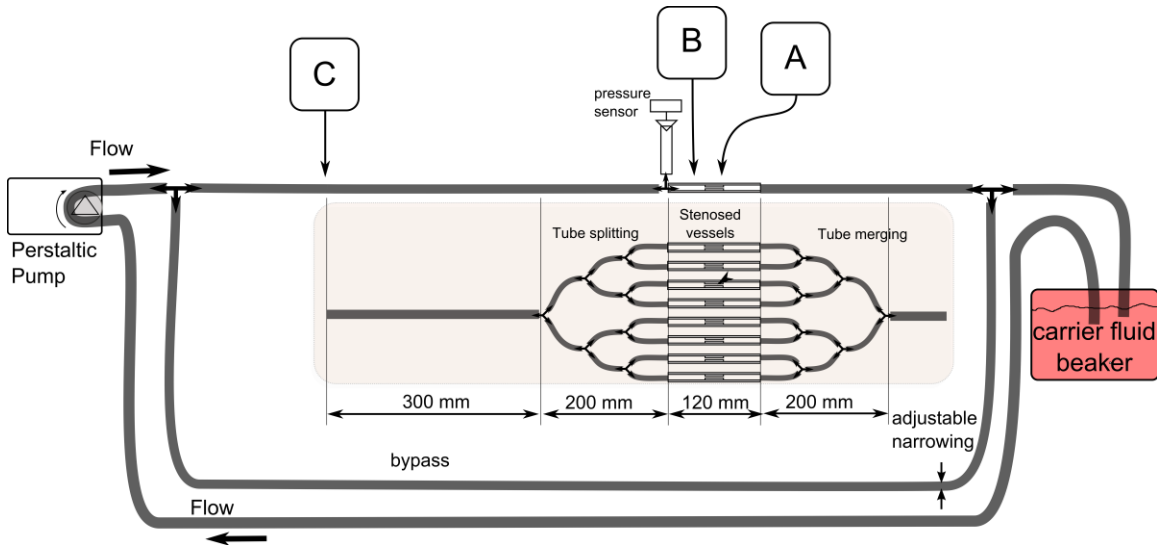
Figure 6. Schematic representation of the experimental setup used in this study with A, B, and C indicating the location of the corresponding actuation sites.

It consists of a heparinized flow system and one of three actuation setups. A rolling peristaltic pump (Manostat 72-300000) induces flow of a buffer fluid (heparinized saline solution) through a tubing system and through eight narrowings modeling the stenosis sites. The fluid was aggregated in a constant temperature bath (Vanlab, VWR Scientific, Inc) and kept at 37°C. For all experiments, a reference setup identical to the test setup but absent the actuation elements was used to provide a baseline result. The two setups (i.e. the reference and the actuated one) shared the buffer fluid in the beaker. Tubing types used to build the flow system were chosen to closely represent the size and the mechanical properties of human arteries. Types, dimensions, and properties of the tubing chosen for each element of the system are reported in Table 1.

A bypass was installed to provide a path around the occlusion sites to simulate more closely an actual obstruction in a living organism, where not all vessels are blocked simultaneously. The lumen of the bypass was adjustable to control the flow rate and the induced pressure. The total capacity of the tubing was between 165 ml and 200 ml

depending on the actuation system used. The fluid pressure was measured at the edge of one of the narrowings, as shown in Figure 1, using a pressure sensor (MPXM2053GS, Freescale Semiconductor, Inc, Austin, TX) connected to an instrumentation amplifier (INA110, Texas Instruments, Dallas, TX). A bi-axial MEMS accelerometer was used to measure motion induced at the actuation site, as described in Actuation section.

Table 4. Materials used to construct the flow system and the clot formation setup.

Vessel	Material	Length	ID (mm)	OD (mm)	Durometer	P/N	Brand
Connectors	Silicone	2 m	4.76	7.95	50 A	SMD-188A-25	X-MED
Clot formation	Silicone	30 m	4.76	7.95	50 A	SMD-188A-25	X-MED
Narrowing outside	PVC	120 mm	4.76	6.35	66 A	TMT-187A-50	Tygon
Narrowing inside	PVC	15 mm	1.59	4.76	66 A	TMT-187A-10	Tygon
Large tube	PVC	120 mm	9.5	12.7	55 A	8000-0120	Thermo Scientific

Data acquisition was done in the LabView environment using a custom made Virtual Instrument and a data acquisition module (NI USB-6009 DAQ, National Instruments, Austin, TX). Continuous data acquisition was performed throughout the experiment at a sampling rate of 1 kHz and the acquired data was stored in a text file on a personal computer.

During the experiment, flow in the system was regulated using the adjustable narrowing on the bypass to 2 ml/s and pressure varying between 25 kPa and 30 kPa (188 mmHg and 225 mmHg respectively).

Stenosis Sites

There was a total of 16 narrowings in the experimental setup used to model stenosis sites, eight for the reference side and eight for the actuated side. Each narrowing in a given setup was identical and created by inserting a 15 mm plastic tube element (narrowing inside in Table 4) into a larger plastic tube (narrowing outside in Table 1), as depicted in Figure 7. In order to insert the smaller tube, the larger tube was

cut in half and then glued around the smaller tube with cyanoacrylate glue (Loctite Pro Liquid) and sealed with a silicon glue-sealant (Dow Corning 732). Finally, the tube was cut into proper length and desired proportions before and after the narrowing with a total length of 120 mm. The resulting structure presented a 90% luminal stenosis. Installation of narrowings in the actuated and the reference systems was randomized. The internal diameter and length of the tubing was chosen to correspond to the internal diameter of the human coronary artery, based on the middle section of the right coronary artery [87].
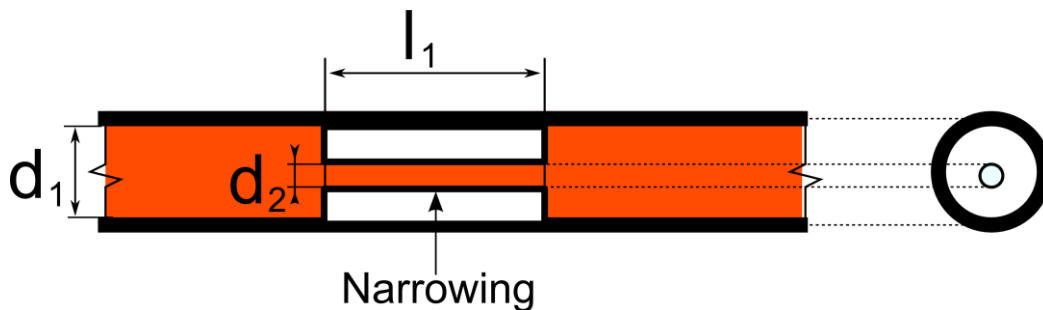
Figure 7. Stenosis site construction, where d1 = 4.76mm, d2 = 1.59mm and l1 = 15mm.

Buffer Fluid

The buffer fluid used in the system was a solution of 2000 Units of heparin (H3393, Sigma-Aldrich, Saint Louis, MI) in 1000 ml of 0.9% Sodium Chloride IV injection USP solution (Baxter International, Deerfield, IL). The fluid was brought to 37 ℃ prior to the experiment and kept at a constant temperature. Very low concentrations of 2 USP units of heparin per ml, much below the amount of heparin needed to prevent coagulation in whole blood which is 20 to 50 units per mL of whole blood were used [88].

Actuation

This work investigates the effect of various types of low frequency mechanical actuation on accelerating vessel reperfusion. In each experiment, one of the three actuation setups described below and depicted in Figure 3 was used and positioned as depicted in Figure 6. The resulting pressure at the narrowings with no actuation, pressure during actuation and the acceleration at the application site are shown for each of the three setups in Figure 8.

27

Setup A

The stenosis sites were directly vibrated at 5 g amplitude (2 mm displacement at 24 Hz). The mechanical stimulus was applied at the occlusion site and the lumen of the vessel was not directly deformed.

Setup B

Deformation was applied to the occluded vessel 20 mm before each stenosis site. In this case, the vessel was directly deformed and the clot was placed between the narrowing and the application site, but was not directly deformed. The vessel was reaching 80% focal occlusion at the deformation site during actuation.

Setup C

Deformation was applied to a vessel with an inside diameter larger than the one of the stenosed vessels, corresponding to the diameter of human aorta in the abdominal region [89]. The actuation site was placed 60 centimeters from the stenosis site. In this case, no mechanical stimuli was applied directly to the narrowings. The amplitude of deformation applied to the large vessel was equal to 3 mm.

In all the three cases, the mechanical movement was generated by a DC motor (Unionwell LW2920D120) with shaft extending from both ends coupled with an aluminum beam through a lever system implying a quasi linear motion, as depicted in Figure 8. The motor location could be adjusted horizontally and vertically to accommodate various configurations of distances.

The aluminum beam was either coupled with a free moving narrowing (setup A) or induced a direct deformation of the vessel immobilized by a wooden spacer (setups B and C). In cases A and B, the actuation was close to the blood clot, and in the case C remote from the clot. The induced displacement was constant independent of frequency.

The actuation frequency was controlled through the DC voltage supplied to the motor and observed using an accelerometer (AD22286, Analog Devices, Cambridge, MA) mounted on the aluminum beam. For all the three experiments, the actuation frequency was between 20 Hz and 24 Hz.
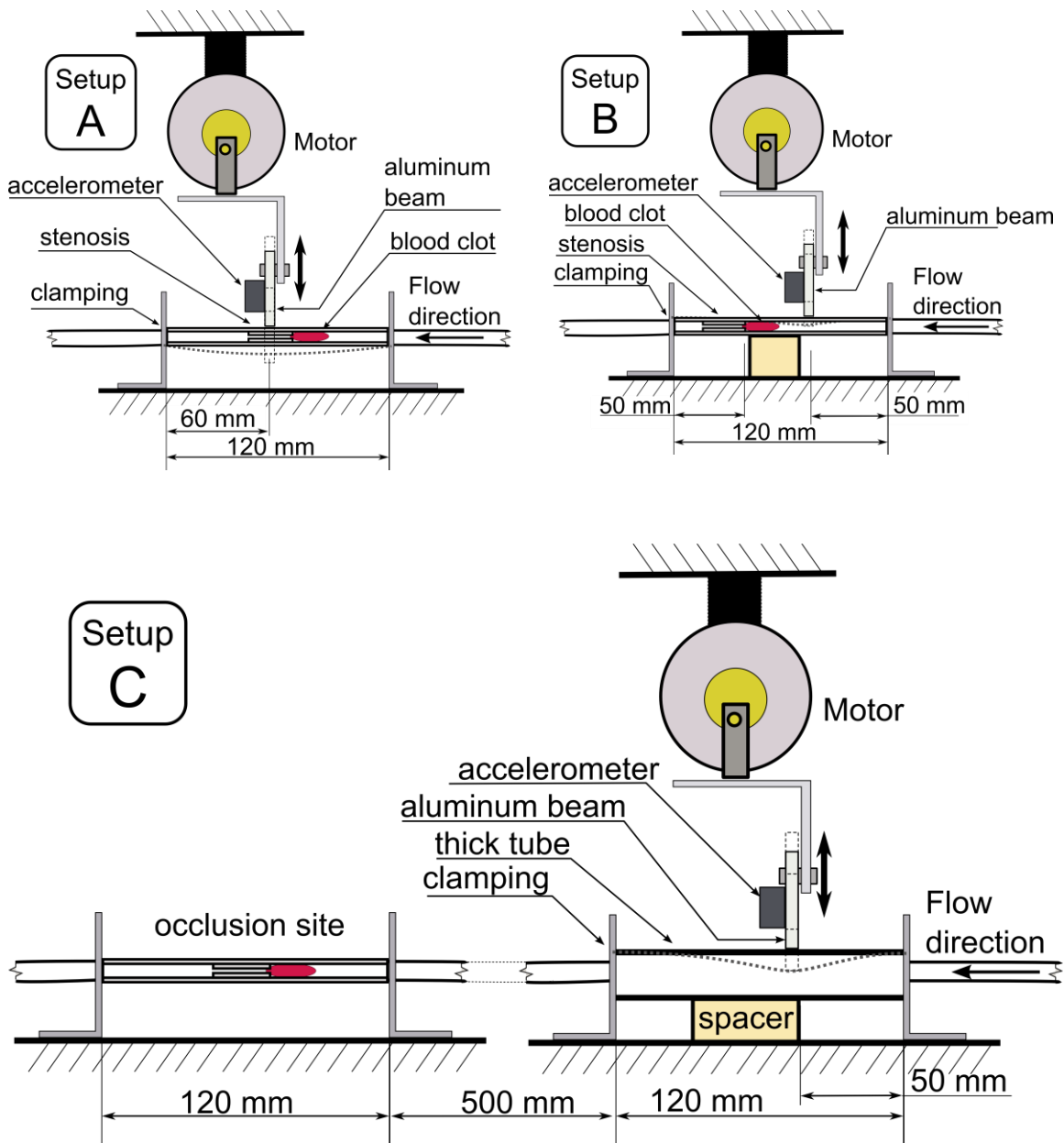
Figure 8. Actuation setups used in this experiment: setup A where the stenosis sites are directly vibrated (a); setup B where mechanical deformation is applied to the vessel proximal to the stenosis site (b); and setup C where mechanical deformation is applied 60 cm from the stenosis site to a larger vessel (c).

A photograph of the complete implementation of the setup used in this work is depicted in Figure 9.
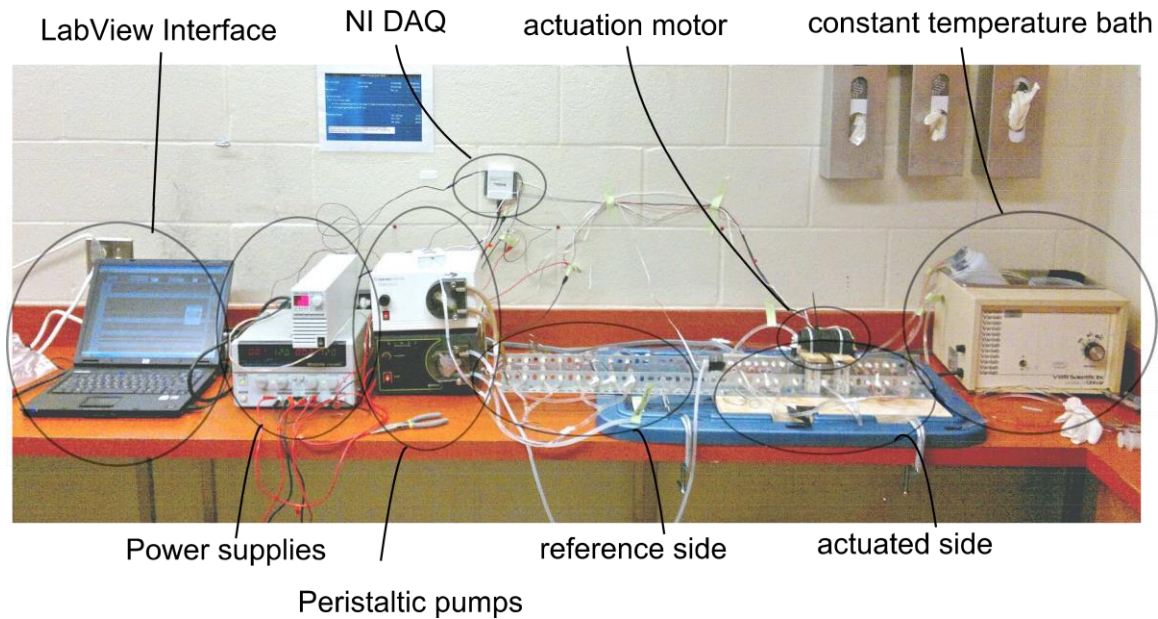
Figure 9. Photograph of the experimental setup used in this work.

3.1.2. Experimental Procedure

A total of 198 occlusions was successfully tested in all experiments with 27 occlusions subject to direct vibrations, 56 subject to local vessel deformation, 37 subject to remote vessel deformation and the remaining 78 providing the baseline result. A total of 28 experiments was discarded due to occlusion instability (immediate perfusions).

Clot Preparation

Whole blood was collected from the left jugular vein of a sheep (female, Ovisaries, Suffolk breed) elevated in a controlled environment at UBC Farm. Blood was drawn under standardized conditions into a 60 ml syringe and immediately distributed into sterile silicon tubing (ID 4.76 mm), sealed inside a double zip-lock bag and placed into a water bath held at 37°C. Ninety minutes from blood extraction, the clotted blood was removed from the bath and inspected visually for retraction. The retracted clot was pressed out of the silicon tube and verified for uniformity. The long columnar clot was then cut into 15 mm pieces and each piece was weighted separately using a digital scale (VB-302A, Virtual Measurements & Control, Santa Rosa, CA). The resulting distribution of clot weights in each experiment is detailed in Figure 10 to Figure 12. Cut and weighted clots were immediately inserted into the flow system by disconnecting the

narrowings separately one by one at clamping, placing a clot inside the tube with a spatula and subsequently flooding it with the fluid from the beaker and reconnecting the narrowing. Upon re-pressurization the clots occluded the closest stenosis site. Special care was taken to remove all air bubbles from the system prior to pressurizing and not to damage the clots mechanically.
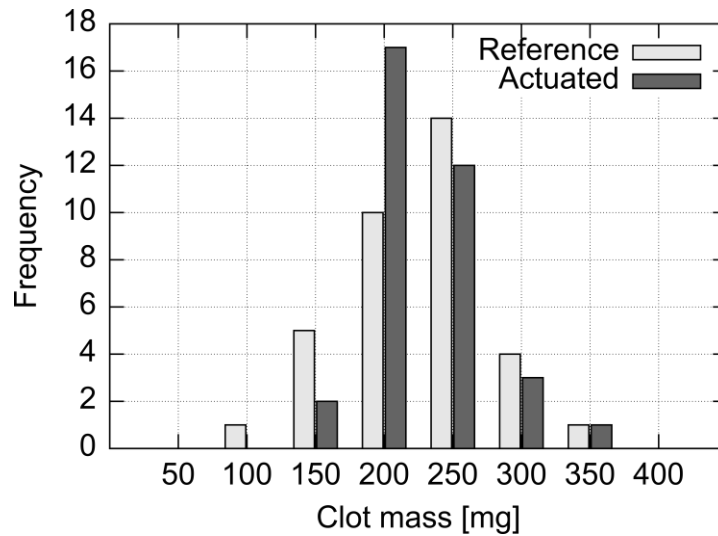
Figure 10. Setup A.
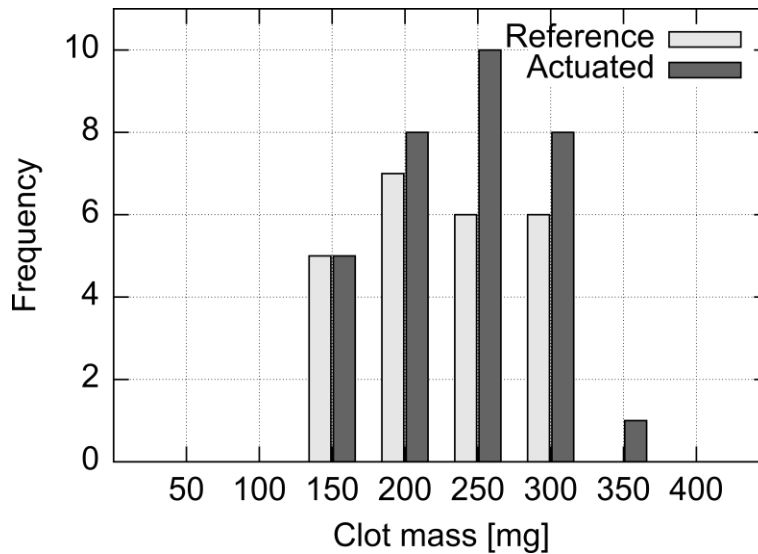
Figure 11. Setup B.
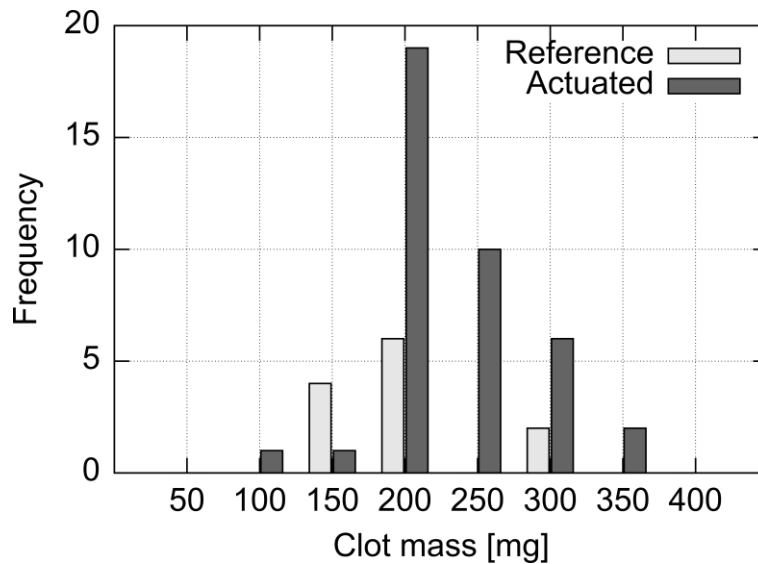
Figure 12. Setup C.

The clot distribution between the stenosed channels and the reference versus the actuated setups was randomized.

Flow System

In order to verify occlusion stability, after insertion of all clots, the system was pressurized using the peristaltic pump for 120 seconds without applying actuation. Narrowings where clots perfused within this period were clamped and labeled as immediate perfusions. The reference and the actuated setups were functionally identical during this period. Throughout all the experiments, 12.23% of clots perfused prior to actuation (immediate perfusions).

Actuation

After the initial test for 120 seconds, the actuation setup was activated. Perfusions were detected through abrupt reduction of the buffer fluid pressure at the narrowings. Each perfused narrowing was immediately clamped to maintain constant pressure in the system. The time to perfusion was noted from the activation of actuation. After 20 minutes from the start of actuation, the system was stopped and all the remaining clots (that did not perfuse) were removed, drained and re-weighted.

3.2. Experimental Results

The three setups described in the previous section were evaluated for their efficiency in accelerating reperfusion of occluded vessels. Setup A

3.2.1. Setup A

In this case, the stenosis sites were directly vibrated. The pressure variations at the occlusion sites both prior to actuation and during actuation along with acceleration during actuation are presented in Figure 13. It can be seen that the mechanical vibrations have minimal impact on the fluid pressure at the narrowings.

Out of 35 tests, only 1 perfusion occurred within the duration of actuation (20 minutes) after 13 minutes on the actuated side resulting in a TIMI 2 flow. Therefore, only the change in the clot masses was evaluated. Figure 14 presents a histogram of clot mass changes evaluated as the difference between the clot mass post experiment versus the clot mass prior to the experiment. The average mass change is -15.89% (σ = 26.4%) for the reference system and -12.16% (σ = 19.1%) for the actuated system. The fact that mass of some clots increased may be due to water absorption, or imperfect soaking method employed.

3.2.2. Setup B

In this case, a direct mechanical deformation of the vessel was imposed near the stenosis site. Figure 15 presents the pressure variations prior to actuation and during actuation along with acceleration at the application site while using setup B to impose vessel deformation. It can be seen that vessel deformation is inducing significant pressure variations at the occlusion site and thus at the blood clot. Contrary to the case where direct vibrations were applied, in the deformation case over 95% of the narrowings were successfully perfused resulting in a TIMI 3 flow within 11 minutes of the onset of actuation while only two perfusions (5.3%) occurred on the reference side within 20 minutes.
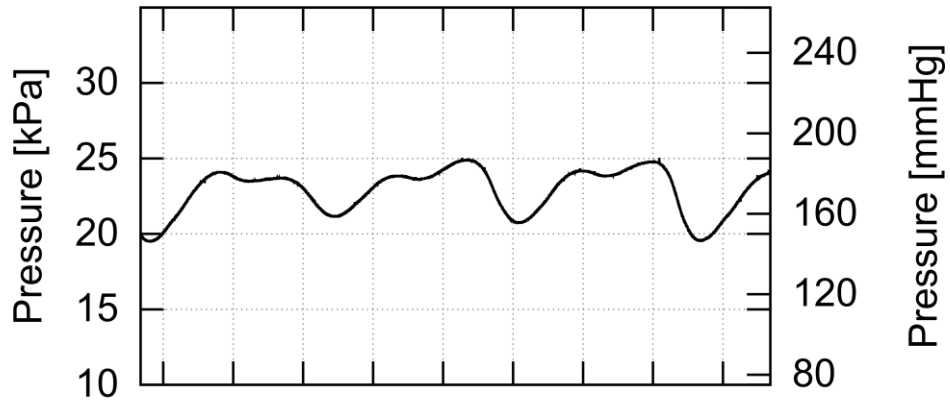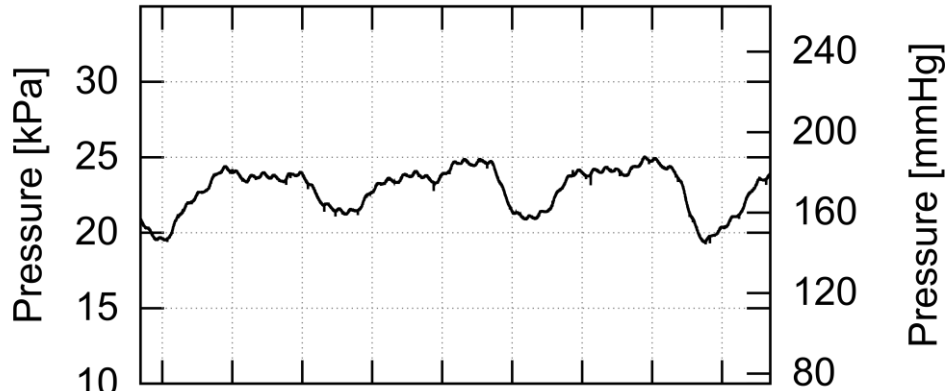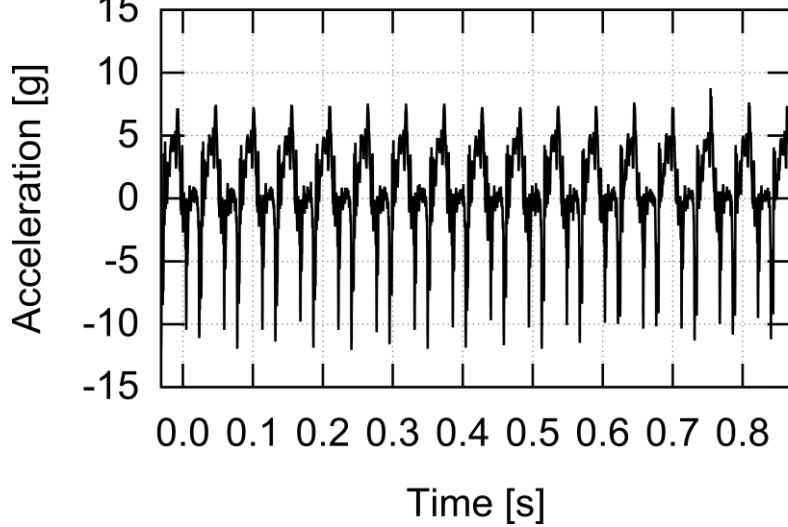
Figure 13. Pressure in the flow system with and without mechanical stimulus and acceleration measured at the actuation site for setup A.
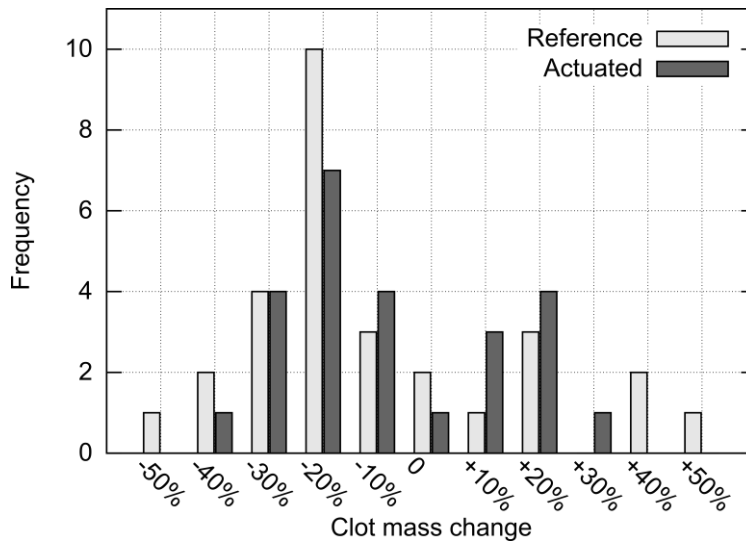
Figure 14. Clot mass change post experiment versus prior to experiment.

3.2.3.   Setup C

In this case, a direct mechanical deformation was imposed 60 centimeters from the stenosis sites to the fluid carrying vessel with a larger ID.

Figure 16 presents the pressure variations at the narrowings with and without actuation and the acceleration at the application site while using setup C. It can be seen that as in the case of using setup B, there are significant pressure variations at the occlusion site induced by the actuation. As a result of actuation induced using setup C, over 95% of narrowings perfused within 16 minutes of application resulting in a TIMI 3 flow, whereas there was no perfusion on the reference side. Only one occlusion out of 37 actuated narrowings did not perfuse within 20 minutes.

Setups B and C have proven to be the most efficient in accelerating reperfusion. Figure 18 presents distribution of times to perfusion for the actuated side for those setups [4]. The average time to perfusion was 3 minutes 50 seconds for setup B and 4 minutes 27 seconds for setup C. Figure 17 summarizes the patency rate for all the experiments. It can be seen that setups B and C have very similar distribution of times to perfusion which indicates that deformation of a large vessel distant from the occlusion

35

site is equally efficient as deformation of vessels very close to the occlusion site. On the other hand, patency rate for setup A is very close to the baseline.
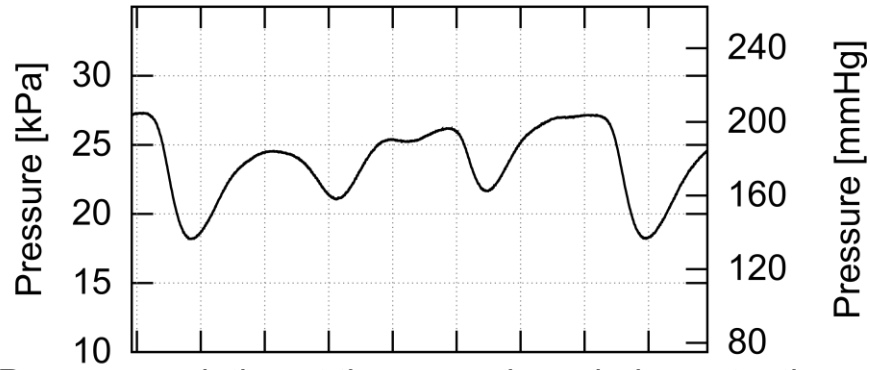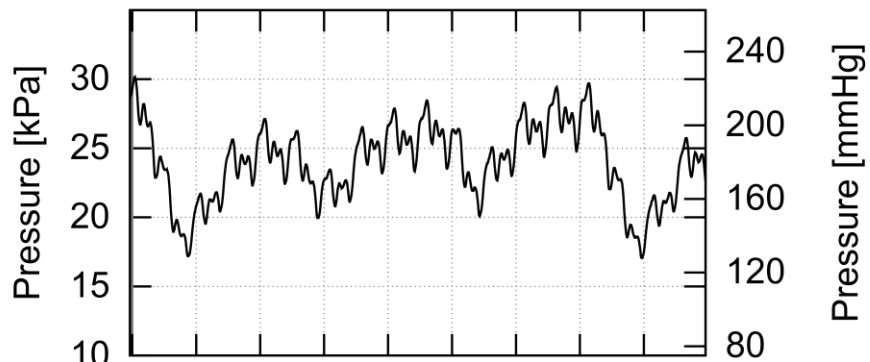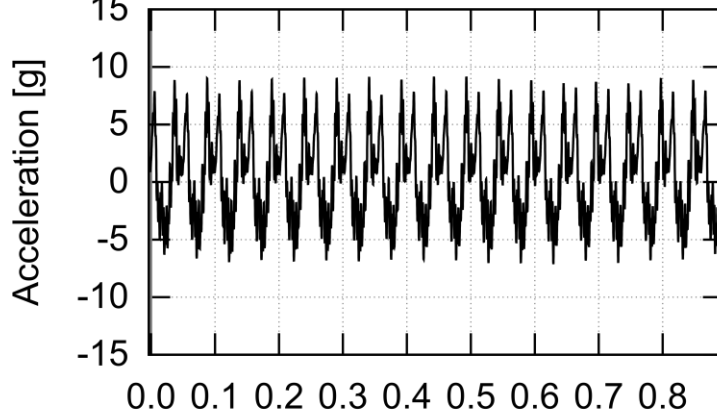
Figure 15. Pressure in the flow system with and without mechanical stimulus and acceleration measured at the actuation site for setup B.
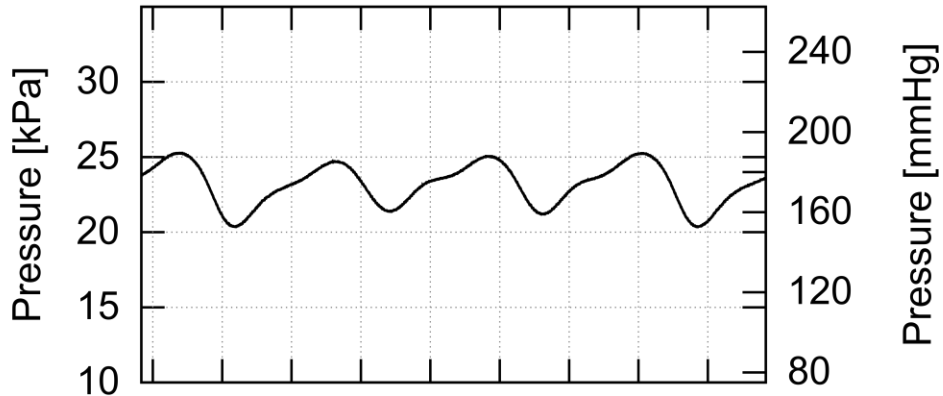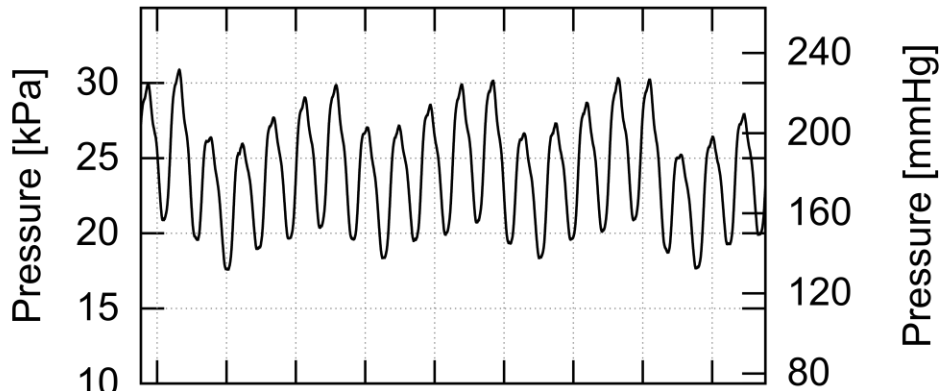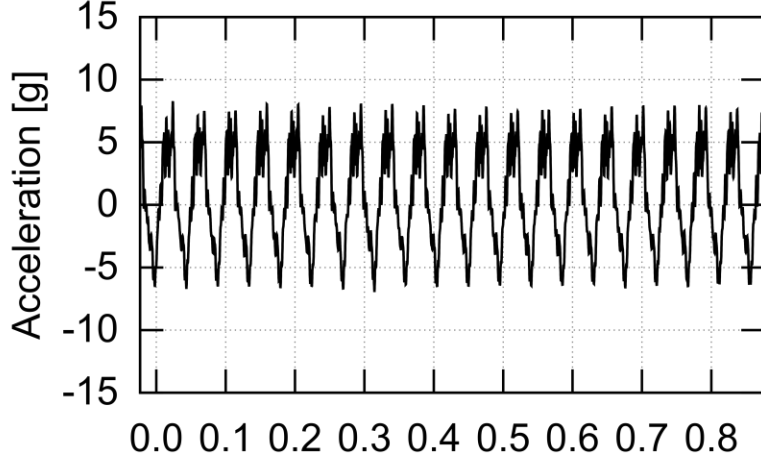
Figure 16. Pressure in the flow system with and without mechanical stimulus and acceleration measured at the actuation site for setup C.
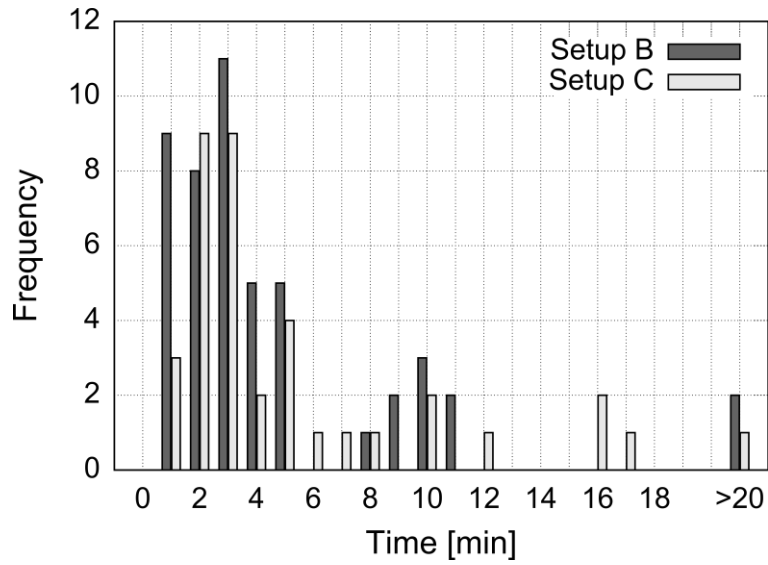
Figure 17. Reperfusion rate among the tested setups for the first 20 minutes of actuation.
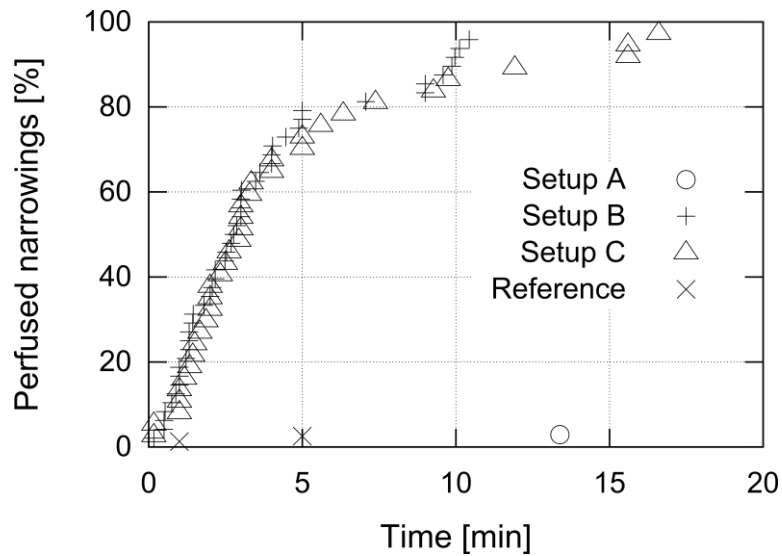
Figure 18. Histogram of times to perfusion while using setup B or setup C to induce vessel deformation.

3.3. Discussion

This study evaluates the effectiveness of various actuation methods in accelerating re-perfusion of occluded vessels in an in-vitro model. The experimental

results show that while keeping pressure in the system at systemic levels, 95% of occlusions perfuse within 11 minutes of application in the case of a mechanical deformation applied at the occlusion site and 95% of the occlusions perfuse within 16 minutes of application if a mechanical deformation is applied 60 centimeters from the occlusion site. Contrary to indications from previous publications, it was demonstrated that direct vibration of the occlusion sites has no significant impact on accelerating reperfusion. The notion that mechanical actuation positively affects the speed at which a blood thrombus disintegrates was suggested in previous publications. However, this study is the first to systematically evaluate the various proposed application methods. The three approaches examined in this study apply either displacement or deformation at specific frequencies.

It was theorized that vessel vibration would induce more mixing in the buffer fluid and promote clot lysis, but the experimental results prove otherwise, as no significant improvement in reperfusion time was observed when occluded vessel was directly vibrated.

It may be due to the very narrow lumen of the vessels and the lack of pressure waves that would deform the clot and stimulate mixing. On the other hand, it was demonstrated that pressure variations induced by vessel deformation drastically improve reperfusion rate. Mechanical stimuli create pressure waves that are transferred by the fluid to the occlusion site. If deformation is applied distant to the occlusion site, the amplitude of pressure variations is reduced due to compliance of vessels (albeit low for aortic walls). Still, as the blood is a non-compressible fluid, the pressure waves are usually well transferred through the circulatory system of a living organism [90]. Fluid viscosity and its traction on the vessel walls imply pressure non-uniformity in the lumen of the vessel, as depicted schematically in Figure 19, which can have further positive impact on clot dissolution. If the central part of the thrombus is subject to higher forces than the outer parts, then clot deformation is more prominent and lysis is further promoted. Furthermore, arterial thrombus is often characterized by presence of alternating layers called Lines of Zahn [91], [92], [93]. Lines of Zahn are characteristic of thrombus formed at rapid arterial blood flow, like the one in the coronary arteries, where laminations are produced by deposition of platelets and fibrin (pale layers) and red blood cells (dark layers). A blood clot presenting such a layered construction would be much

more prone to deformations induced by the non-uniform pressure distribution applied at the front of the thrombus.
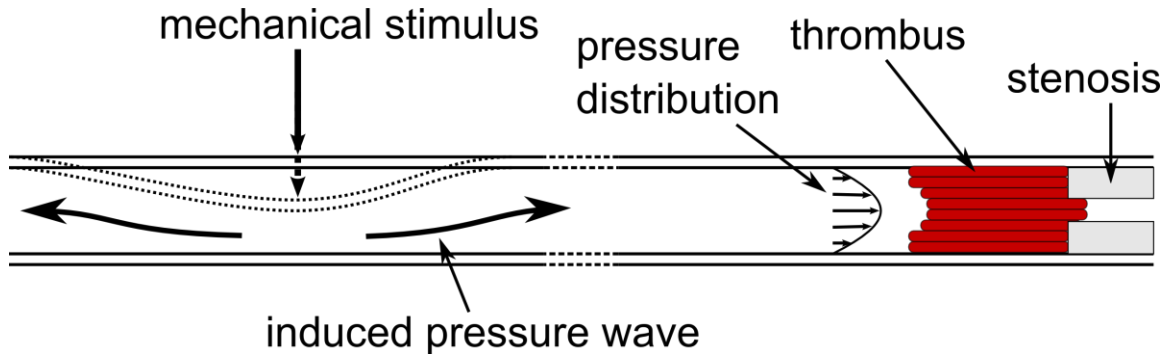
Figure 19. Schematic representation of pressure distribution in a vessel induced by vessel deformation distant from stenosis site.

During these experiments, it was observed that after perfusion the blood clot is split into multiple long and narrow fragments that easily pass through occlusion sites when recirculated in the system. It can be argued that in-vivo such fragments may occlude further arteries leading to a "no reflow" situation known from unsuccessful angioplasty procedures. Nevertheless, in the presented method, the fragments of disintegrated clot are sufficiently large not to spread across all capillaries in the myocardial muscle. Therefore, any displacement of the occlusion site down the bloodstream would enhance delivery of the oxygenated blood thus reducing the extent of myocardial muscle death and increasing the chances of patient survival.

The fact that even distant vessel deformation accelerates clot lysis opens way to application of mechanical stimuli away from the chest area of patients suffering from acute myocardial infarct. Furthermore, as application of the stimulus directly over the occlusion site is not critical, contrary to ultrasound, lack of exact knowledge of the occlusion site location does not exclude efficient treatment, as long as a major artery is targeted. A feedback system, where a high frequency blood pressure monitor would detect pressure waves in an easily accessible artery (e.g. thyroid), could be used to verify the efficiency of application. Thus, such method could be effectively applied in the field using a simple external massager device operated by minimally trained personnel. Finally, as the chest area is very sensitive, any prolonged mechanical deformation is

undesirable, contrary to the more robust abdominal section containing large blood carrying vessels, like the aorta. In order to induce a displacement of 3 mm in amplitude at the aorta level, a significant displacement has to be applied at the surface of the body. The tests indicate that peak to peak displacement of 8 mm at 30 Hz applied using a commercial massager (Max F-209, Brookstone, Merrimack, NH) can be tolerated in the abdominal area for at least 20 minutes with an application force of 50 N. The in-vitro results presented in this chapter indicate that such application would be sufficient to promote reperfusion in case of acute myocardial infarction.

3.4. Summary and Conclusion

The presented study addressed the first objective of this thesis and evaluated the effectiveness of various types of low frequency mechanical actuation in accelerating reperfusion. A simplified in-vitro model of bloodstream during myocardial infarction was created employing a stenosed, heparinized flow system subject to systemic levels of pressure. Complete reperfusion resulting in TIMI 3 flow in 95% of cases after 11 minutes of vessel deformation at the occlusion site and after 16 minutes of vessel deformation 60 centimeters from the occlusion site was observed, while there was only 2.3% perfusions in the reference system within 20 minutes. The presented results demonstrate that low frequency deformation of blood carrying vessels can be used to accelerate reperfusion, which is of great importance in helping patients suffering from acute myocardial infarction. A simple device can be constructed to apply external mechanical stimulus in the abdomen area or any other major distal artery of patient's torso that induces deformation. Such method would be non-invasive, safe, inexpensive and suitable for use by inexperienced emergency personnel in the field.

Next chapter deals with architecture and design of a proof-of-concept apparatus for application of mechanical vibration on the chest of STEMI patients and examining major contributing factors to the efficacy and safety of the device.

41

4.   Diastolic Timed Vibrator[3]

This chapter addresses the second objective of this work by introducing a proof-of-concept device that can induce mechanical vibration on the chest of STEMI patients during the diastole phase. Also addressed are methods to increase the efficacy and major contributing safety factors.

Due to the slow action and possible complications related to pharmacological thrombolytic therapy and not infrequent delays in transportation to PCI centers, there is an ongoing interest in finding alternative, noninvasive, complimentary therapies to assist in increasing the efficacy of treatment both in the pre-hospitalization and the hospitalization phases in dealing with acute coronary syndromes. One of the major factors in increasing the survival rate of patients suffering from acute coronary ischemia is the speed of intervention. The two major techniques currently in use, pharmacological and interventional, can be employed to recanalize coronary arteries, but the former is slow acting and often leads to incomplete reperfusion, while the latter requires specialized personnel in a hospital with a cardiac catheterization laboratory.

Previous studies show that delivery of ultrasound waves to the occlusion site accelerates thrombolysis [34], [48], [94], and also enhances penetration of lytic enzymes into the thrombus [52], [53]. In order to evaluate the possible use of transcutaneous ultrasound accelerated lysis, an investigation was carried out to assess the safety of the method and it was concluded that excessive tissue heating is a possible complication and pulsed ultrasound should be employed [95]. Although animal studies have shown ultrasound to be effective in achieving TIMI 3 flow, recent clinical trials have failed to prove its efficacy in disrupting blood clots or facilitating reach of clot busting agents to the occlusion site, even at lower ultrasound frequencies [34], [96]. Finally, Wright et al. [46] believe that high-intensity focused ultrasound can be used to achieve partial

---

[3] This chapter is based on published and unpublished (at the time of this submission) articles that the author of this thesis has been a major contributor [1], [2], [3], [4].

reperfusion; however, this approach would be reliant on a highly trained technician to target the therapy (not likely available in first line emergency scenarios) and could potentially lead to internal bleeding.

In addition to the ultrasound and the mechanical vibration approaches, Torno et al. [97] reported that magnetically guided tPA loaded microspheres can significantly accelerate the lysis process. Although very promising, this technique cannot be used by minimally trained personnel and requires knowledge of infarct location. Furthermore, this technique requires specific tools that would add to the final cost and reduce the availability of the solution.

This chapter introduces a novel method for pre-hospitalization treatment of patients with acute coronary ischemia that can be safely applied by a minimally trained individual prior to or during patient transportation to hospital. It consists of applying low frequency mechanical vibration to the left intercostal space of patient's chest during diastole of the heart cycle to induce vibrations on the heart and thus on the coronary arteries. Mechanical vibration stimulates mixing of blood which improves drug delivery to the occlusion site, applies mechanical force on the clot leading to, potentially, its faster dissolution and finally acts as a strong vasodilator in case of spasms. The principle of operation and the architecture of the Diastolic Timed Vibrator, vibration pattern generator and active braking methods are introduced in this chapter. Experimental results demonstrate the functionality of the DTV device and pave way for in-vivo tests leading to clinical confirmation of the proposed method.

4.1. Method

The objective of the proposed method is to provide pre-hospitalization treatment to heart attack patients within the recommended door-to-needle and door-to-balloon time frames. Previous research suggests that diastolic timed mechanical vibrations at frequencies around 50 Hz improve the coronary blood flow (CBF) as well as the left ventricular performance in subjects with either normal or impaired CBF [98]. Furthermore, tension and spasm in the coronary arteries can be relieved by application of low frequency vibrations to the chest wall which can potentially help in vasodilating the arteries [85]. Low frequency vibration is therefore beneficial even without the presence of

any thrombolytic agents in patients' system [74]. The goal is to introduce the Diastolic Timed Vibrator (DTV), a device implementing a treatment method consisting in applying low frequency mechanical vibrations to the chest of myocardial infarct patients during the diastole of the heart cycle so as to help in rupturing and/or dissolving the thrombus, increasing thrombolytic agent penetration, as well as improving the overall coronary blood flow. In the absence of clot-busting drugs during the door-to-needle period, DTV can be used as a standalone treatment method, but it can also complement the thrombolytic drug therapy for improved reperfusion. Furthermore, the DTV can be used at hospitals where the STEMI patient is being prepared for the catheterization procedure to reduce the risks of myocardial muscle cell death.

In order to facilitate myocardial relaxation and to minimize additional stress induced to the weakened heart muscle, vibrations, which may have a negative effect on the strength of heart contractions, must be periodically timed to match the diastolic phase of the heart cycle in avoidance of at least the isovolumetric contraction and early to mid-phase of systole, which are the phases responsible for generating left ventricular pressure and the vast majority of cardiac output, respectively. This timing is also believed to improve the contractile strength of the heart muscle [67]. In order to stop vibrations during the systole, a modified version of the Hamilton and Tompkins ECG processing algorithm [99], [100] can be used to detect the onset of the QRS complex as soon as possible. Therefore, the DTV apparatus can detect the start of systole by real time monitoring of patient's ECG and initiate and cease vibrations at the right timings. Gill et al. [76] suggest at least a 10 ms interval between the stop command and the actual cessation of vibrations to avoid vibration overspill into the systole. Additionally, in order to maximize the diastole interval coverage with the mechanical vibrations, DTV must be able to start the application of vibrations within the shortest time following the start command. To this end, various methods of efficient starting and stopping of the DTV motor are presented and discussed in this chapter.

Finally, determination of the most effective vibration frequency value is of paramount importance. In order for the DTV to achieve the best possible outcome, the vibrations should be administered over frequencies between 40 and 60 Hz as it is where the resonance frequency spectrum of the myocardium falls [71]. However, the optimum frequency range is subject dependent and thus cannot be established a priori.

44

Therefore, in this chapter various vibration frequency patterns that can increase the method efficacy are presented and evaluated.

4.2. System Architecture

The system described in this chapter is the platform and a proof-of-concept approach for implementation of a diastolic timed vibration apparatus. It was mostly made of off-the-shelf modules (instead of complete devices). Figure 20 shows the proposed implementation on high level of abstraction.
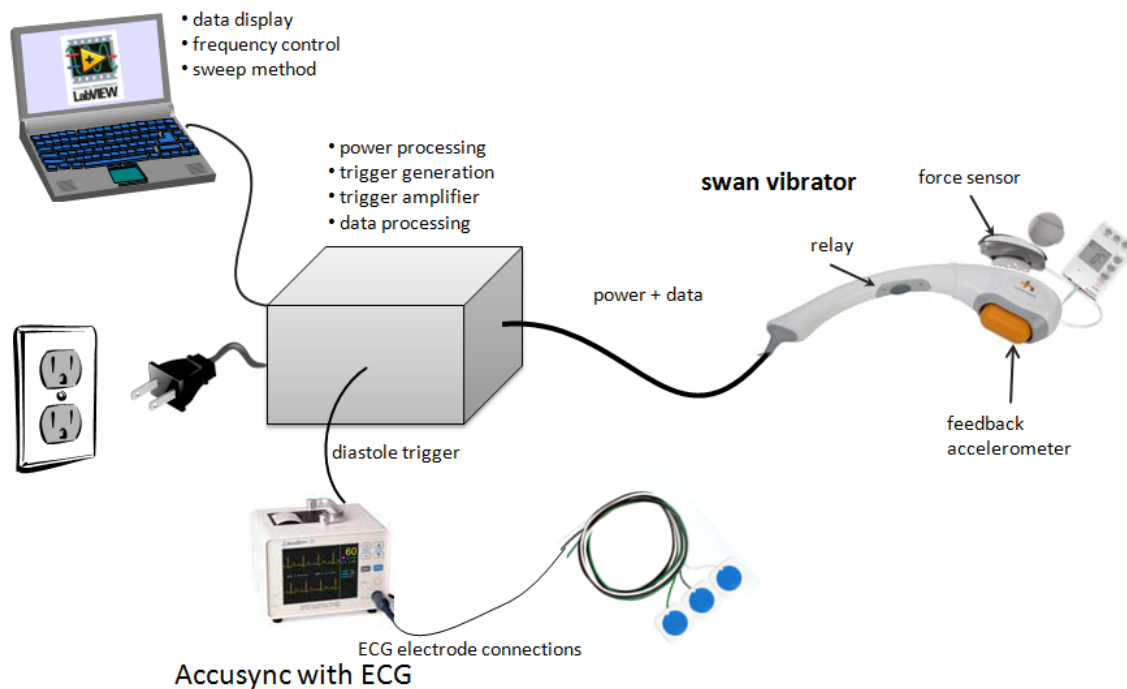
Figure 20. Building Blocks of the DTV System.

Figure 21 shows a simplified version of the DTV system/apparatus [4]. The main feature required from the system is to generate required vibrations in synchronism with the heart cycle. In order to achieve this goal, a standard therapeutic off-the-shelf massager was used to apply vibrations to the chest. It is worth noting that as the displacement of the massager head is invariable with frequency; the amplitude of the generated acceleration increases with the square of the generation frequency.

Frequency and amplitude of vibrations would then be measured by means of a MEMS feedback accelerometer installed on the inner wall of the massager head. The frequency of vibration was tuned by an adjustable power supply controlled by DTV.
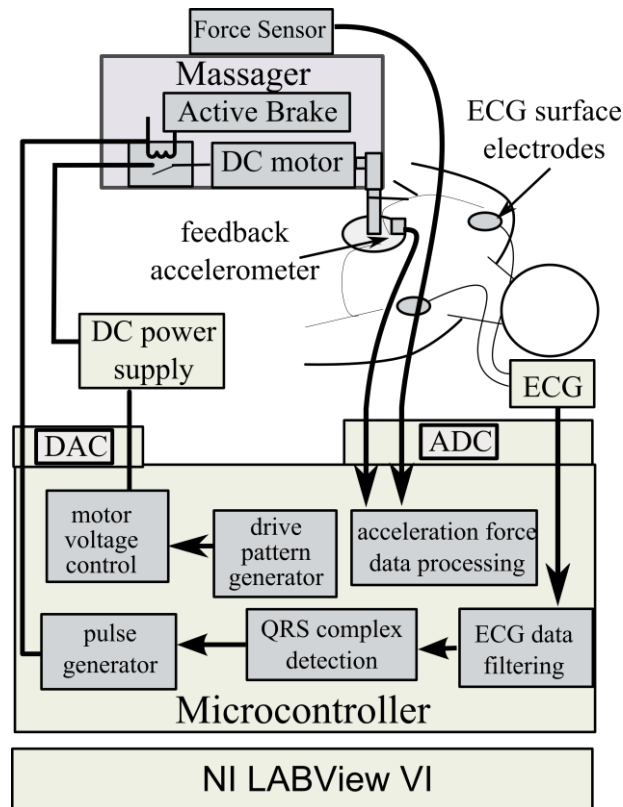
Figure 21. Simplified block diagram of the DTV system architecture.

A power relay, internal to the massager, was used to interrupt power delivery to the DC motor in the massager and engage an active braking device to stop generation of vibrations. An analog ECG signal acquired from the patient was amplified and filtered by the DTV device and subsequently used for QRS complex detection using the custom algorithm. A closed loop feedback system was used to control the relay and thus the timing of vibration generation. A force sensor was mounted on the device to measure the engagement force applied by the device operator. A feedback signal was given to the operator to inform him/her of whether the application force was adequate. A microcontroller was chosen to implement the control logic and the ECG processing algorithms. A PC was used to monitor and display data through a LabView virtual instrument and also interface with the rest of the system. Some elements of the user interface were implemented on the PC as well.

4.2.1. System Specifications

Massager Unit

Human Touch Swan Softouch massager (P/N: HT-1280, shown in Figure 22) was used for generating vibrations applied to the chest of subject. HT-1280 is a CSA[4] approved two-speed muscle massager that operates with 120 Vac. The internal rectifier circuitry was removed so that a high-voltage controllable DC power supply could be used for vibration frequency control. Massager's maximum frequency of vibration was measured to be around 40 Hz with 110 Vdc input. Figure 23 shows the modified version of the Human Touch massager.

Figure 22. Human Touch HT-1280 Massager.
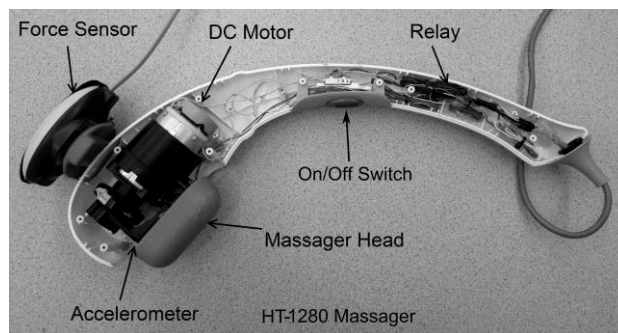
Figure 23. Modified version of the massager.

Force Sensor

JTECH Medical Commander Muscle Tester was used as the force sensor for the DTV system. Commander Muscle Tester is composed of a compact dynamometer and a

---

[4] C22.2 No. 69-92: Motor-operated appliances (household and commercial)

commander unit that is used for storing and displaying force measurements. In order to easily measure the application force, the dynamometer was mounted on the top of the massager unit where the operator could directly press on when applying treatment. Figure 24 shows the force sensor described.

Figure 24. JTECH Medical's Commander Muscle Tester.

ECG Trigger Monitor

The ECG trigger monitor used in this phase of the project was the AccuSync 72 – shown in Figure 25 – from AccuSync Research Medical Corp. AccuSync 72 is designed for gated cardiac studies where automatic R Wave detection is necessary.

Main features of the device include:

- 16-color TFT display

- Operation with 3 or 5 ECG leads

- R trigger output – 5 V TTL/CMOS at R detection, 0 V otherwise

- ECG analog output

Also, the AccuSync 72 device can be powered with an external power supply or a built-in rechargeable battery.

Relay

In order to stop the massager from vibrating during the systole phase, a relay was used to disconnect the 120 Vdc input voltage to the massager. Panasonic APE30006 slim power relay fulfills this requirement and was installed inside the massag-

Figure 25. AccuSync 72 ECG Trigger Monitor.

-er unit for improved system integration. APE30006 is a 6 A, 250 Vac relay with 3.96 V to 6 V pick-up voltage. Nominal operating current and coil resistance are 28 mA and 212 Ω, respectively. The engage and release times of the relay – at nominal 6 V pick-up voltage – are 8 ms and 4 ms, respectively. These timings can add additional delay to the motor start-up and stop times; their impact could be reduced by using fast acting relays or solid state switches.

Accelerometer

The accelerometer in the system was used to quantitatively measure the frequency and amplitude of the applied vibration. The requirements for the DTV system are:

- Vibration stroke: 6 mm max.

- Vibration frequency: 60 Hz max.

Based on the above criteria, the accelerometer range was determined by the following equation:

$$a = -A\omega^2 sin\omega t$$

Where a [m/s^2] is the acceleration, A [m] is the displacement amplitude, and ω [rad/s] is the frequency of vibration. Thus, the maximum acceleration amplitude is equal to:

$$|a| = A\omega^2 = 0.003 \times (2\pi \times 60)^2 = 426.37 \, ^m/_{s^2} = 43.48 \, g$$

The selected accelerometer must have an acceleration range of ~$\pm$44 *g*, and a minimum guaranteed bandwidth of 60 Hz. The sensitivity of the accelerometer must be sufficient to enable measurements of acceleration in m*g* range.

The accelerometer selected – Analog Devices ADXL278 – not only satisfied but also surpassed all the requirements above. It features:

- Range: (X-axis/Y-axis) ±70 g/±35 g

- Bandwidth: 360 Hz min.

- Sensitivity: (X-axis/Y-axis) 25.65 mV/*g*, 52.25 mV/*g*, ratiometric

In order to make accurate measurements and also for better system integration, the accelerometer was glued vertically to the surface of the massager head (Figure 26). All the required components were soldered on the accelerometer in order to avoid use of additional prototyping board.

Mounted Accelerometer
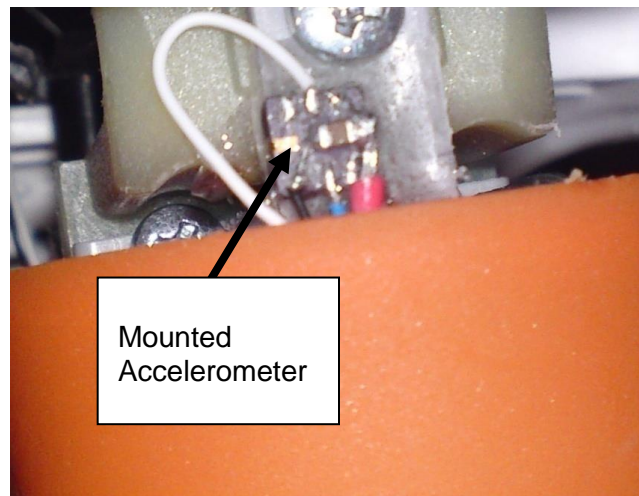
Figure 26: Mounted Accelerometer.

After mounting the accelerometer to the massager head, a simple test was made to measure the frequency of vibration. Figure 20 shows the waveforms for both X and Y

direction acceleration. As shown, the massager head has the most vibration along the Y axis whereas the X axis shows very minor acceleration. The frequency of vibration is ~40 Hz. Maximum acceleration along the X axis is ~9.9 g whereas along the Y axis it is 20 g. Figure 28 shows the measurement done for determining the time from the onset of initiation of stop command to the next start command, which is ~170 ms.
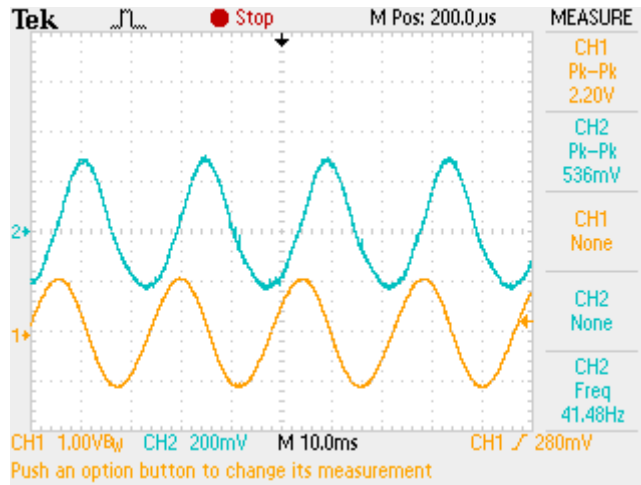
Figure 27. Accelerometer Output: CH1 and CH2 display the Y and X axes outputs, respectively.
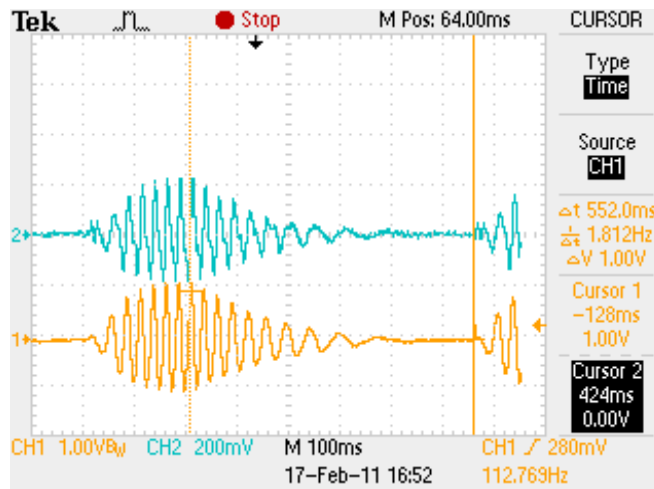
Figure 28. Measurement of Stop - Start Time.

Data Acquisition Devices

NI – 6009 DAQ device, shown in Figure 29, was used for acquiring accelerometer output, ECG waveform, R trigger, and also for controlling the relay built

into the massager. NI – 6009 is a USB bus-powered multifunction DAQ with multiple analog and digital I/Os. It also features an internal 5 V/200 mA power source.

Figure 29. NI - 6009 DAQ.

ECG Simulator

An ECG simulator from Fluke Corporation, PS410 as shown in Figure 30, was used in the system in order to generate ECG waveforms for testing the system. PS410 is capable of generating 35 types of arrhythmic ECG waveforms and eliminates the need for real-time ECG signal capture during development phase.

Figure 30: Fluke PS410 ECG Simulator.

Switch

Since the NI – 6009 DAQ can only sink/source 8.5 mA of current and also considering the fact that the relay inside the massager unit requires ~30 mA of coil current to operate, it was necessary to utilize DAQ 5 V internal supply; however, DAQ internal supply was not controllable by means of LabVeiw, hence the requirement for a controllable switch. The schematic for the switch is shown in Figure 31. When on, it allows for ~40 mA of current.
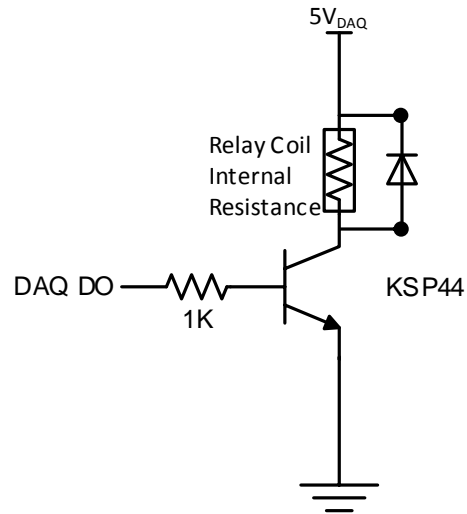
Figure 31: BJT Switch Schematic.

Figure 32 shows how the relay is placed in the massager body to control the start and stop cycles of the DTV system.
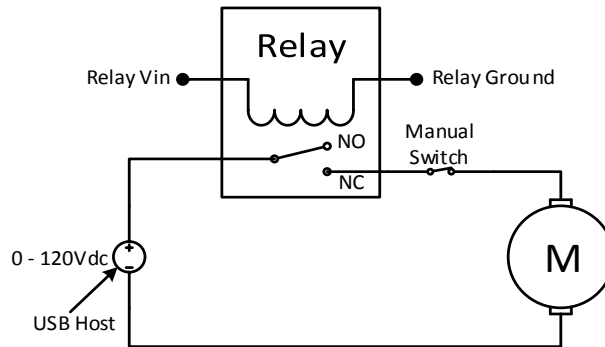
Figure 32. Placement of the relay to control massager start/stop operation.

Power Supply

5V Supply

The 5 V internal supply of the NI – 6009 could source 200 mA of current for powering the accelerometer and relay. No external low voltage supply was required for the prototype.

120 Vdc Supply

A programmable voltage supply allows for varying the frequency of vibration of the massage head. TDK.Lambda ZUP 120-3.6, shown in Figure 33, was used for this purpose. Its output voltage could be directly controlled from the LabView environment, which, in turn, made it possible to control the frequency of vibration from the host computer. In order for the massager to be able to operate with DC input voltages, all the internal AC-to-DC circuitry was removed. The only active circuitry inside the unit is the mechanical on/off switch.

Figure 33: TDK.Lambda Power Supply.

LabView

National Instruments LabView environment version 8.5 was used for developing the code for DTV operation. The program controled the on/off times as well as the frequency of vibration of the motor based on the detection of R waves (Figure 34).

Active Braking System

An active braking system was used to improve the DC motor stopping time to minimize vibration overspill into the systole phase of the heart cycle. In order to reduce the braking time of the massager, several active braking methods were evaluated. A fast double pole double throw relay (V23105, Tyco Electronics, Berwyn, PA) was used to engage the braking system with the ECG trigger signal. The following active stopping methods were considered:

- Short circuiting the motor: the trigger signal disconnects the drive voltage and short circuits the motor coil to quickly dissipate the accumulated magnetic energy.
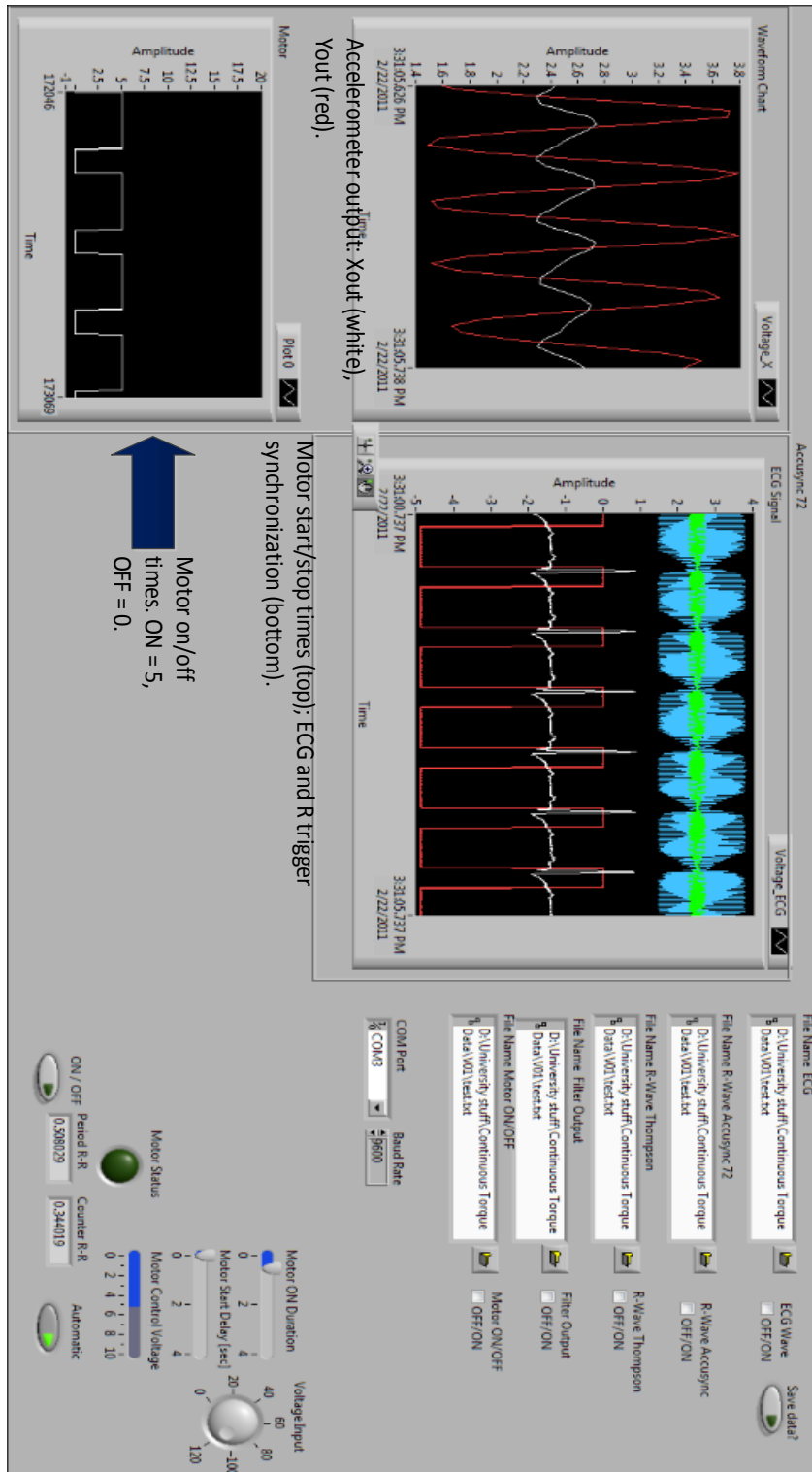
Figure 34: LabView Front Panel for the DTV System.

- Resistive load: in order to avoid excessive discharge currents, instead of short circuiting the motor, a resistive load is connected to the motor coil.

- Capacitive load: a capacitor is connected to the motor coil to form an LC oscillating circuit to invert the voltage applied on the motor.

  - Place a capacitor and a resistor in the regenerative loop to dissipate energy into heat and hold a charge in the capacitor. Once the capacitor is fully charged (energy is transferred from the coil to the capacitor), it starts discharging through the coil. If there were no losses, this periodic action of energy transfer between the capacitor and inductor would result in an electrical oscillation at frequency $\omega = (LC)^{0.5}$, where L is equivalent inductance of the motor and C is the capacity of the connected capacitor. In a real case, the energy transferred from the capacitor to the inductor would cause the motor to stop even more quickly as the induced magnetic flux in the coil would result in electromagnetic force opposing the armature motion. The resistor R dissipates energy as heat during the energy transfer between capacitor and inductor damping the electrical vibrations (Figure 35).

- Inverted supply: the drive signal is briefly applied with the opposite polarity to induce a stopping torque in the motor. The duration of the inverted pulse is controlled in a feedback loop using the accelerometer to ensure that the motor does not start spinning in reverse.

In addition, a user controllable drive pattern generator was implemented to invoke constant, random, or sweep vibrations patterns.

4.3. Vibration Patterns

In order to maximize the beneficial effects of DTV, four possible patterns of frequency application can be considered: constant, random, ramp, and cumulative ramp.
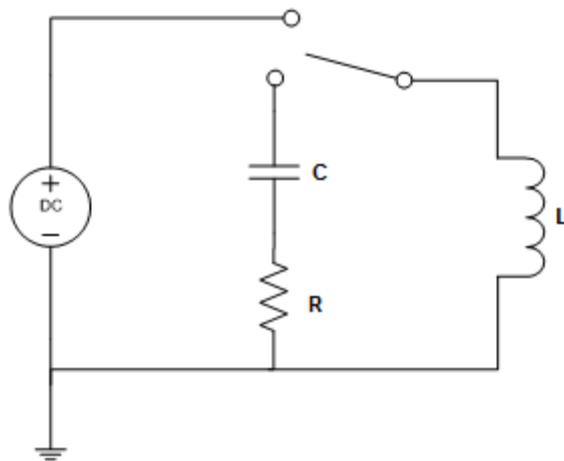
Figure 35. Simplified schematic of the proposed braking system.

4.3.1. Single Constant Frequency

The first and most widely discussed pattern consists in application of vibrations at a single predefined frequency. Naya et al. and Koiwa et al. [67], [98] suggest that the frequency of 50 Hz matches the resonance of the heart muscle and thus induces the highest amplitude of vibrations. Nevertheless, the optimal frequency value can vary between subjects and is very difficult to estimate in rudimentary conditions usually present in emergency situations.

4.3.2. Random Frequency

In order to increase the probability of generating a correct excitation frequency, random frequencies from the preferred range can be generated [101]. Usually, resonance frequency of the heart muscle falls within 40 to 60 Hz. Therefore, application of vibrations with frequency values randomly chosen from within this range can be more beneficial than using the single frequency method. Furthermore, randomized frequency application could potentially add a degree of turbulence within the fluid of an acutely thrombosed artery.

4.3.3. Frequency Ramps

Both the random and the single frequency approaches do not warrant that the optimum frequency for a given individual is reached. Therefore, given that the optimal

frequency for most subjects lies between 40 and 60 Hz, a linear sweep between those frequencies can be the most beneficial. As duration of the diastole, where the mechanical vibrations are applied, is from 1.04 s at 40 BPM to 165 ms at 160 BPM [102], the vibration sweep could be too quick to be efficient. Therefore, the following two possibilities could be considered:

- Ramp: Sweeping between the minimum and the maximum frequency values within one diastole.

- Cumulative Ramp: Partitioning the frequency sweep over multiple heart cycles.

Finally, the frequency sweep can be beneficial in increasing the amplitude of vibrations, if a nonlinear resonance is induced in the heart muscle [103].

4.4. Materials and Methods

The experimental results reported here are aimed at validating the functionality of the proposed Diastolic Timed Vibrator device. All tests have been done on a lab bench; no human testing have been attempted at this stage of the project.

4.4.1. ECG Data

Two sources of ECG signal were used for testing the DTV device:

- Patient simulator (PS410, Fluke, Everett, WA) generating ECG signals including ones with ST elevation patterns for initial device evaluation.

- Custom built ECG generator regenerating ECG signals from saved numerical values obtained from the PhysioNet's Physikalisch-Technische Bundesanstalt Diagnostic ECG database (PTBDB) [104], [105] for evaluation of algorithm efficiency on ECG acquired from MI patients.

Data from the PTBDB ECG database contains 12-lead myocardial infarction ECG traces acquired from patients with various localization, gender, age groups, and

health condition. For evaluation, 763 heart cycles from 31 patients with MI localized in inferior (16 cases), lateral (7), anterior (14), posterior (2) and septal (5) sections of the heart were used. Some patients had multiple infarcts.

4.4.2. Test Setup

The device described in Section 4.2 was used in the experiments. An off-the-shelf ECG machine was used for ECG acquisition, filtering and amplification (AccuSync 72, AccuSync, Milford, CT). Lead I was selected for the purpose of this experiment with left and right arm electrodes as well as left leg electrode as the reference.

A digital to analog conversion (DAC) with attenuation was required in order to generate a proper ECG signal from the PTBDB data sets. Upon experimentation, signals were generated via a data acquisition device (PXI-6251, National Instruments, Austin, TX) at 16-bit digital to analog precision attenuated by a factor 1200:1 and then using a resistive voltage divider for further attenuation with a factor 100:1, as depicted in Figure 36. Left arm electrode was directly connected to the voltage divider and both the right arm and the left leg electrodes were grounded. The entire software interface was developed in LabView. The VI would automatically read ECG files stored on a physical drive, and generate the attenuated ECG signal. Also included were provisions for recording the ECG waveform from the AccuSync machine and recording the R-wave trigger both for duration of 40 seconds.
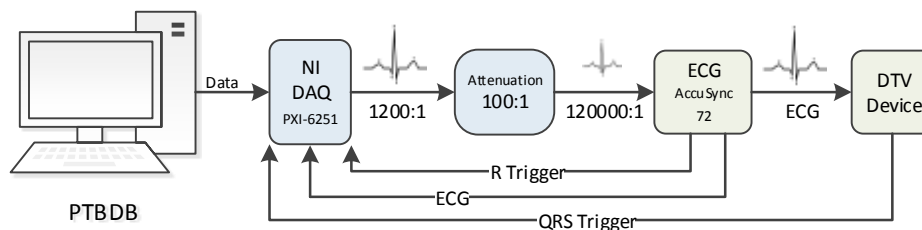
Figure 36. Setup for ECG signal regeneration based on records from the PTBDB Database.

The generated ECG signals were acquired using an ECG monitor for filtering, amplification and optional reference R-wave trigger generation, as explained earlier

herein. The filtered and amplified signal was then supplied to the DTV device for analog to digital conversion and further processing. The resulting timing signals were used to activate the relay built into the massager. A data acquisition device (PXI-6251, National Instruments, Austin, TX) was used to acquire signals generated by the DTV device and interfacing it to the custom created LabView VI. The vibration frequency and the pattern of vibrations were achieved by varying the DC input voltage supplied to the massager by a power supply (ZUP1203.6, TDK-Lambda Americas, Inc., San Diego, CA) controlled by the DTV device. The LabView VI was used to observe the processed ECG signals, the acceleration feedback from the massager head, and to calculate the starting and stopping delays in reference to the onset of systole and the onset of diastole in the input ECG signal used. In order to provide a robust timing estimation, the feedback acceleration signal was low pass filtered with 400 Hz cut-off frequency and then its DC component was removed.

4.5. Experimental Results

4.5.1. ECG Synchronization

In order to evaluate the precision and efficiency of the proposed MHT algorithm in [100], the results of QRS complex detection obtained with the proposed algorithm versus a state of the art R-wave detection device AccuSync 72 (AccuSync Medical Research Corporation, Milford, CT) were compared. As explained earlier, the ECG signals were generated based on data from the PTBDB ECG database.

Regarding the R-wave detection, the results provided by the MHT algorithm [100] and AccuSync 72 were very similar with an average difference of 3 ms (σ = 12.47 ms). On the other hand, if the P-wave detection in the MHT algorithm was successful (in 82% of cases for this dataset), the onset of the R-wave could be predicted on average 29 ms (σ = 14.52 ms) earlier than with the AccuSync device. Figure 37 presents histograms detailing the distribution of detection times in reference to the actual location of the R-wave in the analyzed ECG traces.
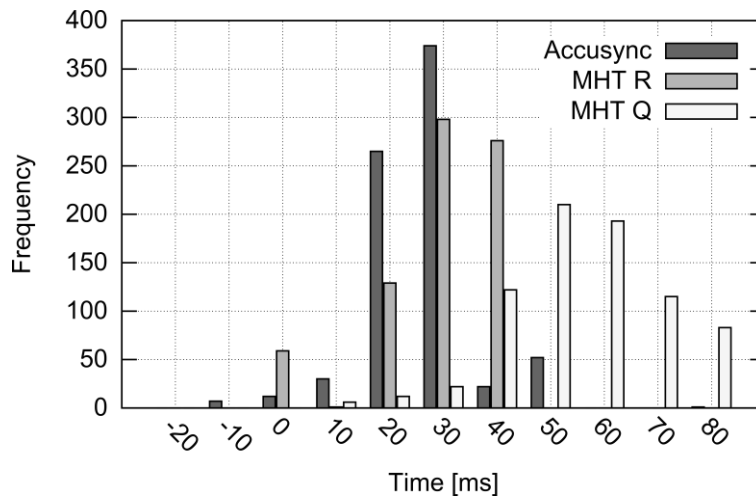
***Figure 37. Histogram of QRS complex detection times in relation to actual location
of the peak of the R-wave, with results obtained with the Accusync
72 device and the proposed MHT algorithm, where MHT R indicates
the case where the MHT algorithm was set the detection was made
before the actual peak of the R-wave.***

4.5.2. Frequency Patterns

As discussed previously, the DTV device implements four methods of vibration frequency generation: constant frequency, random, ramp, and cumulative ramp. An experiment to verify the correct functionality of the frequency generation module implemented for the DTV device was performed. The results were obtained at 30 N force applied on the massager and using an ECG signal (with ST-elevations) generated by the patient simulator. Figure 38 shows the vibration frequency and the detected vibrations for the proposed patterns along with the input ECG signal to present the synchronization concept [3].

4.5.3. Start and Stop Delays

There are two factors that impact the safety and efficacy of the DTV device. Safety is affected by the amount of vibration that remains generated during the systole, i.e. after the termination trigger has been issued. The efficacy of the device on the other hand, is affected by the delay after the start trigger, after which the vibration generated reaches the desired amplitude - the Start Delay.
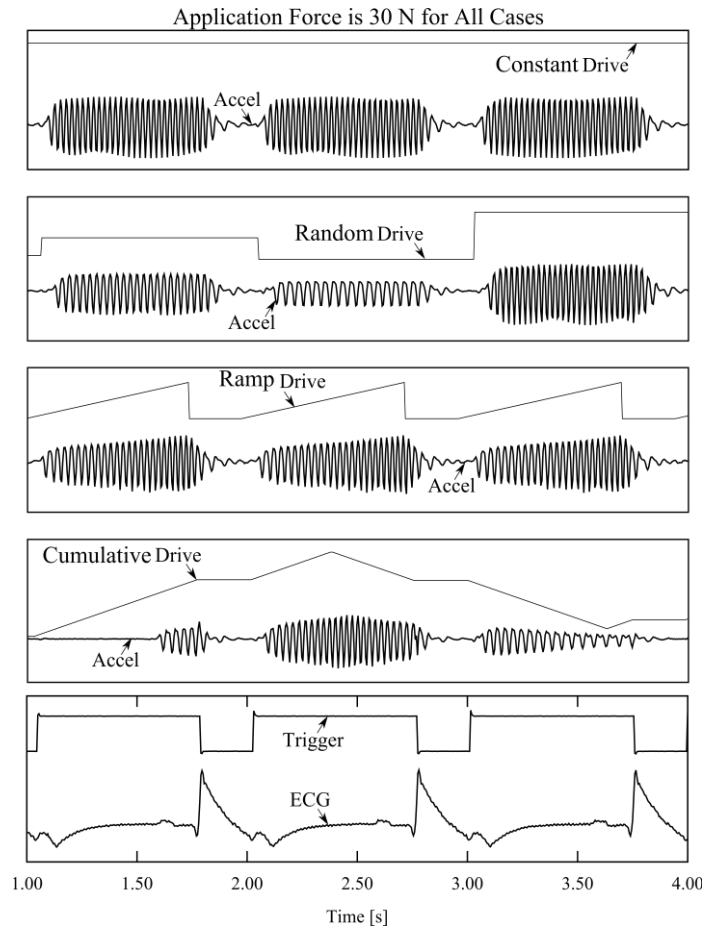
Figure 38. Vibration frequency, induced mechanical vibrations (Acceleration), R trigger, and ECG (with ST elevation) for the four vibration patterns discussed [3].

The acceleration signal acquired at the massager head was used to estimate the amount of vibration still present after the termination signal was issued. After filtering, the acceleration signal was separated into the starting part, the steady part, and the stopping part. The steady amplitude was calculated as the mean amplitude of acceleration during the steady state. The starting time values were calculated from the rising edge of the driving signal to a point where the steady amplitude was achieved. For the stopping time, two exponential functions were fitted: one to peaks of the stopping signal and one to the valleys of the stopping signal. The obtained fitted functions were used to calculate the time delay after the falling edge of the trigger signal for which the vibration amplitude decreased by 1/e from the initial amplitude calculated for the steady state. This method allows to precisely indicate the stopping time, even when the 1/e point does not fall on one of the peaks. The acceleration signal was acquired

62

synchronously with the ECG signal supplied to the DTV device allowing for precise definition of acceleration timing in reference to the ECG signal.

Engagement Force

The start delay is mostly affected by the amplitude of the engagement force applied on the DTV device. This force is an important factor affecting the efficiency of transferring mechanical vibrations to the heart. Experiments indicate that application forces of up to 50 N are tolerated by the subjects. In a real use, the application force level will depend on the subject's tolerance and will vary between 30 N and 50 N. The average start and stop delays for vibration frequency of 42 Hz were measured. Obviously, for the 50 N application force the start delay is the longest at 162 ms and the stop time is the shortest at 44 ms. Table 5 summarizes the average start and stop delays obtained in this experiment.

Table 5. Average start and stop times for different levels of engagement force.

Engagement Force	Start Time [ms]	Stop Time [ms]
0N	110	166
30N	155	62
50N	162	44

Active braking

Braking time of the massager defines the amount of vibration that is still applied to the chest of the subject after the stop trigger was received. The average timings obtained for the proposed active braking methods are listed in Table 6.

Table 6. Average stop times with active braking methods.

Method	Average Stop Time [ms]	Standard Deviation
Open circuit	54.7	45.6
Short circuit	48.3	14.7
68uF capacitor	44.6	18.0
28 ohm resistor	37.5	20.9
Inverted drive	11.7	0.31

Implication of these intervals is further analyzed in the discussion section of this work.

4.6. Discussion

This study presents and discusses the performance of Diastolic Timed Vibrator. The most important aspect affecting the safety and efficacy of the device is the vibration timing in synchronism with the diastole of the heart cycle. In order to prevent overspill of vibrations into the systole, which may have detrimental effects on the heart muscle, the motor must be stopped just before the onset of systole indicated by the mitral valve closure (MC). The length of the diastole for male subjects can be approximated using the formula proposed by Weissler et al. Figure 39 shows the possible vibration period versus the duration of diastole for various heart rate values, with and without application force [3]. It can be seen that the elevated motor start time induces a delay that significantly reduces the useful time of application of vibrations. At 50 N, the start time of 162 ms leaves no space for vibrations for heart rates above 120 BPM. A more efficient scheme of motor starting, using voltage boost or reducing the amplitude of vibration during systole instead of stopping the motor can be used to overcome this limitation.

Vibrations are stopped when the R-wave is detected, which occurs a minimum of 40 ms before the mitral valve closure indicating the actual start of systole [74]. Given the relatively short amount of time between the R-wave and the MC and its variability, early detection of the QRS complex is crucial for assuring safety of the device. To this end, the MHT algorithm aiming at detecting the QRS complex based on early P- and Q-wave detections is studied in the literature and by different members of this team [100]. The P-wave detection algorithm resulted in an average of 29 ms earlier detection of the QRS complex relative to the middle of the R-wave.

If the DTV controller was to issue a stop command to the massager motor using the MHT algorithm processing real time ECG data, the hardware would have, on average, an additional 29 ms [100] to cease the vibrations in 82% of heart beats. It should be noted that the algorithm finds the approximate location of the P and Q-waves based on dynamically updated templates customized for each patient in the learning phase. On the other hand, it is not always that the P-wave can be clearly identified. In

such cases, the regular R-wave detection algorithm is invoked. Even in this worst case scenario, the motor would have on average at least 40 ms to stop before the onset of systole indicated by the mitral valve closure, which is enough when the inverted drive is used for active braking (11.7 ms stop delay). Considering that the application force on the massager can further dampen motor vibrations and further improve the stop time, it would be fair to believe that the massager can be effectively stopped well before the onset of systole when triggered by the R-wave. Finally, it should be noted that the proposed algorithm was designed for minimum footprint so that it can be implemented on an inexpensive micro-controller.
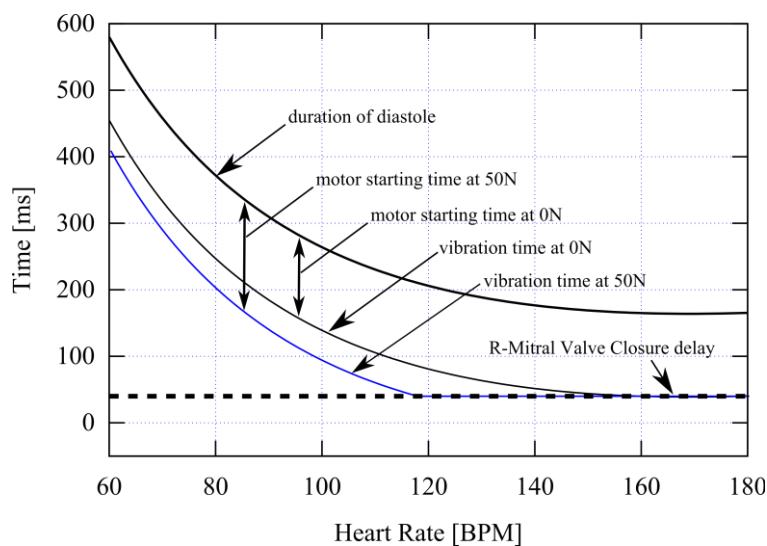
Figure 39. Possible timing of vibrations versus the duration of diastole measured from aortic valve closure to mitral valve closure (MC) for various heart rates and engagement forces. R-MC delay shows the time between the peak of the R-wave and MC [3].

Another research is currently performed within the DTV project to improve the prediction of the QRS complex and use seismocardiography (SCG) signals to verify the correct timing of application [107].

Another aspect affecting the effectiveness of the DTV device is the frequency of the applied vibrations. The optimal frequency value depends on the physique of the subject. In order to ensure that the vibrator generates the optimum frequency, a randomized drive and two variants of a frequency sweep drive were implemented. While the sweep methods ensure that the optimum frequency is applied at least momentarily,

the random method provides longer application time at each frequency, but does not guarantee that the optimum frequency for a given patient is applied.

4.7. Summary and Conclusions

As the second objective, the presented work introduces the Diastolic Timed Vibrator, a device offering a potential method for improving re-canalization time and enhancing coronary blood flow in heart attack patients that can be safely applied in the pre-hospitalization phase by minimally trained personnel. The features of the device affecting its performance were analyzed along with discussion of the major challenges related to its safety and efficacy. The major challenge in implementing the device consists in reliable synchronization of the generated vibrations with the heart cycle of the patient. Vibrations applied during the diastole have beneficial effect, but any vibration overspill into the systole can have detrimental effects on the contractile action of the weakened heart muscle. In order to address this issue, a modified Hamilton-Tompkins (MHT) ECG processing algorithm for early detection of QRS complexes in MI patients followed by a custom ECG annotation algorithm was used in this project [100]. It was demonstrated that on average the QRS complex can be detected 29 ms prior to the R-wave, which is sufficient to stop the vibrator well before the onset of systole indicated by the mitral valve closure. Furthermore, various active braking methods to further decrease the time required to stop the application motor were presented and evaluated. Finally, the capability of the device to generate various frequency patterns, assuring that the optimum vibration frequency for a given patient is used, were described in this chapter.

5. Effects of Direct Distal Arterial Mechanical Deformation on Blood Flow: a Preliminary Investigation

While the Diastolic Timed Vibration apparatus presented in chapter 4 can be beneficial to STEMI patients, delivery of mechanical vibration to the coronary artery is limited by the chest wall. This is due to the boniness and rigidity of the rib cage, which limits inward deformation and displacement toward coronary arteries. Similar to the purpose of DTV, a device that can noninvasively be used by minimally trained individuals to assist STEMI patients is of high interest. In chapter 3, it was discussed that distant vessel deformation could accelerate clot lysis, which opens a way to application of mechanical stimuli away from the chest area of patients suffering from acute myocardial infarct.

The purpose of this chapter is to address objective three of this work by presenting different approaches taken to quantitatively determine the turbulence change in blood flow caused by external mechanical vibration on a human artery. Not all the approaches were successful in the experiments presented; however, this would be the very first step in examining the effects of direct, distal, external low frequency mechanical deformation on a human subject artery as well as a follow-up to the in-vitro study. Noninvasive measurement devices, i.e. force sensor, accelerometer, pulse sensor, and ultrasound, were used for data gathering purposes. The author of this work volunteered as the test subject. The procedure was to apply low frequency mechanical vibration to a major distal artery and determine whether vibration would reach the desired proximal arterial site through bloodstream. If proven effective, a device similar to the architecture of DTV with various feedback sensors and adjustable vibration frequency and stroke level could be designed so that it could be used by minimally trained individuals to commence treatment of STEMI patients.

5.1. Method

The measurement consisted of vibrating an artery with an off-the-shelf massager, operating at 32 Hz, and measuring the transferred vibrations at any of the common carotid arteries (or similar) and also to see whether the actuation can cause turbulence in the blood flow. Two different methods were used for this measurement: measurements via superficial electromechanical transducers, and via ultrasound.

5.1.1. Measurements

Four different approaches were tried to measure the turbulence from over the surface of the skin: force sensor, accelerometer, pulse sensor, and ultrasound; however, only two of the approaches were used.

Force Sensor

A precision gram sensor load cell with a capacity of 25 grams was used to perform the measurements. The excitation range for this sensor is 10 V with a rated output range of 1 mV/V. Therefore, for every gram of mass the output would change by 400 μV. The output was amplified and low-pass filtered in hopes to generate a clean and readable signal. The issue with this sensor was that it was hard to have the sensor fixed in place at the carotid artery while mechanical actuation was being applied to the femoral artery. As a result, the captured signal included artifacts caused by the instability of the load sensor. Even after performing some signal processing, the data proved to be of low quality. Eventually, after several trials, no further measurements were performed.

Accelerometer

A sensitive accelerometer was also tried to determine the blood turbulence due to external arterial mechanical deformation. However, similar to the force sensor case, this approach was dismissed. The main issue was lack of physical stability of the sensor when put on the carotid artery, mostly due to shape of the sensors. If pressed too hard on the artery, it would severely dampen the pulsations leading to inaccurate readings.

Pulse Transducer

A piezo-electric pulse transducer was used to perform blood turbulence measurement. This transducer is typically used in research settings for measurement of pulse rate. Also, among many other applications, the sensor is used to measure carotid pulse and peripheral pulse in the finger. It has an ergonomic shape and sits on the tip of index finger very easily; it can also be stuck to the carotid or brachial artery with minimal impact on the signal quality. The pulse sensor was connected to a DAQ (USB-9162, National Instruments, Austin, TX) for recording and analyzing the data after the output was amplified and conditioned. In addition, a VI was created in LabView in order to extract major frequency components of the signal.

In this approach, vibration was applied to the left brachial artery and the results were measured at the index finger of the same hand.

Ultrasound

In order to better and more accurately understand the effect of low frequency mechanical vibration on the stenosis site with vibration applied to a site distal to the stenosed site, an experiment was performed with use of an ultrasound imaging machine. The carotid artery, was probed with vibration applied to four different sites: left femoral artery, descending aorta in the abdomen, left brachial artery, and left shoulder. The following parameters were measured:

Peak Systolic Velocity (PSV)

It is defined as the maximum blood flow velocity during a cardiac cycle, normally occurring during the systole phase [107]. It is a measure of plaque size (stenosis tightness) and turbulence. Higher PSV values indicate tighter stenosis and greater turbulence in the blood flow. Values lower than 125 cm/s with no spectral broadening indicate a normal flow [108].

End-Diastolic Velocity (EDV)

It is defined as the minimum flow velocity during a cardiac cycle, normally occurring at the end of diastole phase [107]. It usually remains intact until the stenosis causes 70% occlusion; this is when EDV significantly increases [108].

Resistive Index (RI)

It is defined as:

$$[(PSV - EDV) / PSV]$$

Turbulence and instantaneous reversal of diastolic flow lead to higher RI indices. Normal RI is approximately at 0.7 [109], [110].

Systolic / Diastolic (SD) Ratio

It is the ratio of PSV/EDV. Similar to RI, it is used to describe relative difference in flow velocity between systole and diastole [110].

5.2. Results

5.2.1. Pulse Transducer

Figure 40 shows the FFT signal of the pulse measured at the index finger with the pulse transducer.

As expected, the major component was at the 1 Hz indicating a 60 beats per minute heart rate. Measuring the heart rate manually confirmed the obtained result. In this scenario, no vibration was applied. A similar result was also recorded with the sensor positioned on the carotid artery. Figure 41 shows the FFT of the pulse measured at the index finger with vibration applied to the left brachial artery of the same hand. The frequency of vibration from the massager was measured and recorded at 32 Hz. As seen in Figure 41, the major frequency components are at 1 and 32 Hz which correspond to the human pulse frequency and the massager motor vibration frequency, respectively. Application of higher vibration frequencies (up to 50 Hz) lead to same results with the second major component showing at the corresponding frequency of the massager.
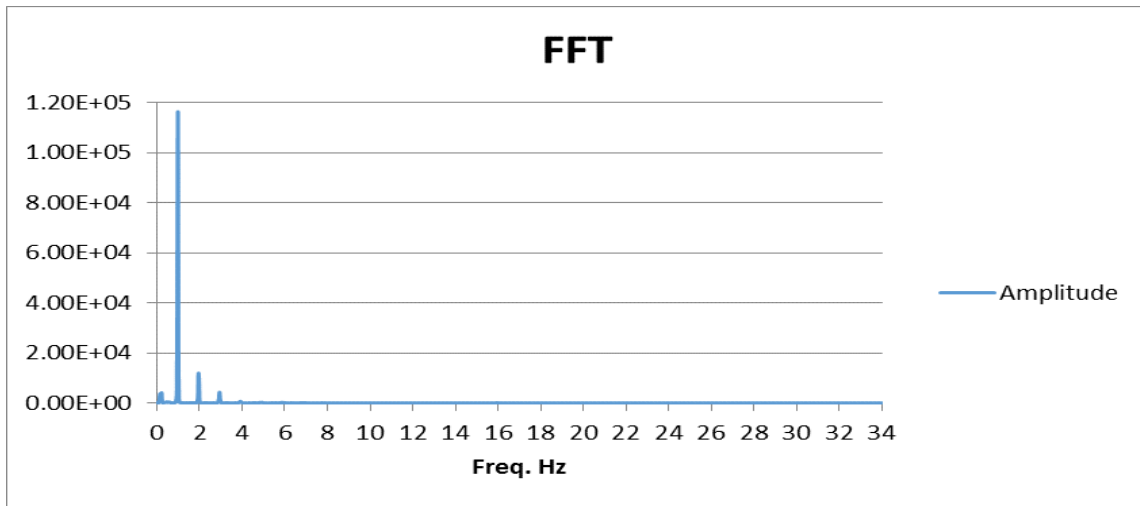
Figure 40. FFT Results for the No-Vibration Case at the Index Finger.
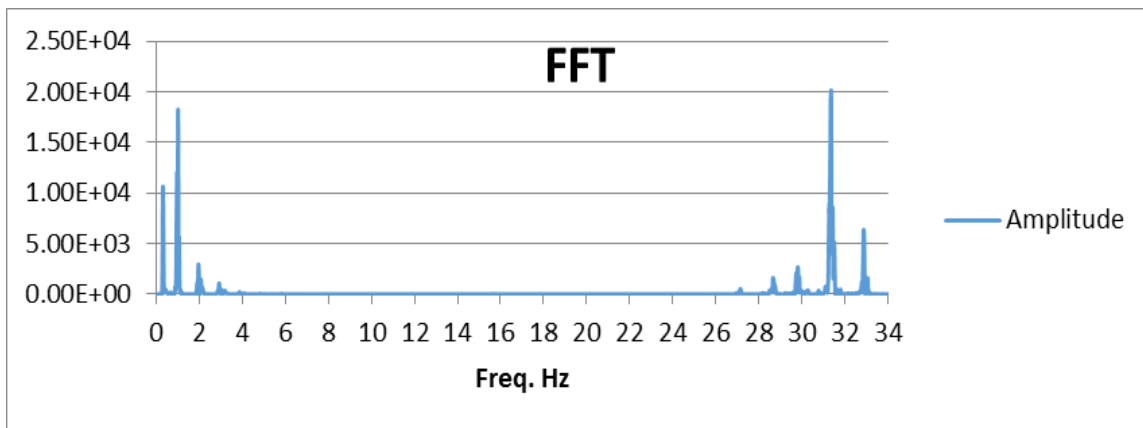
Figure 41. Vibration Applied to the Brachial Artery. Pulse Measured at the Index Finger.

5.2.2. Ultrasound

Figure 42 shows the ultrasound acquired from the left carotid artery. The PSV is registered at 101.24 cm/s with RI at 0.73. EDV was recorded at 26.9 cm/s and the S/D ratio at 3.76. Figure 42 represents the case with no vibration applied to the subject. The subject was in supine position for all the cases in this experiment.

Figure 43 shows the case where vibration was applied to the left brachial artery of the subject with a frequency of 32 Hz. PSV was recorded at 91.11 cm/s with RI at 0.73. EDV was slightly reduced to 24.41 cm/s and the S/D ratio showed minor reduction to 3.73. With a 32 Hz vibration applied to the left femoral artery the PSV increased to

96.17 cm/s. RI also increased to 0.78. EDV was recorded at 21 cm/s with S/D ratio increasing to 4.57 (Figure 44).
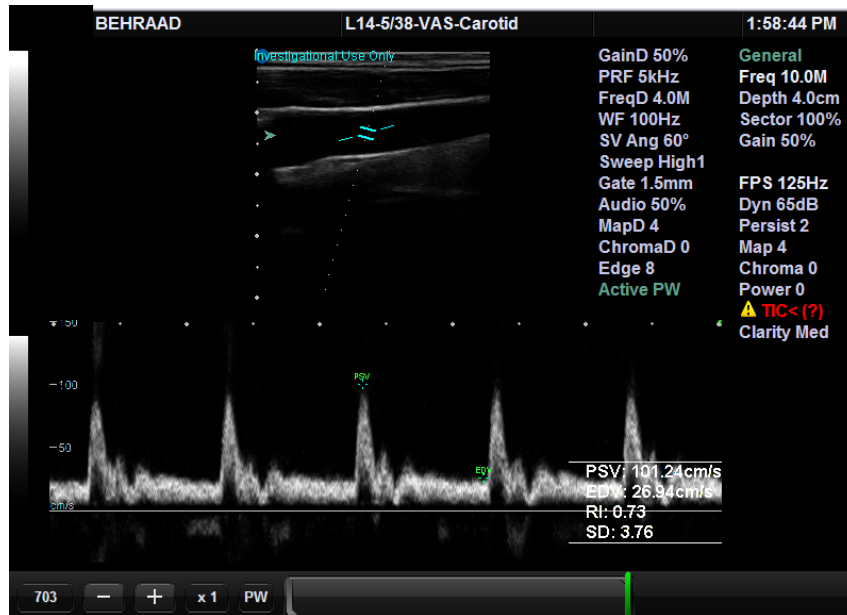
Figure 42. Ultrasound image of the left ceratoid artery with no vibration applied to the subject.
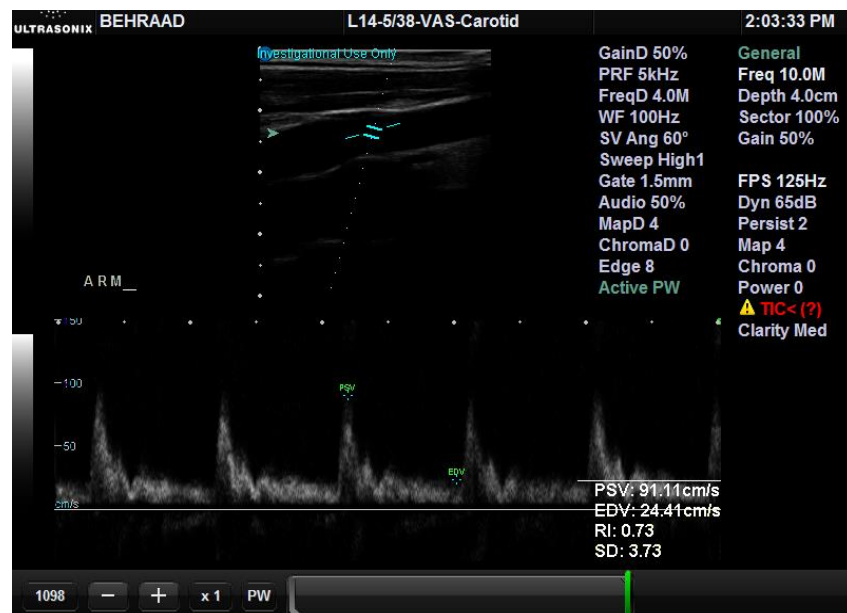
Figure 43. Ultrasound image of the left ceratoid artery with vibration applied to the left brachial artery of the subject.
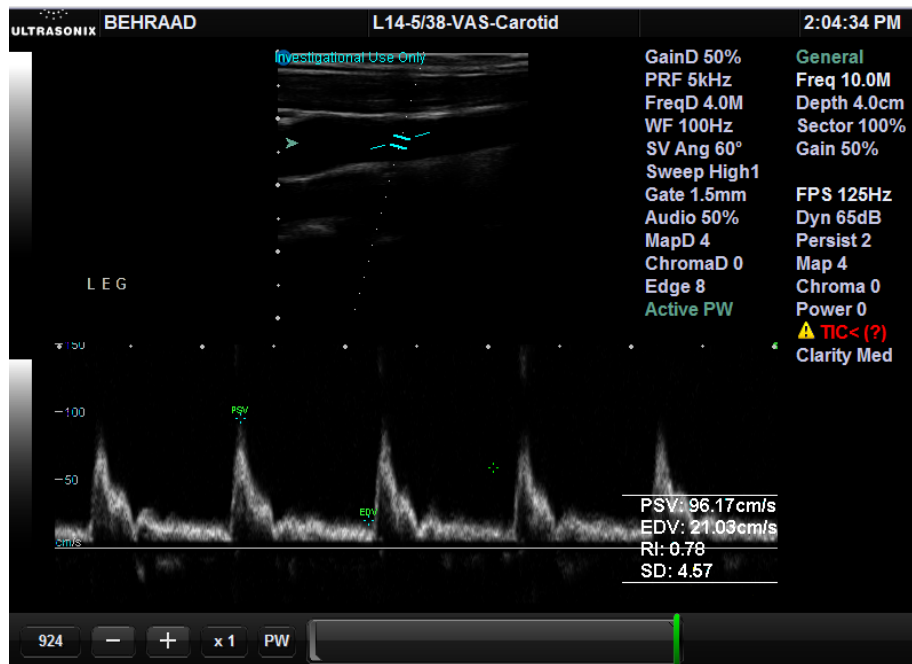
Figure 44. Ultrasound image of the left ceratoid artery with vibration applied to the left femoral artery of the subject.

In another experiment, the massager was placed on the descending aorta in the abdomen and applied vibration at frequency of 32 Hz on the aorta. This experiment lead to a PSV of 97.86 cm/s with an RI at 0.75. EDV and S/D ratio were recorded at 24.41 cm/s and 4.01, respectively. Figure 45 shows the waveform captured for this experiment.

Finally, 32 Hz vibration was applied to the shoulder of the subject close to the left subclavian artery. In this round of experiment, the peak systolic velocity increased to 106.3 cm/s with RI of 0.76. The EDV, however, remained approximately the same as in previous cases at 25.25 cm/s. S/D ratio in this case was registered at 4.21. Figure 46 shows the acquired ultrasound image for this experiment. Table 7 shows the summary of the results.

Table 7. Summary of the ultrasound experiment.

Location	PSV [cm/s]	EDV [cm/s]	RI	S/D Ratio
Brachial Artery	91.11	24.41	0.73	3.73
Femoral Artery	96.17	21.03	0.78	4.57
Descending Artery	97.86	24.41	0.75	4.01
No-vibration	101.24	26.94	0.73	3.76
Subclavian Artery	106.3	25.25	0.76	4.21
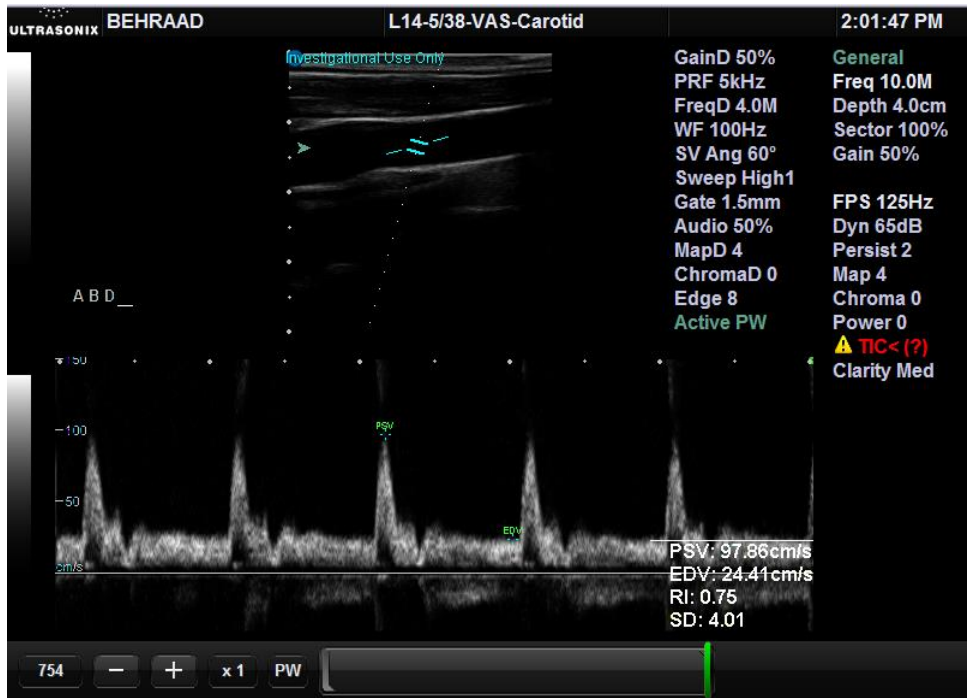
Figure 45. Ultrasound image of the left ceratoid artery with vibration applied to the descending aorta in the abdomen of the subject.
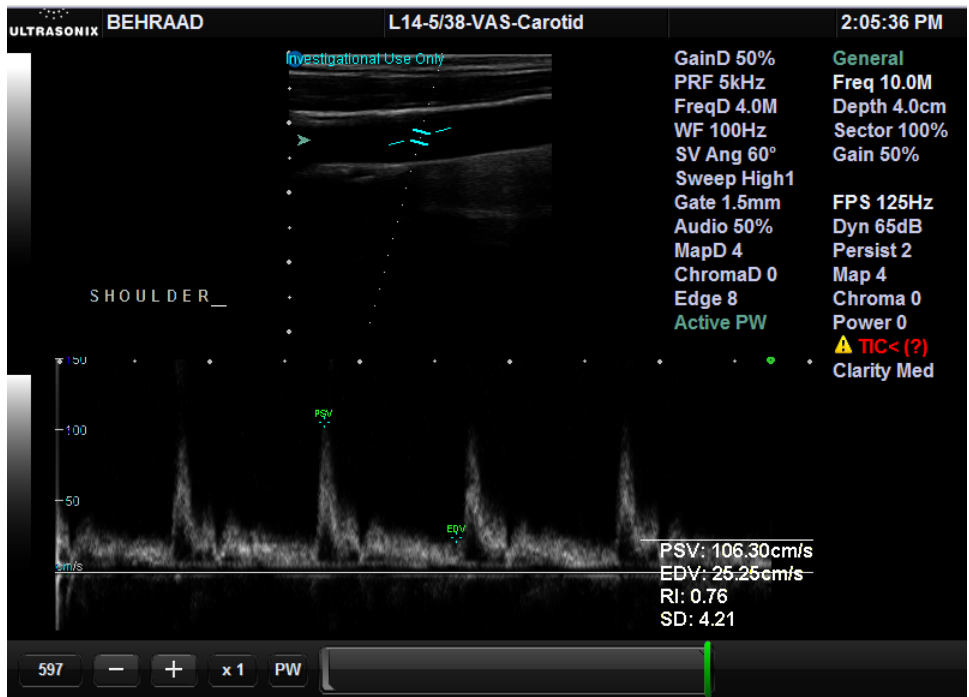
Figure 46. Ultrasound image of the left ceratoid artery with vibration applied to the left subclavian artery of the subject.

5.3. Discussion

Among the approaches presented in this chapter, only the ones with pulse transducer and ultrasound imaging met the requirements of the experiment.

In the pulse transducer method, to test the system, a Fast Fourier Transform (FFT) of the signal from the index finger of the subject was taken in order to determine the prominent frequency component. As expected, the prominent frequency component was equal to 1 Hz, which is equal to 60 beats per minute or a pulse rate of 60 BPM (Figure 40). When external mechanical vibration with a frequency of 32 Hz was applied to subject's left brachial artery, two major frequency components at the index finger and also carotid artery were identified at 1 and 32 Hz frequencies, which correspond to the subject's pulse rate and massager operating frequency, respectively; however, it is very difficult to determine whether the same frequency has been transferred to the index finger via the bloodstream. In other words, although the same frequencies have been sensed at the assumed proximal location, it is hard to quantitatively determine the portion of mechanical strokes transferred via bloodstream to the stenosis site versus strokes transferred via surface. Given the viscous nature of blood [111], it would be fair to assume that strokes probably get dampened significantly before reaching the clot site. Furthermore, there are no other major frequency components that could be contributed to turbulence in the bloodstream. Consequently, this method does not provide quantitative results in order to measure turbulence, but it gives an indication of the fact that mechanical strokes at a distal region do transfer to the proximal region.

The ultrasound method, on the other hand, provided quantitative results that can be compared. In the no-vibration experiment, all the measured parameters, i.e. PSV, EDV, RI, and S/D ratio, were recorded as reference values. EDV shows significant change in presence of 70% or more stenosis sites [108]. Therefore, no major conclusions can be drawn from EDV changes. Actuation on the brachial artery causes the most decrement on the PSV. This can be justified by resorting to the fact that external mechanical actuation does assist in smoother blood flow depending on the location of mechanical actuation application. In addition, brachial artery has the least diameter size. Mechanical deformation on femoral artery causes an increase in the RI, which is a parameter for assessing turbulence in the blood [108]. Vibration on the

abdomen lead to greater RI with respect to the two previous cases and increased PSV compared to the femoral artery case. This difference could be due to greater diameter of the descending aorta and also existence of more soft tissue (dampening) around the aorta. Finally, vibration on subclavian artery lead to the highest PSV and almost the second highest RI in this trial. This means that mechanical strokes at this location do transfer to the carotid artery and cause turbulence. This might be because of closer proximity of the subclavian artery to the carotid artery and also presence of lesser number soft/dampening tissues around this location, which leads to easier transfer of mechanical actuations via the bloodstream.
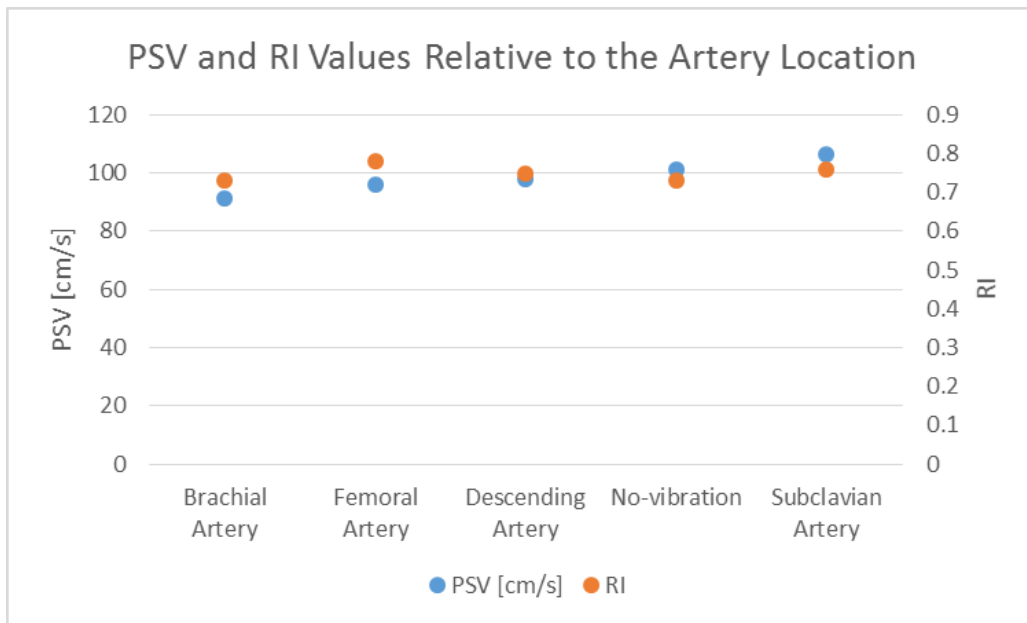
Figure 47. Values of PSV and RI based on the artery location.

Figure 47 shows the measured values for RI and PSV with respect to the artery at which mechanical deformation was applied. Once again, PSV provides a means for determining the stenosis size, turbulence, and reverse flow. It is also worth noting that since the EDV values for this experiment are not representative of stenosis in this particular experiment (EDV shows significant change in presence of 70% or more stenosis sites), the RI values obtained may not be true representations of the results of this experiment as RI values depend on EDV. However, they can be used to show the change in the trend of turbulence.

5.4. Summary and Conclusions

In this chapter, objective three of this work was addressed. Different methods for determining whether external mechanical vibration distal to a stenosis site would cause turbulence in the blood flow detectable at the stenosis site were discussed. Various approaches were examined, out of which, pulse transduce method and ultrasound imaging were selected. Other methods did not provide results accurately enough.

A piezo-electric pulse transducer was placed on the index finger of a subject, and mechanical deformation was applied to the brachial artery of the subject. Although useful in showing transfer of mechanical actuations to the proximal site (visible 32 Hz frequency component from the FFT calculations), it was difficult to conclude that the all the mechanical actuations were transferred through the bloodstream. Blood is viscous and, consequently, can dampen the mechanical strokes.

In the second approach, ultrasound imaging was used to determine blood velocity characteristics with and without mechanical deformation at different arteries. Carotid artery was assumed to be the stenosis site. Four separate experiments were conducted with vibration applied on brachial artery, femoral artery, descending abdominal artery, and subclavian artery. Contrary to results from the case with pulse sensor, with ultrasound imaging it was possible to measure blood velocity profile (PSV, EDV, RI, S/D ratio) in different test scenarios and compare results. Based on the results, it was obvious that application of mechanical vibration on a major artery distal to carotid artery, indeed, changed turbulence in the blood flow. Maximum value for PSV was recorded at 106.3 cm/s resulting from mechanical actuations on the left subclavian artery. The reference PSV value was recorded at 101.24 cm/s. Least PSV was recorded at 91.11 cm/s and was due to application of deformation on the left brachial artery, which indicated a reduction in turbulence and smoother flow. The variation seems to come from the distance of the artery from the stenosis site, surrounding tissue dampening traits, and diameter size of the artery. Therefore, it is of paramount importance to perform arterial deformation on an artery that imposes the highest turbulence on the distal stenosis site. More in-depth experiments are required to fully prove statistical significance of the method and identify arteries with greatest capability of inducing turbulence.

6. Discussion

Given the comprehensive background information provided in chapter 2, it is obvious that there is need for a noninvasive method that can be used in conjunction with anti-thrombolytic drugs by initiating pre-hospitalization treatment right after the onset of STEMI symptoms. Current methods either require specialized equipment and trained personnel or lack availability. The method and equipment must be easy to use so that minimally trained individuals could operate the device and commence treatment until the arrival of EMS and transferal to a hospital equipped with cath lab.

The results of the in-vitro study in chapter 3 show that lysis with use of mechanical deformation is most successful when either directly applied to the occlusion site or at a distance relative to the occlusion site. The results indicate 95% of the occlusions were perfused within 11 minutes of direct application of mechanical deformation on the occlusion site while the same success rate, 95%, but within 16 minutes of applying direct actuations was observed when deformation was applied 60 cm away from the stenosis. However, vibration applied to the stenosed region does not assist in dissolving the clot (2.3% success rate in 20 minutes after start of application of vibration), which may be as a result of very narrow flow sites that impede the process of mixing blood with clot busting agents. Also, no pressure waves can be directed at the thrombi when vibration is directly applied to the stenosed region possibly due to limited availability of blood and flow around the region; however, direct application of mechanical deformation on the thrombi imposes direct and severe shear stress leading to deformation, displacement, and eventually, disruption of the clots, hence the highest success rate in the shortest time (95% in 11 minutes).

Direct application of mechanical deformation on an occlusion site is not always possible. In case of coronary thrombosis, access to coronary arteries is limited by the stiffness and downward movability range of the rib cage. Consequently, it may not be practical to apply direct mechanical deformation on the coronary arteries of the STEMI patients noninvasively. On the other hand, as mentioned earlier, distal application of

arterial mechanical deformation leads to 95% success rate, although it takes 16 minutes on average for the clot to break down. Mechanical stimuli generate pressure waves in the bloodstream, which are transferred through the blood [90], moving toward the stenosis site, hitting the thrombus and causing deformation. Also, fluid viscosity and its traction on the vessel walls imply pressure non-uniformity in the lumen of the vessel, as depicted schematically in Figure 19, which can have further positive impact on clot dissolution. Traction of the thrombus to the vessel walls causes the central part of the clot experience greater degree of deformation. Moreover, Lines of Zahn, a characteristic of thrombus in the coronary arteries, as discussed in chapter 3, make deformation and displacement of thrombi more feasible.

An argument can be made that disrupted clot fragments, after passing through the stenosis site, could end up blocking other narrower blood vessels and impede or block blood flow at another location. The response to such an argument would require stating the fact that the disintegrated fragments are generally large and therefore cannot generally spread to all capillaries. In addition, removal or displacement of a large thrombus in a patient with severe myocardial infarction increases their chance of survival as opposed to complete necrosis of the myocardium and patient mortality.

On the other hand, in chapter 4, it was hypothesized that application of diastolic timed mechanical vibration to the chest of myocardial infarct patient could potentially help in mixing fibrinolytic agents with the clot and also cause stress, which, collectively, would lead to disruption of the thrombus. This hypothesis was made at the time where different areas of the project were moving forward in parallel. However, it can now be dismissed based on the in-vitro experiment results as the success rate was shown to be only 2.3% within 20 minutes of application of vibration. But the facts that studies show vibration can increase coronary blood flow and also improve the relaxation of the weak heart during diastole and reduce spasms are of great importance.

The DTV chapter analyzed the two major aspects impacting the proper operation of a Diastolic Timed Vibrator [3]: vibration patterns and vibration timing. The effectiveness of the applied vibrations relies on the application of the optimal frequency, whose value differs in every subject. In order to ensure that the vibrator generates the optimum vibration frequency, randomized drive and two variants of a sweep drive were

implemented. While the sweep methods ensure that the optimum frequency is applied at least momentarily, the random method provides longer application time at each frequency, but does not guarantee that the optimum frequency for a given patient is used. Furthermore, vibration timings were evaluated. In order to prevent overspill of vibrations into the systole, the motor must be stopped just before its onset (Mitral Valve closure). The length of the diastole for male subjects can be approximated using a formula proposed by Weissler et al. [102]. The duration of diastole can be as short as 170 ms in some individuals at heart rate of 150 BPM. As a result, the motor must be able to effectively vibrate during this period and cease all motion just before the onset of the systole. Therefore, the limitations of the motor start and stop times must always be considered in the design of DTV (Figure 39). Based on the results obtained from the active braking system (Table 6), it was possible to stop the unloaded motor (worst case scenario) in less than 12 ms. Given the application force on the massager, which is deemed to be between 30 and 50 N, can further dampen motor vibrations and further improve the stop time, the massager can be effectively stopped well before the onset of systole when triggered by the R-wave [3]. Consequently, application force is an important factor affecting the efficiency of transferring mechanical vibrations to the heart. In a real use, the application force level will depend on the subject's tolerance and will vary between 30 and 50 N [3]. Subject's tolerance, based on the author's experiments, depends on the size of the subject and the rib cage, amount of fat, and bone density. In the design of this test, the damping induced by the chest was estimated. The estimation was based on results of in-vivo trials performed on human subjects, where an accelerometer was placed in the esophagus (back wall of the heart) and vibrations at 50 Hz were applied to the chest [67]. Assuming a good coupling between the vibrator and the chest (high engagement force), it might be possible to obtain 5 g acceleration at the front of the heart and thus at the coronary arteries with 8 mm vibration stroke at the chest. A noninvasive feedback system must be developed to read the observed vibration by the heart and coronary arteries. However, further in-depth experiments are required to determine the exact tolerated values and all the contributing factors based on using the proposed system.

In order to examine effects of direct distal external mechanical vibration and deformation on the blood flow, experiments in chapter 5 were conducted. The measurement method consisted of applying direct arterial mechanical deformation on an

artery distal to a presumed arterial stenosis site and determining whether the actuations get transferred to the stenosis site through bloodstream in form of turbulence or other. Four different measurement devices were examined: load cell, surface accelerometer, pulse transducer, and ultrasound imaging system. Load cell and surface accelerometer methods were dismissed in the initial phase of the experiment; due to their physical shape, it was difficult to position the devices on an artery correctly with stability to capture the changes. After numerous trials the resulting capture signals were of low quality and even further signal processing did not yield better results. Therefore, only the pulse transducer and ultrasound imaging methods were used. In measurements with the pulse transducer the reference frequency component (no actuations applied) at the index finger and carotid artery was at 1 Hz. This figure corresponded to heart rate of the subject (60 BPM). However, with application of mechanical deformation on the left brachial artery, in addition to 1 Hz, a secondary component at 32 Hz was observed. The 32 Hz was due to the application of mechanical deformation as the vibrating node of the massager operated at 32 Hz for this experiment. No other major components were observed (Figure 41). The results, however, are inconclusive since it is difficult to determine whether the measured vibration was transferred through the bloodstream or was it simply a transfer of energy through body surface using this method. The only solid conclusion that could be drawn was that mechanical actuation does transfer to a distal site. To further investigate, an ultrasound imaging system was used to quantitatively measure blood velocity profile change under distal mechanical deformation at the left carotid artery. Peak Systolic Velocity (PSV) was chosen as the primary turbulence measurement parameter. The minimum measured PSV value was for the left brachial artery at 91.11 cm/s and the maximum at 106.3 cm/s for the left subclavian artery. The reference case (no actuation applied) yielded a PSV value of 101.24 cm/s. Looking at the data points in Figure 47 one can see that PSV values are dependent on the specific artery deformed; it is possibly a function of distance to the measurement site, diameter of the artery, and surrounding tissue dampening properties. Also, depending on the artery, mechanical actuations may reduce turbulence and lead to smoother flow as in the case with brachial, femoral, and abdominal arteries with PSV values of 91.11, 96.17, and 97.86 cm/s, respectively. Further experiments are required understand the impact of different variables on blood flow velocity change and for selection of best distal artery. Contrary to the pulse transducer case, ultrasound imaging shows that application of

distal arterial mechanical deformation leads to increase or reduction of turbulence and imposes blood flow velocity change.

Based on the discussion and analysis presented, it can be seen that a combinational method consisting of concurrent application of mechanical vibration during diastole phase of the heart to the chest as well as direct application of mechanical vibration to an artery distal to the stenosis site could greatly benefit STEMI patients. Diastolic timed vibration applied to the heart of the STEMI patient increases the coronary blood flow and improves relaxation of the heart while direct application of mechanical strokes to certain arteries distal to the stenosis site causes increased turbulence in the blood flow, which, in turn, could help in mixing clot busting agents with the clot. It also changes the blood flow velocity profile and cause turbulence, which can eventually help in displacing/disrupting the clot and allowing oxygen to reach myocardium and prevent myocardial cell death. Therefore, an apparatus consisting of two separate and controllable vibrating devices with the ability to stop vibration during systole phase of the heart and adjustable stroke amplitude can be envisioned for this purpose.

7.   Summary and Conclusion

This thesis introduced a noninvasive adjunct therapeutic device as a means for starting pre-hospitalization treatment of STEMI patients. It included application of diastolic timed vibration along with distal arterial deformation to improve coronary blood flow, release of heart muscle spasms, impose turbulence on the clot wall and to better mix clot busting agents with thrombi. The presented work aimed at achieving three objectives: introduction of the proposed method and study of the method in-vitro, introduction of design and architecture of the corresponding device as part of the method, and finally, determining whether distal arterial actuations would cause turbulence in the blood flow of human subjects as a preliminary investigation to back up feasibility of the claimed method herein.

7.1. Study of Current Thrombolysis Methods

Various common and/or of interest methods of thrombolysis were reviewed. Present methods have one or more of the following shortcomings:

- Limited availability of specialized treatment centers, hospitals, and/or staff in certain geographic locations.

- Delays due to prolonged door-to-balloon and door-to-EMS intervals.

- Invasiveness of current common methods.

- Safety of some of the common methods.

Due to the reasons mentioned above, need for a noninvasive adjunct therapeutic method was clear. Therefore, the following three projects, were started to address this need.

7.2. In-vitro Study (Thesis Objective 1)

In this study, an electromechanical setup was developed to allow for studying the efficacy of mechanical vibration and deformation on disrupting thrombi in-vitro. Three different approaches were examined: vibration of the occlusion site, application of direct deformation on the occlusion site, and application of direct deformation on a site 60 cm away from the occlusion site. It was shown that 95% of the occlusions achieved TIMI 3 flow within 11 minutes of the start of experiment with direct application of actuations on the occlusion site. Direct distal deformation at a 60 cm distance to the occlusion site also showed 95% success rate in achieving TIMI 3 flow within 16 minutes of the start of actuation. However, with direct vibration of the occlusion site, only 2.3% of the cases showed TIMI 3 flow and only after 20 minutes. Therefore, it was concluded that deformation of the occlusion site and also application of deforming mechanical strokes to an artery distal to the stenosis site drastically improved reperfusion rates when compared to the case where the occlusion site was only vibrated. Use of ultrasound imaging also showed that blood velocity profile changed with application of direct mechanical strokes to an artery distal to stenosis site due to induction of turbulence in the flow.

7.3. Diastolic Timed Vibrator (Thesis Objective 2)

A diastolic timed vibrator device was introduced as a means to effectively apply diastolic timed vibration to the chest of STEMI patients with the initial intention of disrupting the clots, improving coronary blood flow, and releasing spasms of the heart muscle in the STEMI patients. DTV applies mechanical strokes during the diastole phase of the heart cycle, is able to adjust and feedback frequency of vibration, and monitor the application force; however, based on the results from objective 1 of this thesis, the first goal of this chapter was dismissed; it was realized that application of mechanical vibration on the stenosed region has little to no effect in disrupting thrombi with only 2.3% success rate.

One of the major challenges of DTV is the ability to stop the motor in time to avoid vibration spillage into the systole phase. Similarly, it is important to start the motor

as quick as possible after the "start" command is initiated to increase the efficacy of the treatment and cover the diastole phase for its duration. As a result, various braking and stopping systems were examined. The fastest stop time could be achieved by use of the inverted drive method, which lead to 11.7 ms average stop time. Motor startup times were also examined. At 50 N application force, the motor start time was recorded at 162 ms. Based on Figure 28, 162 ms start time imposed a limitation on patients with heart rates above 120 BPM as there would be no time left for vibration. Therefore, the limitation of the motor start and stop times must be taken into account when designing the DTV. In addition, based on the author's experiments, 30 to 50 N of application force on the chest was very well tolerated by the subjects that underwent the experiment. Although, this claim needs to be further investigated.

Since resonance frequency of the heart can vary in different subjects, various vibration patterns were studied to ensure maximum coverage of the different frequencies so that the resonance frequency of the heart could always be covered. Among constant, random, and cumulative ramp patterns presented, cumulative ramp pattern with a sweep frequency between 40 and 60 Hz was proposed to more ideally cover the resonance frequency of the heart of different subjects.

7.4. Distal Arterial Deformation and Turbulence in the Bloodstream (Thesis Objective 3)

As a follow-up on the in-vitro study conclusion, which suggested that distal arterial deformation would lead to TIMI 3 flow, and to study the effect of direct mechanical deformation on human arteries, experiments in chapter 5 were performed. Four approaches were examined, out which only two proved accurate: pulse transducer and ultrasound imaging. Using a pulse transducer, effect of 32 Hz direct distal deformation – applied on the left brachial artery – on the left carotid artery and index finger were studied. The major frequency components measured at the index finger and carotid artery were 1 and 32 Hz. 1 Hz component corresponded to the pulse rate of the subject while the 32 Hz component was from vibrating node of the motor, which could have been either transferred through the surface or through the bloodstream. No conclusions with respect to the amount of turbulence through bloodstream could have

been drawn. Therefore, experiments with use of ultrasound imaging were performed to analyze blood velocity profile and its respective changes with application of mechanical deformation. It was shown that direct arterial mechanical deformation does indeed impose turbulence in the bloodstream by changing the peak systolic velocity (PSV), an indicator of presence of turbulence. Maximum value for PSV was recorded at 106.3 cm/s resulting from mechanical actuations on the left subclavian artery. Least PSV was recorded at 91.11 cm/s and was due to application of deformation on the left brachial artery. The reference PSV value was measured at 101.24 cm/s. Therefore, values less than the reference PSV, e.g. the case in the left brachial artery, indicate a smoother flow whereas PSV values greater than 101.24 cm/s indicate turbulence as the case with subclavian artery. The varying results seemed to be dependent on the distance, material of the surrounding tissue and their damping properties, and the diameter of the artery. Regardless, it was obvious that application of direct distal mechanical deformation on an artery does, indeed, affect the blood velocity profile and depending on the specific artery, it can increase or decrease turbulence. Therefore, it is important to apply mechanical deformation on arteries that have the best turbulence imposition capability, although this would require further investigation and characterization.

7.5. Conclusion

Based on the summary of experiments above, it is reasonable to propose use of a combinational method consisting of a diastolic timed vibrator and a mechanical deformation device for increased coronary blood flow, improved relaxation of the ill myocardium spasm, better mixing of the fibrinolytic agents with clot and, finally, added blood flow turbulence for imposing turbulence and pressure on the clot wall to displace and/or disrupt thrombi. The proposed system must be compact and easy to use such that minimally trained individuals or even bystanders at the scene with a STEMI patient can utilize the device and start the pre-hospitalization treatment until arrival of the EMS and transferal to a cath lab. Further experiments must be conducted to gain more detailed understanding of presented limitations.

7.6. Future Work

The limitations of the in-vitro study mostly consisted in limited fidelity with which the in-vitro system represents an actual circulatory system. The effect of various methods of application without analyzing the mechanism of mechanical stimulus transfer through tissues in a living organism [83] were studied. Furthermore, the presented study was limited to the use of heparin, while application of more potent thrombolytic drugs could positively affect the results. Future in-vitro studies of the proposed method should use various anti-thrombolytic agents dissolved in the buffer fluid. Upon successful verification of this technique, an in-vivo experiment must be performed.

The next goal for the DTV would be to determine the best possible approach for detecting the vibration perceived by the heart and the coronary arteries, which must be followed by the design and implementation of such method as a feedback system that can safely and noninvasively read the amount of vibration observed by the heart and thrombosed coronary artery. This is needed to adjust the frequency and amplitude of the strokes to guarantee optimized transfer of energy. In addition, the feedback system can help the operator to understand how accurate the placement of the vibrating node on the patient's chest is and adjust accordingly. Upon successful validation of the device, the method will be evaluated first in-vitro and only then in-vivo. More research is required to further verify the safety of the method and the setup to allow clinical trials on human subjects.

Further experiments with ultrasound imaging are required to determine the best location for applying mechanical deformation, and also to obtain more accurate relationship between the type of artery and respective change in blood flow profile. Presented experiment only focused on very few trials with limited number of data points due to time limitations and unavailability of an appropriate ultrasound machine at our facility. Various frequencies at different stroke amplitudes need to be examined. Different arteries on the left and right side of the body must be experimented on. Enough data must be gathered to statistically draw conclusions on efficacy of the approach.

Finally, a prototype device must be developed that could incorporate both DTV and a second device for applying controllable mechanical actuation on the artery.

Although more complicated in design, the final product must be very simple and intuitive to be used by minimally trained individuals.

References

[1] M. Marzencki, B. Kajbafzadeh, F. Khosrow-Khavar, K. Tavakolian, M. Soleimani-Nouri, J. Hamburger, B. Kaminska, and C. Menon, "Low Frequency Mechanical Actuation Accelerates Reperfusion In-vitro," *To be submitted for publication.*

[2] M. Marzencki, B. Kajbafzadeh, F. Khosrow-Khavar, K. Tavakolian, B. Kaminska, and C. Menon, "Diastolic Timed Vibrator: Noninvasive Pre-Hospitalization Treatment of Acute Coronary Ischemia," *To be submitted for publication.*

[3] B. Kajbafzadeh, M. Marzencki, N. Alavi, F. Khosrow-Khavar, K. Tavakolian, C. Menon, and B. Kaminska, "Preferred patterns of diastolic timed vibrations for pre-hospitalization treatment of acute coronary ischemia," in *Engineering in Medicine and Biology Society,EMBC, 2011 Annual International Conference of the IEEE*, 2011, pp. 2480 –2483.

[4] M. Marzencki, B. Kajbafzadeh, F. Khosrow-Khavar, B. Kaminska, and C. Menon, "Accelerating Reperfusion with low frequency vessel deformation during myocardial infarction," in *Computing in Cardiology (CinC), 2012*, 2012, pp. 737–740.

[5] W. H. Organization, "The Top Ten Causes of Death," World Health Organization, 310, May 2011.

[6] E. Falk, P. K. Shah, and P. J. de Feyter, *Ischaemic Heart Disease*. Manson Publishing, 2007.

[7] S. Mendis and P. Puska, "What are cardiovascular diseases (CVDs)?," in in *Global Atlas on Cardiovascular Disease Prevention and Control*, World Health Organization, 2011, pp. 2–7.

[8] V. L. Roger, A. S. Go, D. M. Lloyd-Jones, E. J. Benjamin, J. D. Berry, W. B. Borden, D. M. Bravata, S. Dai, E. S. Ford, C. S. Fox, H. J. Fullerton, C. Gillespie, S. M. Hailpern, J. A. Heit, V. J. Howard, B. M. Kissela, S. J. Kittner, D. T. Lackland, J. H. Lichtman, L. D. Lisabeth, D. M. Makuc, G. M. Marcus, A. Marelli, D. B. Matchar, C. S. Moy, D. Mozaffarian, M. E. Mussolino, G. Nichol, N. P. Paynter, E. Z. Soliman, P. D. Sorlie, N. Sotoodehnia, T. N. Turan, S. S. Virani, N. D. Wong, D. Woo, and M. B. Turner, "Heart Disease and Stroke Statistics—2012 Update A Report From the American Heart Association," *Circulation*, Dec. 2011.

[9] D. B. Foster, "Myocardial Infarction," in in *Twelve-Lead Electrocardiography*, Springer London, 2007, pp. 64–83.

[10]P. I. Aaronson and J. P. T. Ward, "Pathophysiology of acute myocardial infarction," in in *The Cardiovascular System at a Glance*, 3rd ed., Wiley-Blackwell, 2007, pp. 94–95.

[11]M. Lavallee, D. Cox, T. A. Patrick, and S. F. Vatner, "Salvage of myocardial function by coronary artery reperfusion 1, 2, and 3 hours after occlusion in conscious dogs.," *Circ Res*, vol. 53, no. 2, pp. 235–247, Aug. 1983.

[12]W. J. Cantor, "Overview, Rationale, and Lexicon: Primary Percutaneous Coronary Intervention in Acute Myocardial Infarction," in in *Primary Angioplasty in Acute Myocardial Infarction*, J. E. Tcheng and C. P. Cannon, Eds. Humana Press, 2009, pp. 1–8.

[13]G. I. per lo S. della S. nell'Infarto M. (GISSI), "Effectiveness of intravenous thrombolytic treatment in acute myocardial infarction," *Lancet*, vol. 1, no. 8478, pp. 397–402, Feb. 1986.

[14]M. O'Rourke, D. Baron, A. Keogh, R. Kelly, G. Nelson, C. Barnes, J. Raftos, K. Graham, K. Hillman, and H. Newman, "Limitation of myocardial infarction by early infusion of recombinant tissue-type plasminogen activator.," *Circulation*, vol. 77, no. 6, pp. 1311–1315, Jun. 1988.

[15]P. W. Armstrong, R. S. Baigrie, P. A. Daly, A. Haq, M. Gent, R. S. Roberts, M. R. Freeman, R. Burns, P. Liu, and C. D. Morgan, "Tissue plasminogen activator: Toronto (TPAT) placebo-controlled randomized trial in acute myocardial infarction.," *J Am Coll Cardiol*, vol. 13, no. 7, pp. 1469–1476, Jun. 1989.

[16]C. J. Lavie, B. J. Gersh, and J. H. Chesebro, "Reperfusion in acute myocardial infarction." *Mayo Clin Proc*, vol. 65, no. 4, pp. 549–564, Apr. 1990.

[17]C. Bode, R. W. Smalling, G. Berg, C. Burnett, G. Lorch, J. M. Kalbfleisch, R. Chernoff, L. G. Christie, R. L. Feldman, A. A. Seals, and W. D. Weaver, "Randomized Comparison of Coronary Thrombolysis Achieved With Double-Bolus Reteplase (Recombinant Plasminogen Activator) and Front-Loaded, Accelerated Alteplase (Recombinant Tissue Plasminogen Activator) in Patients With Acute Myocardial Infarction," *Circulation*, vol. 94, no. 5, pp. 891–898, Sep. 1996.

[18]R. W. Smalling, C. Bode, J. Kalbfleisch, S. Sen, P. Limbourg, F. Forycki, G. Habib, R. Feldman, S. Hohnloser, and A. Seals, "More Rapid, Complete, and Stable Coronary Thrombolysis With Bolus Administration of Reteplase Compared With Alteplase Infusion in Acute Myocardial Infarction," *Circulation*, vol. 91, no. 11, pp. 2725–2732, Jun. 1995.

[19]J. H. Gurwitz, J. M. Gore, R. J. Goldberg, H. V. Barron, T. Breen, A. C. Rundle, M. A. Sloan, W. French, and W. J. Rogers, "Risk for intracranial hemorrhage after tissue plasminogen activator treatment for acute myocardial infarction. Participants in the National Registry of Myocardial Infarction 2," *Annals of Internal Medicine*, vol. 129, no. 8, pp. 597–604, Oct. 1998.

[20] H. M. Krumholz, J. Herrin, L. E. Miller, E. E. Drye, S. M. Ling, L. F. Han, M. T. Rapp, E. H. Bradley, B. K. Nallamothu, W. Nsa, D. W. Bratzler, and J. P. Curtis, "Improvements in Door-to-Balloon Time in the United States, 2005 to 2010 Clinical Perspective," *Circulation*, vol. 124, no. 9, pp. 1038–1045, Aug. 2011.

[21] S. S. Rathore, J. P. Curtis, J. Chen, Y. Wang, B. K. Nallamothu, A. J. Epstein, H. M. Krumholz, and for the National Cardiovascular Data Registry, "Association of door-to-balloon time and mortality in patients admitted to hospital with ST elevation myocardial infarction: national cohort study," *BMJ*, vol. 338, no. may19 1, pp. b1807–b1807, May 2009.

[22] C. B. Granger, T. D. Henry, W. E. R. Bates, B. Cercek, W. D. Weaver, and D. O. Williams, "Development of Systems of Care for ST-Elevation Myocardial Infarction Patients The Primary Percutaneous Coronary Intervention (ST-Elevation Myocardial Infarction–Receiving) Hospital Perspective," *Circulation*, vol. 116, no. 2, pp. e55–e59, Jul. 2007.

[23] A. Y. K. Chan, "Electrocardiograph," in in *Biomedical device technology: principles and design*, Springfield, Ill.: Charles C. Thomas, 2008.

[24] "Electrocardiography," *Wikipedia, the free encyclopedia*. 20-Apr-2013.

[25] "PVC," *Learn EKGs*. [Online]. Available: http://www.learnekgs.com/pvc.htm. [Accessed: 24-Apr-2013].

[26] "ECG ST Segment elevation," *Life in the Fast Lane medical education blog*. [Online]. Available: http://lifeinthefastlane.com/2012/01/ecg-st-segment-evaluation/. [Accessed: 24-Apr-2013].

[27] P. M. Rautaharju, B. Surawicz, and L. S. Gettes, "AHA/ACCF/HRS Recommendations for the Standardization and Interpretation of the ElectrocardiogramPart IV: The ST Segment, T and U Waves, and the QT Interval A Scientific Statement From the American Heart Association Electrocardiography and Arrhythmias Committee, Council on Clinical Cardiology; the American College of Cardiology Foundation; and the Heart Rhythm Society Endorsed by the International Society for Computerized Electrocardiology," *J Am Coll Cardiol*, vol. 53, no. 11, pp. 982–991, Mar. 2009.

[28] S. A. Joshi, *Nutrition and dietetics : with Indian case studies*. New Delhi: Tata McGraw-Hill, pp. 281-282, 2010.

[29] K. O. Md and M. C. Md, "Vulnerable plaque: Definition, detection, treatment, and future implications," *Curr Atheroscler Rep*, vol. 7, no. 2, pp. 121–126, Mar. 2005.

[30] J. Loscalzo and A. I. Schafer, *Thrombosis and hemorrhage*, 3rd ed. Philadelphia: Lippincott Williams & Wilkins, pp. 688, 2003.

[31] Lippincott Williams & Wilkins, "Cardiovascular Care," in in *Lippincott's nursing procedures*, 5th ed., Philadelphia: Lippincott Williams & Wilkins, 2009, p. 508.

[32] H. P. Mattle, "Intravenous or Intra-Arterial Thrombolysis? It's Time to Find the Right Approach for the Right Patient," *Stroke*, vol. 38, no. 7, pp. 2038–2040, Jul. 2007.

[33] J. Wasiak, J. Law, P. Watson, and A. Spinks, "Percutaneous transluminal rotational atherectomy for coronary artery disease," in in *Cochrane Database of Systematic Reviews*, The Cochrane Collaboration and J. Wasiak, Eds. Chichester, UK: John Wiley & Sons, Ltd, 2012.

[34] R. J. Siegel and H. Luo, "Ultrasound thrombolysis.," *Ultrasonics*, vol. 48, no. 4, pp. 312–320, Aug. 2008.

[35] G. Trübestein, C. Engel, F. Etzel, A. Sobbe, H. Cremer, and U. Stumpff, "Thrombolysis by ultrasound.," *Clin Sci Mol Med Suppl*, vol. 3, p. 697s–698s, Dec. 1976.

[36] U. Rosenschein, A. Frimerman, S. Laniado, and H. I. Miller, "Study of the mechanism of ultrasound angioplasty from human thrombi and bovine aorta," *Am. J. Cardiol.*, vol. 74, no. 12, pp. 1263–1266, Dec. 1994.

[37] U. Rosenschein, J. J. Bernstein, E. DiSegni, E. Kaplinsky, J. Bernheim, and L. A. Rozenzsajn, "Experimental ultrasonic angioplasty: disruption of atherosclerotic plaques and thrombi in vitro and arterial recanalization in vivo," *J. Am. Coll. Cardiol.*, vol. 15, no. 3, pp. 711–717, Mar. 1990.

[38] C. W. Hamm, W. Steffen, W. Terres, I. de Scheerder, J. Reimers, D. Cumberland, R. J. Siegel, and T. Meinertz, "Intravascular therapeutic ultrasound thrombolysis in acute myocardial infarctions," *Am. J. Cardiol.*, vol. 80, no. 2, pp. 200–204, Jul. 1997.

[39] A. S. Hong, J. S. Chae, S. B. Dubin, S. Lee, M. C. Fishbein, and R. J. Siegel, "Ultrasonic clot disruption: an in vitro study," *Am. Heart J.*, vol. 120, no. 2, pp. 418–422, Aug. 1990.

[40] W. Steffen, M. C. Fishbein, H. Luo, D.-Y. Lee, H. Nitams, D. C. Cumberland, S. W. Tabak, M. Carbonne, G. Maurer, and R. J. Siegel, "High intensity, low frequency catheter-delivered ultrasound dissolution of occlusive coronary artery thrombi: An in vitro and in vivo study," *Journal of the American College of Cardiology*, vol. 24, no. 6, pp. 1571–1579, Nov. 1994.

[41] "Safety of diagnostic ultrasound.," in in *Diagnostic ultrasound: physics and equipment*, 2nd ed., Cambridge, UK ; New York: Cambridge University Press, 2010, pp. 160–161.

[42] U. Rosenschein, A. Roth, T. Rassin, S. Basan, S. Laniado, and H. I. Miller, "Analysis of Coronary Ultrasound Thrombolysis Endpoints in Acute Myocardial Infarction (ACUTE Trial) Results of the Feasibility Phase," *Circulation*, vol. 95, no. 6, pp. 1411–1416, Mar. 1997.

[43] R. J. Gibbons, D. R. Holmes, G. S. Reeder, K. R. Bailey, M. R. Hopfenspirger, and B. J. Gersh, "Immediate angioplasty compared with the administration of a thrombolytic agent followed by conservative treatment for myocardial infarction. The Mayo Coronary Care Unit and Catheterization Laboratory Groups," *N. Engl. J. Med.*, vol. 328, no. 10, pp. 685–691, Mar. 1993.

[44] C. L. Grines, K. F. Browne, J. Marco, D. Rothbaum, G. W. Stone, J. O'Keefe, P. Overlie, B. Donohue, N. Chelliah, and G. C. Timmis, "A comparison of immediate angioplasty with thrombolytic therapy for acute myocardial infarction. The Primary Angioplasty in Myocardial Infarction Study Group," *N. Engl. J. Med.*, vol. 328, no. 10, pp. 673–679, Mar. 1993.

[45] U. Rosenschein, V. Furman, E. Kerner, I. Fabian, J. Bernheim, and Y. Eshel, "Ultrasound Imaging–Guided Noninvasive Ultrasound Thrombolysis Preclinical Results," *Circulation*, vol. 102, no. 2, pp. 238–245, Jul. 2000.

[46] C. Wright, K. Hynynen, and D. Goertz, "In Vitro and In Vivo High-Intensity Focused Ultrasound Thrombolysis," *Investigative Radiology*, vol. 47, no. 4, pp. 217–225, Apr. 2012.

[47] K. Tachibana and S. Tachibana, "Ultrasound Energy for Enhancement of Fibrinolysis and Drug Delivery: Special Emphasis on the Use of a Transducer-Tipped Ultrasound System," in in *Ultrasound Angioplasty*, R. J. Siegel, Ed. Springer US, 1996, pp. 121–133.

[48] K. Tachibana and S. Tachibana, "Prototype therapeutic ultrasound emitting catheter for accelerating thrombolysis.," *J Ultrasound Med*, vol. 16, no. 8, pp. 529–535, Aug. 1997.

[49] P. A. Dijkmans, L. J. M. Juffermans, R. J. P. Musters, A. van Wamel, F. J. ten Cate, W. van Gilst, C. A. Visser, N. de Jong, and O. Kamp, "Microbubbles and ultrasound: from diagnosis to therapy," *Eur J Echocardiogr*, vol. 5, no. 4, pp. 245–246, Aug. 2004.

[50] S. Atar, H. Luo, T. Nagai, and R. J. Siegel, "Ultrasonic thrombolysis: catheter-delivered and transcutaneous applications," *European Journal of Ultrasound*, vol. 9, no. 1, pp. 39–54, Mar. 1999.

[51] S. Atar, H. Luo, T. Nagai, R. A. Sahm, M. C. Fishbein, and R. J. Siegel, "Arterial Thrombus Dissolution In Vivo Using a Transducer-Tipped, High-Frequency Ultrasound Catheter and Local Low-Dose Urokinase Delivery," *Journal of Endovascular Therapy*, vol. 8, no. 3, pp. 282–290, Jun. 2001.

[52] J. V. Braaten, R. A. Goss, and C. W. Francis, "Ultrasound reversibly disaggregates fibrin fibers.," *Thromb Haemost*, vol. 78, no. 3, pp. 1063–1068, Sep. 1997.

[53] V. Suchkova, F. N. Siddiqi, E. L. Carstensen, D. Dalecki, S. Child, and C. W. Francis, "Enhancement of fibrinolysis with 40-kHz ultrasound.," *Circulation*, vol. 98, no. 10, pp. 1030–1035, Sep. 1998.

[54] H. Luo, W. Steffen, B. Cercek, S. Arunasalam, G. Maurer, and R. J. Siegel, "Enhancement of thrombolysis by external ultrasound," *American Heart Journal*, vol. 125, no. 6, pp. 1564–1569, Jun. 1993.

[55] Luo, Nishioka, Berglund, Kim, Carbone, Cercek, and Siegel, "Effect of External Ultrasound Frequency on Thrombus Disruption In Vitro," *J. Thromb. Thrombolysis*, vol. 3, no. 1, pp. 63–66, 1996.

[56] H. Luo, Y. Birnbaum, M. C. Fishbein, T. M. Peterson, T. Nagai, T. Nishioka, and R. J. Siegel, "Enhancement of thrombolysis in vivo without skin and soft tissue damage by transcutaneous ultrasound," *Thromb. Res.*, vol. 89, no. 4, pp. 171–177, Feb. 1998.

[57] T. Nishioka, H. Luo, M. C. Fishbein, B. Cercek, J. S. Forrester, C.-J. Kim, H. Berglund, and R. J. Siegel, "Dissolution of Thrombotic Arterial Occlusion by High Intensity, Low Frequency Ultrasound and Dodecafluoropentane Emulsion: An In Vitro and In Vivo Study," *Journal of the American College of Cardiology*, vol. 30, no. 2, pp. 561–568, Aug. 1997.

[58] Y. Birnbaum, H. Luo, T. Nagai, M. C. Fishbein, T. M. Peterson, S. Li, D. Kricsfeld, T. R. Porter, and R. J. Siegel, "Noninvasive In Vivo Clot Dissolution Without a Thrombolytic Drug Recanalization of Thrombosed Iliofemoral Arteries by Transcutaneous Ultrasound Combined With Intravenous Infusion of Microbubbles," *Circulation*, vol. 97, no. 2, pp. 130–134, Jan. 1998.

[59] R. J. Siegel, V. N. Suchkova, T. Miyamoto, H. Luo, R. B. Baggs, Y. Neuman, M. Horzewski, V. Suorsa, S. Kobal, T. Thompson, D. Echt, and C. W. Francis, "Ultrasound energy improves myocardial perfusion in the presence of coronary occlusion," *J Am Coll Cardiol*, vol. 44, no. 7, pp. 1454–1458, Oct. 2004.

[60] V. N. Suchkova, R. B. Baggs, and C. W. Francis, "Effect of 40-kHz ultrasound on acute thrombotic ischemia in a rabbit femoral artery thrombosis model: enhancement of thrombolysis and improvement in capillary muscle perfusion," *Circulation*, vol. 101, no. 19, pp. 2296–2301, May 2000.

[61] D.-S. Jeon, H. Luo, M. C. Fishbein, T. Miyamoto, M. Horzewski, T. Iwami, J. M. Mirocha, F. Ikeno, Y. Honda, and R. J. Siegel, "Noninvasive transcutaneous ultrasound augments thrombolysis in the left circumflex coronary artery—an in vivo canine study," *Thrombosis Research*, vol. 110, no. 2–3, pp. 149–158, May 2003.

[62] R. J. Siegel, S. Atar, M. C. Fishbein, A. V. Brasch, T. M. Peterson, T. Nagai, D. Pal, T. Nishioka, J. S. Chae, Y. Birnbaum, C. Zanelli, and H. Luo, "Noninvasive, transthoracic, low-frequency ultrasound augments thrombolysis in a canine model of acute myocardial infarction.," *Circulation*, vol. 101, no. 17, pp. 2026–2029, May 2000.

[63] R. J. Siegel, S. Atar, M. C. Fishbein, A. V. Brasch, T. M. Peterson, T. Nagai, D. Pal, T. Nishioka, J. S. Chae, Y. Birnbaum, C. Zanelli, and H. Luo, "Noninvasive transcutaneous low frequency ultrasound enhances thrombolysis in peripheral and coronary arteries," *Echocardiography*, vol. 18, no. 3, pp. 247–257, Apr. 2001.

[64] Y. Birnbaum, H. Luo, S. Atar, M. C. Fishbein, A. V. Brasch, T. Nagai, D. Pal, T. Nishioka, J. S. Chae, C. Zanelli, T. M. Peterson, and R. J. Siegel, "Noninvasive transthoracic low frequency ultrasound augments thrombolysis in a canine model of acute myocardial infarction--evaluation of the extent of ST-segment resolution," *J. Thromb. Thrombolysis*, vol. 11, no. 3, pp. 229–234, May 2001.

[65] L. A. Frizzell, D. L. Miller, and W. L. Nyborg, "Ultrasonically induced intravascular streaming and thrombus formation adjacent to a micropipette," *Ultrasound Med Biol*, vol. 12, no. 3, pp. 217–221, Mar. 1986.

[66] C. L. Kerr, D. W. Gregory, K. K. Chan, D. J. Watmough, and D. N. Wheatley, "Ultrasound-induced damage of veins in pig ears, as revealed by scanning electron microscopy," *Ultrasound Med Biol*, vol. 15, no. 1, pp. 45–52, 1989.

[67] Y. Koiwa, H. Honda, T. Takagi, J. Kikuchi, N. Hoshi, and T. Takishima, "Modification of human left ventricular relaxation by small-amplitude, phase-controlled mechanical vibration on the chest wall.," *Circulation*, vol. 95, no. 1, pp. 156–162, Jan. 1997.

[68] J. Thomas, D. J. Cook, and D. Brooks, "Chest physical therapy management of patients with cystic fibrosis. A meta-analysis.," *Am J Respir Crit Care Med*, vol. 151, no. 3 Pt 1, pp. 846–850, Mar. 1995.

[69] D. Smith, T. Ishimitsu, and E. Craige, "Mechanical vibration transmission characteristics of the left ventricle: implications with regard to auscultation and phonocardiography," *J. Am. Coll. Cardiol.*, vol. 4, no. 3, pp. 517–521, Sep. 1984.

[70] J. J. Farber and J. H. Purvis, "Conduction of Cardiovascular Sound Along Arteries," *Circulation Research*, vol. 12, no. 3, pp. 308–316, Mar. 1963.

[71] Y. K. et al, "Measurement of instantaneous viscoelastic properties by impedance-frequency curve of the ventricle," *The American Journal of Physiology*, vol. 250, no. 4 Pt 2, pp. H672–84, Apr. 1986.

[72] R. Hashiguchi, Y. Koiwa, T. Ohyama, T. Takagi, J. Kikuchi, J. P. Butler, and T. Takishima, "Dependence of instantaneous transfer function on regional ischemic myocardial volume," *Circ. Res.*, vol. 63, no. 6, pp. 1003–1011, Dec. 1988.

[73] E. Wobser and U. Stumpff, "Intragastral Disintegration of Blood Coagula by Mechanical Vibration Intragastrale Thrombenauflösung durch mechanische Schwingungen," *Endoscopy*, vol. 10, no. 1, pp. 15–19, 1978.

[74] W. R. Dubrul and M. A. Evans, "United States Patent: 6287271 - Motion catheter," 628727111-Sep-2001.

[75] J. Folts, "An in vivo model of experimental arterial stenosis, intimal damage, and periodic thrombosis.," *Circulation*, vol. 83, no. 6 Suppl, pp. IV3–I14, Jun. 1991.

[76] H. Gill and A. Hoffmann, "The timing of onset of mechanical systole and diastole in reference to the QRS-T complex: a study to determine performance criteria for a non-invasive diastolic timed vibration massage system in treatment of potentially unstable cardiac disorders," *Cardiovascular engineering*, vol. 10, no. 4, pp. 235–245, Dec. 2010.

[77] F. Pipp, S. Boehm, W.-J. Cai, F. Adili, B. Ziegler, G. Karanovic, R. Ritter, J. Balzer, C. Scheler, W. Schaper, and T. Schmitz-Rixen, "Elevated fluid shear stress enhances postocclusive collateral artery growth and gene expression in the pig hind limb," *Arterioscler. Thromb. Vasc. Biol.*, vol. 24, no. 9, pp. 1664–1668, Sep. 2004.

[78] F. R. Arko, C. M. Davis, E. H. Murphy, S. T. Smith, C. H. Timaran, J. G. Modrall, R. J. Valentine, and G. P. Clagett, "Aggressive percutaneous mechanical thrombectomy of deep venous thrombosis: early clinical results.," *Arch Surg*, vol. 142, no. 6, pp. 513–9, Jun. 2007.

[79] F. G. Yohannes and A. K. Hoffmann, "Non-invasive low frequency vibration as a potential emergency adjunctive treatment for heart attack and stroke. An in vitro flow model.," vol. 25, no. 3, pp. 251–258, Jun. 2008.

[80] Y. Koiwa, T. Takagi, J. Kikuchi, H. Honda, N. Hoshi, and T. Takishima, "The improvement of systolic function of depressed left ventricle by external vibration at diastole.," *Tohoku J Exp Med*, vol. 159, no. 2, pp. 169–170, Oct. 1989.

[81] Y. Koiwa, T. Ohyama, T. Takagi, J. Kikuchi, H. Honda, N. Hoshi, and T. Takishima, "Clinical demonstration of vibration-induced depression of left ventricular function.," *Tohoku J Exp Med*, vol. 159, no. 3, pp. 247–248, Nov. 1989.

[82] J. Kikuchi, Y. Koiwa, T. Takagi, H. Honda, N. Hoshi, J. P. Butler, and T. Takishima, "Effects of mechanical vibration on left ventricular diastolic properties during global ischemia.," *Am J Physiol*, vol. 263, no. 1 Pt 2, pp. H88–H95, Jul. 1992.

[83] T. Takagi, Y. Koiwa, J. Kikuchi, H. Honda, N. Hoshi, J. P. Butler, and T. Takishima, "Diastolic vibration improves systolic function in cases of incomplete relaxation," *Circulation*, vol. 86, no. 6, pp. 1955–1964, Dec. 1992.

[84] L. E. Lindblad, R. R. Lorenz, J. T. Shepherd, and P. M. Vanhoutte, "Effect of vibration on a canine cutaneous artery.," *Am J Physiol*, vol. 250, no. 3 Pt 2, pp. H519–H523, Mar. 1986.

[85] P. B. Oliva and J. C. Breckinridge, "Arteriographic evidence of coronary arterial spasm in acute myocardial infarction," *Circulation*, vol. 56, no. 3, pp. 366–374, Sep. 1977.

[86] M. Marzencki, F. Khosrow-Khavar, S. A. Zaidi, C. Menon, and B. Kaminska, "Diastolic Timed Vibrations for Pre-hospitalization Treatment of Myocardial Infarction.," in *BIOSIGNALS*, 2011, pp. 405–408.

[87] J. T. Dodge, B. G. Brown, E. L. Bolson, and H. T. Dodge, "Lumen diameter of normal human coronary arteries. Influence of age, sex, anatomic variation, and left ventricular hypertrophy or dilation.," vol. 86, no. 1, pp. 232–246, Jul. 1992.

[88] S. C. Division, "Technical Bulletin #870," Sigma Aldrich, 2012.

[89] B. Sonesson, F. Hansen, H. Stale, and T. Länne, "Compliance and diameter in the human abdominal aorta—The influence of age and sex," vol. 7, no. 6, p. 690, 1993.

[90] H. J. Schröder, M. Tchirikov, and C. Rybakowski, "Pressure pulses and flow velocities in central veins of the anesthetized sheep fetus.," vol. 284, no. 4, pp. H1205–H1211, Apr. 2003.

[91] R. Lee, D. Adlam, C. A. Clelland, and K. M. Channon, "Lines of Zahn in coronary artery thrombus.," Feb. 2012.

[92] V. Kumar, A. K. Abbas, and J. Aster, *Robbins & Cotran Pathologic Basis of Disease, 8th Edition*. Elsevier Saunders, 2009.

[93] F. Bajd, J. Vidmar, A. Blinc, and I. Sersa, "Microscopic clot fragment evidence of biochemo-mechanical degradation effects in thrombolysis.," vol. 126, no. 2, pp. 137–143, Aug. 2010.

[94] D. Harpaz, X. Chen, C. W. Francis, and R. S. Meltzer, "Ultrasound accelerates urokinase-induced thrombolysis and reperfusion.," *Am Heart J*, vol. 127, no. 5, pp. 1211–1219, May 1994.

[95] M. G. Cohen, E. Tuero, J. Bluguermann, R. Kevorkian, D. H. Berrocal, O. Carlevaro, E. Picabea, M. P. Hudson, R. J. Siegel, L. Douthat, A. B. Greenbaum, D. Echt, W. D. Weaver, and L. R. Grinfeld, "Transcutaneous ultrasound-facilitated coronary thrombolysis during acute myocardial infarction.," *Am J Cardiol*, vol. 92, no. 4, pp. 454–457, Aug. 2003.

[96] M. Hudson, A. Greenbaum, L. Brenton, C. M. Gibson, R. Siegel, L. R. Reeves, M. F. Sala, G. McKendall, J. Bluguermann, D. Echt, E. M. Ohman, and W. D. Weaver, "Adjunctive Transcutaneous Ultrasound With Thrombolysis: Results of the PLUS (Perfusion by ThromboLytic and UltraSound) Trial," *JACC: Cardiovascular Interventions*, vol. 3, no. 3, pp. 352–359, Mar. 2010.

[97] M. D. Torno, M. D. Kaminski, Y. Xie, R. E. Meyers, C. J. Mertz, X. Liu, W. D. O'Brien Jr, and A. J. Rosengart, "Improvement of in vitro thrombolysis employing magnetically-guided microspheres," *Thromb. Res.*, vol. 121, no. 6, pp. 799–811, 2008.

[98] T. N. et al, "Diastolic mechanical vibration on the chest wall increases human coronary blood flow," *Japanese circulation journal*, vol. 58, no. 7, p. 476, 1994.

[99] P. S. Hamilton and W. J. Tompkins, "Quantitative investigation of QRS detection rules using the MIT/BIH arrhythmia database," *Biomedical Engineering, IEEE Transactions on*, no. 12, pp. 1157–1165, 1986.

[100] F. Khosrow-khavar, M. Marzencki, K. Tavakolian, B. Kajbafzadeh, B. Kaminska, and C. Menon, "Diastolic Timed Vibrator: Applying Direct Vibration in Diastole to Patients with Acute Coronary Ischemia during the Pre-hospitalization Phase," in in *Autonomous and Intelligent Systems*, vol. 6752, M. Kamel, F. Karray, W. Gueaieb, and A. Khamis, Eds. Berlin, Heidelberg: Springer Berlin Heidelberg, 2011, pp. 355–365.

[101] A. K. Hoffmann, "Percussion assisted angiogenesis," 200802753432008.

[102] A. M. W. et al, "Systolic time intervals in heart failure in man," *Circulation*, vol. 37, no. 2, p. 149, 1968.

[103] L. D. Landau and E. M. Lifshitz, *Mechanics*. Pergamon, 1960.

[104] R. Bousseljot, D. Kreiseler, and A. Schnabel, "Nutzung der EKG-Signaldatenbank CARDIODAT der PTB über das Internet," *Biomedizinische Technik/Biomedical Engineering*, vol. 40, no. s1, pp. 317–318, 1995.

[105] A. L. Goldberger, L. A. N. Amaral, L. Glass, J. M. Hausdorff, P. C. Ivanov, R. G. Mark, J. E. Mietus, G. B. Moody, C. K. Peng, and H. E. Stanley, "PhysioBank, PhysioToolkit, and PhysioNet: Components of a new research resource for complex physiologic signals," *Circulation*, vol. 101, no. 23, pp. e215–e220, 2000.

[106] K. Tavakolian, F. Khosrow-khavar, M. Marzencki, B. Kajbafzadeh, B. Kaminska, and C. Menon, "Seismocardiographic Adjustment of Diastolic Timed Vibrations," in *Proc. IEEE EMBS Conference*, 2012.

[107] D. N. Chen and J. Clarke, "Analysis of a clinical sign in traditional Chinese medicine using Doppler ultrasound," *Australas Radiol*, vol. 45, no. 4, pp. 452–456, Nov. 2001.

[108] "Carotid Artery Disease," in in *Clinical sonography: a practical guide*, 4th ed., Baltimore: Lippincott Williams & Wilkins, 2007, pp. 537–540.

[109] M. Nemati, A. S. Bavil, and N. Taheri, "Comparison of normal values of Duplex indices of vertebral arteries in young and elderly adults," *Cardiovascular Ultrasound*, vol. 7, no. 1, p. 2, Jan. 2009.

[110] "Doppler and Color Flow Principals," in in *Clinical sonography: a practical guide*, 4th ed., Baltimore: Lippincott Williams & Wilkins, 2007, p. 27.

[111] G. Elert, "Viscosity - The Physics Hypertextbook." [Online]. Available: http://physics.info/viscosity/. [Accessed: 21-Apr-2013].